

# High-Dimensional Sparse Clustering via Iterative Semidefinite Programming Relaxed K-Means

Jongmin Mun

Paromita Dubey

Yingying Fan

University of Southern California

{jongmin.mun, paromita, fanyingy}@marshall.usc.edu

October 6, 2025

## Abstract

We study high-dimensional clustering where the true signal is sparse among features. To help design algorithms that do not rely on precise estimation of sparse nuisance parameters or signal feature set, we establish minimax separation for exact cluster recovery of semidefinite programming (SDP) relaxation of  $K$ -means using varying subsets of features. It highlights the critical role of feature selection and, at the same time, shows that the signal feature set can be slightly overestimated without compromising clustering performance. Guided by this theory, our method alternates between rough feature selection and clustering: feature selection is performed by thresholding a rough estimate of the discriminative direction, while clustering is carried out via an SDP-relaxed  $K$ -means. We further extend the method to settings with unknown sparse precision matrices, avoiding full model parameter estimation by computing only the minimally required quantities.

**Keywords:** exact recovery; Gaussian mixture models; high-dimensional data; K-means; precision matrix; semidefinite relaxation; sparsity; unsupervised learning; variable selection

## 1 INTRODUCTION

High-dimensional clustering methods group unlabeled observations when the number of features exceeds or matches the sample size. They are widely applied to high-cost recordings with limited sample sizes such as gene expression (Curtis et al., 2012; He et al., 2021) and

neurophysiological signals (Cunningham and Yu, 2014; Kadir et al., 2014; Park et al., 2024). They are also used in machine learning tasks such as reinforcement learning (Liu and Frank, 2022), privacy protection (Javanmard and Mirrokni, 2023), and federated learning (Kim et al., 2024). In many such problems, only a small subset of features is relevant to the clustering. For example, in document clustering, each document contains only a few informative words out of a large corpus (Bing et al., 2020; Wu et al., 2023; Yi et al., 2014). In disease subtype discovery from gene expression data, only a handful of genes out of thousands differ across subtypes (Golub et al., 1999).

If sparsity is present and effectively leveraged, clustering performance improves, as demonstrated in broad applications such as genomics (Lu et al., 2017), neuroimaging data analysis (Mishra et al., 2017; Zhang et al., 2021; Namgung et al., 2024), and financial modeling (Nystrup et al., 2021). However, sparsity in clustering introduces a key challenge of interdependence between the two unsupervised tasks of feature selection and clustering. On one hand, with unknown sparsity, including too many noise features in the clustering algorithm hinders the results. On the other hand, it is challenging to pinpoint the signal features when the true cluster structure is unknown. This interplay motivates two-step or iterative algorithms that alternates between feature selection and clustering, leading to the identification of the true clusters.

**Sparse Clustering Model** We use the following Gaussian mixture model to study the role of sparsity in clustering. Let  $\mathbf{X} \in \mathbb{R}^{p \times n}$  be the data matrix with columns  $\mathbf{X}_1, \dots, \mathbf{X}_n$  independently generated as

$$\mathbf{X}_i \sim \mathcal{N}(\boldsymbol{\mu}_k^*, \boldsymbol{\Sigma}^*) \text{ if } i \in G_k^*, \quad (1)$$

where the non-random sets  $G_1^*, \dots, G_K^*$  partition  $\{1, \dots, n\}$ . The number of clusters  $K$  is assumed known. The unknown cluster centers are denoted by  $\boldsymbol{\mu}_1^*, \dots, \boldsymbol{\mu}_K^* \in \mathbb{R}^p$ , and  $\boldsymbol{\Sigma}^* \in \mathbb{R}^{p \times p}$  is the common covariance matrix. We consider both cases where  $\boldsymbol{\Sigma}^*$  is known and where it is unknown but  $\boldsymbol{\Omega}^* := (\boldsymbol{\Sigma}^*)^{-1}$  has a sparse structure. The goal is to recover  $G_1^*, \dots, G_K^*$ , treating  $\boldsymbol{\mu}_k^*$ 's and  $\boldsymbol{\Sigma}^*$  as nuisance parameters. We assume the existence of an unknown signal feature set

$$S_0 := \bigcup_{1 \leq k \neq l \leq K} \text{supp}(\boldsymbol{\Omega}^*(\boldsymbol{\mu}_k^* - \boldsymbol{\mu}_l^*)) \subset \{1, \dots, p\}, \quad (2)$$

which encodes the complete clustering signal. This assumption aligns with results from classification of two-class Gaussian mixtures, where the optimal decision boundary maximizing the signal-to-noise ratio is proportional to  $\boldsymbol{\Omega}^*(\boldsymbol{\mu}_1^* - \boldsymbol{\mu}_2^*)$  (Fan et al., 2013).

**Previous Two-Step Methods** Conventional dimension reduction, such as PCA (Ghosh and Chinnaian, 2002; Liu et al., 2003; Tamayo et al., 2007), can fail to capture a sparse clustering signal (Chang, 1983). Consequently, many methods adopt models such as (1) and (2) to perform feature selection guided by the clustering signal. They select features using multiple testing based on goodness-of-fit (Jin and Wang, 2016) or moments (Azizyan et al., 2013; Verzelen and Arias-Castro, 2017), model selection (Maugis et al., 2009; Raftery and Dean, 2006), sparse PCA (Löffler et al., 2022), merging algorithm (Banerjee et al., 2017), or an estimated sparse discriminating direction (defined in Section 3.1; Azizyan et al., 2015). Other relevant works include Bouveyron and Brunet-Saumard (2014); Brodinová et al. (2019); Kadir et al. (2014); Liu et al. (2023). Jin et al. (2017) show that, in certain regimes of signal strength and sparsity, accurate feature selection is not required for accurate clustering. Even et al. (2025) use data thinning (Leiner et al., 2025; Dharamshi et al., 2025) to decouple feature selection from clustering and achieves optimality among polynomial-time

clustering algorithms. They further show that the separation required for the success of their method differs from the minimax separation needed for optimal statistical performance without computational constraints.

**Previous Iterative Methods** Iterative methods repeatedly refine cluster assignments and model parameters estimates. Most methods alternate between clustering and regularized estimation of model parameters, such as feature weights (Chakraborty et al., 2023; Huo and Tseng, 2017; Li et al., 2018; Tsai and Chiu, 2008; Witten and Tibshirani, 2010; Yuan et al., 2024), cluster centers (Sun et al., 2012; Yi et al., 2014), and feature rankings (Arias-Castro and Pu, 2017; Zhang et al., 2020). Regularized EM algorithms follow the same principle: the E-step updates cluster assignments, while the M-step performs regularized estimation of sparse model parameters (Bouveyron et al., 2007; Dong et al., 2024; Fraley and Raftery, 2007; Fu et al., 2021; Guo et al., 2010; Pan and Shen, 2007; Wang and Zhu, 2008; Xie et al., 2008; Zhou et al., 2009). Notably, Cai et al. (2019) establish a minimax rate for the excess clustering risk based on estimating  $\beta^*$  from the training data using  $\ell_1$ -regularized EM. Sparse Bayesian hierarchical models (Tadesse et al., 2005; Yao et al., 2025) and sparse convex clustering (Chakraborty and Xu, 2023; Wang et al., 2018) also follow the iterative paradigm, as their fitting procedures, such as MCMC or ADMM, progressively refine parameter estimates and feature selection.

**Limitations of Existing Approaches** In each iteration of existing iterative methods, sparse model parameters are first estimated, which then define the clustering optimization problem. Estimation requires tuning sparsity-inducing regularization parameters, which is challenging in unsupervised settings and computationally heavy. However, across the computer science (Wilder et al., 2019; Bengio et al., 2021), operations research (Bertsimas

and Kallus, 2020; Elmachtoub and Grigas, 2022; Sadana et al., 2025), and statistics (Perdomo et al., 2020; Cutler et al., 2024) literature, it is recognized that when estimation supports a downstream task, prioritizing task quality over estimation accuracy is often preferable. This motivates an algorithm that avoids precise estimation of nuisance parameters and instead focuses on clustering quality.

**Our Contributions** SDP  $K$ -means is a minimax-optimal clustering algorithm for fixed  $p$  that bypasses cluster center estimation (Chen and Yang, 2021). We quantify its sensitivity to feature selection accuracy by deriving the minimax separation under varying feature subsets. Uniformly over all subsets  $S$ , SDP  $K$ -means restricted to  $S$  exactly recovers the clusters if the separation with respect to  $S \cap S_0$ , as defined in (8), exceeds  $\log n + (|S| \log p)/n + \sqrt{(|S| \log p)/n}$ . We show that it is minimax optimal in the regime where  $\frac{|S| \log p}{n} \lesssim \log n$ . This indicates that slight overestimation of  $S_0$  is not highly detrimental. Guided by this theory, we propose an iterative algorithm that alternates between feature selection and SDP  $K$ -means, where feature selection does not require precise estimation of nuisance parameters. Features are roughly selected by thresholding an estimate of the discriminating direction  $\beta^*$  (defined in Section 3.1), which guides  $S_0$  estimation but does not directly affect clustering. Based on the roughly estimated  $S_0$ , we run SDP  $K$ -means on a transformed dataset  $\Omega^* \mathbf{X}$  (innovated transformation; Fan and Lv, 2016), avoiding precise estimation of cluster centers or covariance matrix. To obtain the transformed dataset, we adapt a high-dimensional precision matrix estimation tool (Fan and Lv, 2016), estimating only the minimally required quantities and bypassing high-dimensional nuisance parameter estimation.

**Notations** We denote vectors and matrices by boldface letters, and their individual elements by the corresponding non-boldface letters. For a matrix  $\mathbf{A}$ , single and double subscripts

denote columns and (row, column) elements, respectively. A subscript may be a single index or an index set. For vectors not derived from a matrix, a subscript denotes an element or a sub-vector. If the vector or matrix already contains a subscript, we use parentheses to avoid ambiguity, for example,  $(\tilde{\mu}_1^*)_S$ . We write  $\mathbf{A} \geq 0$ ,  $\mathbf{A} > 0$ , and  $\mathbf{A} \succeq 0$  to denote elementwise nonnegativity, elementwise positivity, and positive semidefiniteness of a matrix, respectively. For a set  $S$ , let  $|S|$  denotes its cardinality. For an integer  $a > 0$ , let  $\mathbf{1}_a \in \mathbb{R}^a$  denote the *all-one vector*, and  $[a]$  denote  $\{1, \dots, a\}$ . For a set  $G_k \subset [n]$ , let  $\mathbf{1}_{G_k} \in \{0, 1\}^n$  denote the indicator vector that takes the value 1 at indices in  $G_k$  and 0 elsewhere.

## 2 THEORETICAL MOTIVATION

We first introduce SDP  $K$ -Means and highlight its limitations in high dimensions through the lens of minimax analysis.

**SDP  $K$ -means** The partition  $G_1, \dots, G_K$  maximizing the  $K$ -means objective is the solution of the following NP-hard mixed integer program (Peng and Wei, 2007; Zhuang et al., 2023):

$$\max_{\mathbf{H} \in \{0,1\}^{n \times K}} \langle \mathbf{X}^\top \boldsymbol{\Omega}^* \mathbf{X}, \mathbf{H} \mathbf{B} \mathbf{H}^\top \rangle, \text{ s.t. } \mathbf{H} \mathbf{1}_K = \mathbf{1}_n, \quad (3)$$

where the inner product denotes the Frobenius inner product,  $\mathbf{B} := \text{diag}(|G_1|, \dots, |G_K|)$ , and each row of  $\mathbf{H}$  is a one-hot cluster indicator, formally  $H_{i,k} := \mathbb{1}(\mathbf{X}_i \in G_k)$  for  $i \in [n]$  and  $k \in [K]$ . Appendix E.1 connects the objective (3) to the log likelihood function in the Gaussian mixture model. Since the change of variable  $\mathbf{Z} = \mathbf{H} \mathbf{B} \mathbf{H}^\top$  satisfies  $\mathbf{Z}^\top = \mathbf{Z}$ ,  $\mathbf{Z} \succeq 0$ ,  $\text{tr}(\mathbf{Z}) = K$ ,  $\mathbf{Z} \mathbf{1}_n = \mathbf{1}_n$ , and  $\mathbf{Z} \geq 0$ , we can lift  $\mathbf{Z}$  into the convex space and relax (3) into a semidefinite program:

$$\max_{\mathbf{Z} \in \mathbb{R}^{n \times n}} \langle \mathbf{X}^\top \boldsymbol{\Omega}^* \mathbf{X}, \mathbf{Z} \rangle \quad \text{s.t.} \quad \mathbf{Z}^\top = \mathbf{Z}, \quad \mathbf{Z} \succeq 0, \quad \text{tr}(\mathbf{Z}) = K, \quad \mathbf{Z} \mathbf{1}_n = \mathbf{1}_n, \quad \mathbf{Z} \geq 0. \quad (4)$$

The SDP  $K$ -means algorithm recovers cluster labels by applying spectral clustering to the solution of (4). When  $\Sigma^*$  is known to be  $\mathbf{I}_p$  and the dimensionality  $p$  is fixed, SDP  $K$ -means achieves the minimax separation under the exact cluster recovery loss (Chen and Yang, 2021), where the separation is defined as in (8) with  $S = [p]$ . The minimax separation  $\log n + \sqrt{(\log n)^2 + (Kp \log n)/n}$  increases with  $p$  at a square-root rate. This shows that any clustering method that does not adapt to sparsity, including SDP  $K$ -means, may fail in high-dimensional settings where  $p$  is comparable to or larger than  $n$ , unless the separation also scales quickly at the square-root rate with  $p$  — an assumption that can be very stringent for large  $p$ . This motivates us to modify the SDP  $K$ -means to incorporate sparsity in high dimensions and explore the corresponding separation rate.

**Minimax Separation under Sparsity** We study how the separation needed for SDP  $K$ -means to achieve exact recovery scales with sample size, ambient dimension, sparsity and estimation quality of  $S_0$ . We assume that  $\Sigma^*$  is known to be  $\sigma^2 \mathbf{I}_p$ . Given any variable subset  $S$ , consider SDP  $K$ -means restricted to  $S$ , which solves the SDP problem (4) over the subset  $S$ :

$$\max_{\mathbf{Z} \in \mathbb{R}^{n \times n}} \langle \mathbf{X}_{S,\cdot}^\top \mathbf{X}_{S,\cdot}, \mathbf{Z} \rangle \quad \text{s.t.} \quad \mathbf{Z}^\top = \mathbf{Z}, \quad \mathbf{Z} \succeq 0, \quad \text{tr}(\mathbf{Z}) = K, \quad \mathbf{Z} \mathbf{1}_n = \mathbf{1}_n, \quad \mathbf{Z} \geq 0, \quad (5)$$

and then obtain cluster labels by applying spectral clustering to the solution. The minimax analysis proceeds in two steps. First, we show that if the clustering signal (or separation) in  $S \cap S_0$ , defined in (8), exceeds a certain threshold explicitly depending on the sample size  $n$ , ambient dimension  $p$ , and subset size  $|S|$ , then exact recovery of cluster labels is possible with high probability. This high-probability event is established uniformly over all possible subsets  $S$ . Second, we identify the minimax optimal regime for our result. Together, these results reveal the role of sparsity in clustering difficulty. They also motivate our iterative

algorithm, which incorporates feature selection to address sparsity and solves a sequence of SDPs corresponding to the sequence of selected feature subsets.

We begin by specifying the problem setting. For each parameter tuple  $\boldsymbol{\theta} = (\boldsymbol{\mu}_1, \dots, \boldsymbol{\mu}_K, \mathbf{H})$ , with  $\boldsymbol{\mu}_k \in \mathbb{R}^p$  cluster centers and  $\mathbf{H} \in \{0, 1\}^{n \times K}$  cluster assignment matrix, let  $\mathbb{P}_{\boldsymbol{\theta}}$  be the corresponding joint distribution of  $n$  independent Gaussian random vectors. Each random vector has mean given by the assigned cluster center and covariance  $\sigma^2 \mathbf{I}_p$ . For all  $1 \leq k \neq l \leq K$ , we impose two restrictions on  $\boldsymbol{\mu}_k - \boldsymbol{\mu}_l$ . First, it has at most  $s$  nonzero entries. Second, its squared  $\ell_2$  norm exceeds a specified threshold  $\Delta^2$ . These conditions define the following Gaussian mixture distribution class:

$$\Theta(s, \Delta, K) := \mathcal{M}(s, \Delta, K) \times \mathcal{H}(K), \quad (6)$$

where  $\mathcal{M}(s, \Delta, K) := \{(\boldsymbol{\mu}_1, \dots, \boldsymbol{\mu}_K) : \boldsymbol{\mu}_k \in \mathbb{R}^p, \|\boldsymbol{\mu}_k - \boldsymbol{\mu}_l\|_2^2 \geq \Delta^2, \text{ for all } 1 \leq k \neq l \leq K,$

$$\cup_{k,l} \text{supp}(\boldsymbol{\mu}_k - \boldsymbol{\mu}_l) = S_0 \subset [p], |S_0| \leq s\},$$

$$\text{and } \mathcal{H}(K) := \{\mathbf{H} = (H_{i,k}) \in \{0, 1\}^{n \times K} : \sum_{k=1}^n H_{i,k} = 1 \text{ for all } i = 1, \dots, n\}.$$

For a given clustering algorithm  $\hat{\mathbf{H}} : \mathbb{R}^{p \times n} \rightarrow \mathcal{H}(K)$ , we assess its performance using the worst-case probability of exact cluster recovery over the distribution class  $\Theta(s, \Delta, K)$ :

$$\sup_{\boldsymbol{\theta} \in \Theta(s, \Delta, K)} \min_{\pi \in \mathcal{S}_K} \mathbb{P}_{\boldsymbol{\theta}}(\hat{\mathbf{H}}(\mathbf{X}) \neq \mathbf{H}), \quad (7)$$

where  $\mathcal{S}_K$  is the set of label permutations of  $[K]$ . For brevity, we omit  $\min_{\pi \in \mathcal{S}_K}$  henceforth.

Given a problem instance  $\boldsymbol{\theta}^* = (\boldsymbol{\mu}_1^*, \dots, \boldsymbol{\mu}_K^*, \mathbf{H}^*) \in \Theta(s, \Delta, K)$ , the true cluster assignment  $\mathbf{H}^*$  has one-to-one correspondence to the block-diagonal matrix  $\mathbf{Z}^* := \mathbf{H}^* \mathbf{B}^* (\mathbf{H}^*)^\top = \sum_{k=1}^K |G_k^*|^{-1} \mathbf{1}_{G_k^*} \mathbf{1}_{G_k^*}^\top$ , up to label permutations. Let the clustering signal (or separation) of a feature subset  $S$  be defined as

$$\Delta_{S \cap S_0}^2 := \min_{1 \leq k \neq l \leq K} \|(\boldsymbol{\mu}_l^* - \boldsymbol{\mu}_k^*)_{S \cap S_0}\|_2^2. \quad (8)$$

We next define the collection of feature subsets with sufficiently strong signal:

$$\begin{aligned} \mathcal{S} &:= \{S : S \subset [p], |S| \leq \sqrt{p}, \Delta_{S \cap S_0}^2 \gtrsim \bar{\Delta}_S^2\}, \quad (9) \\ \text{where } \bar{\Delta}_S^2 &:= \sigma^2 \left( \log n + \frac{|S| \log p}{m} + \sqrt{\frac{|S| \log p}{m}} \right), \\ \text{and } m &:= 2 \min_{1 \leq k \neq l \leq K} \left\{ \left( \frac{1}{|G_k^*|} + \frac{1}{|G_l^*|} \right)^{-1} \right\}. \end{aligned}$$

Theorem 1 gives the separation required for SDP  $K$ -means restricted to  $S$  to achieve exact recovery:

**Theorem 1.** *Assume that there exists a universal constant  $C_1$  such that  $m \geq C_1 n / \log n$ . Also assume  $|G_k^*| \geq 2$  for all  $k \in [K]$ . Let  $\hat{\mathbf{Z}}(S)$  be the solution of (5) corresponding to the subset  $S \in \mathcal{S}$ . Then*

$$\mathbb{P}(\hat{\mathbf{Z}}(S) = \mathbf{Z}^*, \forall S \in \mathcal{S}) \geq 1 - C_3 K / n,$$

where  $C_3 > 0$  is some constant.

The proof of Theorem 1 is presented in Appendix C. The stated probability in Theorem 1 holds uniformly over all feature subsets in  $\mathcal{S}$ . This ensures the validity of iterative algorithms that solve a sequence of SDPs corresponding to the sequence of selected feature subsets: once the algorithm lands on a ‘good’  $S$ , that step ensures accurate clustering. The assumption  $m \geq C_1 n / \log n$  prevents overly imbalanced clusters. Such conditions are essential for theoretical guarantees in clustering and are similarly imposed in previous works (Azizyan et al., 2013; Cai et al., 2019; Chen and Yang, 2021; Chen and Zhang, 2024; Jin and Wang, 2016; Löffler et al., 2021; Verzelen and Arias-Castro, 2017; Giraud and Verzelen, 2019; Royer, 2017; Even et al., 2025). By definition of  $m$  as a harmonic average, the restriction on  $m$  implies a restriction on the cluster size  $K \lesssim \log n$ , which allows a known  $K$  to diverge slowly

with  $n$ . This restriction is milder than most of the previous literature, which often requires  $K$  bounded above by a constant (Verzelen and Arias-Castro, 2017; Jin and Wang, 2016).

Next, we show the optimality of result in Theorem 1.

**Theorem 2.** *Consider the regime  $(s \log p)/n = o(1)$ . For  $n \geq 2$ , no clustering rule can guarantee exact recovery in the worst case over the class*

$$\overline{\Theta} := \Theta(s, C_4 \sigma^2 \log n, K),$$

with  $C_4$  some small positive constant. In other words,

$$\inf_{\hat{\mathbf{H}}: \mathbb{R}^{p \times n} \rightarrow \mathcal{H}(K)} \sup_{\boldsymbol{\theta} \in \overline{\Theta}} \mathbb{P}_{\boldsymbol{\theta}}(\hat{\mathbf{H}}(\mathbf{X}) \neq \mathbf{H}) \geq C_5,$$

with  $C_5$  a positive constant.

The proof of Theorem 2 is presented in Appendix D. Theorem 2 implies that no clustering rule can provide a worst-case guarantee of exact recovery across all subsets  $S$  whose signal strength is of order  $\sigma^2 \log n$ . Under the regime of  $(|S| \log p)/m \lesssim \log n$ , the separation condition in Theorem 1 (i.e., lower bound for  $\Delta_{S \cap S_0}^2$ ) is of order  $\log n$  and thus matches the bound in Theorem 2 up to a constant, demonstrating the minimax optimality of Theorem 1 result.

Theorems 1 and 2 also indicate that, in the sparse regime where  $|S_0| \ll p$ , feature selection can be critical for clustering accuracy. To see this, consider the simple scenario where  $K = 2$ ,  $|G_1^*| = |G_2^*|$  and  $(\boldsymbol{\mu}_1^* - \boldsymbol{\mu}_2^*)_{S_0} = \mu_0 \mathbf{1}_{|S_0|}$ . Then Theorems 1 and 2 prove that for any set  $S$  satisfying  $|S| \lesssim \sqrt{p}$  and  $|S| \lesssim (n \log n)/\log p$ , exact recovery is possible if and only if

$$|S \cap S_0| \mu_0^2 \gtrsim \log n + \frac{|S| \log p}{n} + \sqrt{\frac{|S| \log p}{n}} \asymp \log n.$$

This condition becomes very stringent if  $S$  is a very noisy estimate of  $S_0$  (i.e., missing too many signal variables). It also suggests that a slight overestimate of  $S_0$  may not be very

damaging. These motivate us to design an algorithm that incorporates some conservative feature selection method into clustering.

### 3 PROPOSED INNOVATED TRANSFORMATION-BASED ITERATIVE ALGORITHMS

We propose our algorithms under scenarios of known covariance (Section 3.1), which includes the settings of Theorems 1 and 2, and unknown covariance (Section 3.2). The algorithms are presented for  $K = 2$  for simplicity, although they naturally extend to larger  $K$ .

#### 3.1 Known Covariance Case

The success of feature selection hinges on signal strength. In the related but different problem of classification, it has been recognized (Fan et al., 2013, 2015) that the innovated transformation  $\tilde{\mathbf{X}} = \Omega^* \mathbf{X}$  maximally boosts the signal strength of important features for a general precision matrix that may not be identity matrix. See Fan et al. (2013) for detailed arguments and optimality study for the innovated transformation in Gaussian classification. Our algorithms work with the innovated transformation  $\tilde{\mathbf{X}}$  (or its estimate when  $\Omega^*$  unknown, in Section 3.2). It alternates between a feature selection and SDP  $K$ -Means, detailed below, with the complete procedure summarized in Algorithm 2.

**Feature Selection** As argued in Cai et al. (2019), Gaussian clustering is closely related to classification where the optimal rule is the Bayes rule with linear classification boundary  $\mathbf{x}^T \beta^*$  for a given test point  $\mathbf{x} \in \mathbb{R}^p$ . Here,  $\beta^* := \Omega^* (\mu_1^* - \mu_2^*)$ . It is seen that the magnitudes of entries in  $\beta^*$  reflect the feature importance. Motivated by this, we select features by

thresholding a rough estimate of  $\beta^*$ , used solely to guide feature selection without aiming for precise support recovery. Note that if the true clusters  $G_1^*$  and  $G_2^*$  were known,  $\beta^*$  can be accurately estimated by the sample mean difference  $\tilde{\mathbf{X}}_{G_1^*} - \tilde{\mathbf{X}}_{G_2^*}$ , where  $\tilde{\mathbf{X}}_{G_k^*} \in \mathbb{R}^p$  stands for the sample mean vector formed by columns of  $\tilde{\mathbf{X}}$  in cluster  $k = 1, 2$ .

However, in the clustering problems  $G_1^*$  and  $G_2^*$  are unknown. We propose to iteratively construct an estimate of  $\beta^*$  based on the previous step clustering result. Specifically, at iteration  $t$ , let the estimated cluster assignments from the previous step be  $\hat{G}_1^{t-1}$  and  $\hat{G}_2^{t-1}$ . We estimate  $\beta^*$  by the difference of empirical cluster centers:  $\hat{\beta}^t = \tilde{\mathbf{X}}_{\hat{G}_1^{t-1}} - \tilde{\mathbf{X}}_{\hat{G}_2^{t-1}}$ , and form the set of selected features in the current step as

$$\hat{S}^t := \left\{ j \in [p] : |\hat{\beta}_j^t| > \sqrt{\frac{2\omega_{jj}n \log(2p)}{|\hat{G}_1^{t-1}| \cdot |\hat{G}_2^{t-1}|}} \right\}. \quad (10)$$

We provide some intuition on the above proposed feature selection method. Note that if  $j \notin S_0$ , then  $\tilde{X}_{ji} \stackrel{i.i.d.}{\sim} \mathcal{N}(\tilde{\mu}_j, \omega_{jj})$ , where  $\omega_{jj}$  is the  $j$ th diagonal entry of  $\Omega^*$  and  $\tilde{\mu}_j$  is the mean value that is invariant to class label. For any data partition  $G_1 \cup G_2 = [n]$  and  $j \notin S_0$ , the  $j$ th entry of the mean difference vector  $\tilde{\mathbf{X}}_{G_1} - \tilde{\mathbf{X}}_{G_2}$  follows the distribution  $\mathcal{N}(0, (w_{jj}n)/(|G_1| \cdot |G_2|))$ . Then we can derive that for any  $\delta > 0$ , with probability at least  $1 - \delta$ ,

$$\max_{G_1, G_2} \max_{j \in S_0^c} \left| \sqrt{\frac{|G_1| \cdot |G_2|}{\omega_{jj}}} (\tilde{\mathbf{X}}_{G_1} - \tilde{\mathbf{X}}_{G_2})_j \right| \leq \sqrt{2n \log(2(p - |S_0|)/\delta)}, \quad (11)$$

by the Gaussian maximal inequality (see Appendix F.1 for details). Our threshold in (10) is slightly more conservative than the right-hand side of (11), reflecting the intuition that mild over-selection does not harm clustering, as formalized by Theorems 1 and 2.

**Clustering** At iteration  $t$ , the clustering step solves the reduced version of SDP-relaxed  $K$ -means problem (4), formulated with the selected variables  $\hat{S}^t$  and using the identity

---

**Algorithm 1** SDP  $K$ -means for  $K = 2$  : `clust`


---

**Require:** Transformed and truncated data matrix  $\tilde{\mathbf{X}}_{\hat{S}^t,:}$ , covariance sub-matrix  $\Sigma_{\hat{S}^t,\hat{S}^t}$

- 1:  $\hat{\mathbf{Z}}^t \leftarrow \arg \max_{\mathbf{Z} \in \mathbb{R}^{n \times n}} \langle \tilde{\mathbf{X}}_{\hat{S}^t,:}^\top, \Sigma_{\hat{S}^t,\hat{S}^t} \tilde{\mathbf{X}}_{\hat{S}^t,:}, \mathbf{Z} \rangle$   
s.t.  $\mathbf{Z}^\top = \mathbf{Z}$ ,  $\mathbf{Z} \succeq 0$ ,  $\text{tr}(\mathbf{Z}) = 2$ ,  $\mathbf{Z}\mathbf{1}_n = \mathbf{1}_n$ ,  $\mathbf{Z} \geq 0$
- 2:  $\hat{G}_1^t, \hat{G}_2^t \leftarrow$  spectral clustering result on  $\hat{\mathbf{Z}}^t$
- 3: Output  $\hat{G}_1^t, \hat{G}_2^t$

---

$\mathbf{X}^\top \boldsymbol{\Omega}^* \mathbf{X} = \tilde{\mathbf{X}}^\top \boldsymbol{\Sigma}^* \tilde{\mathbf{X}}$ . Since this step is reused in unknown covariance scenario, we present it as Algorithm 1. In line 1 of Algorithm 1,  $\tilde{\mathbf{X}}_{\hat{S}^t,:}^\top, \Sigma_{\hat{S}^t,\hat{S}^t} \tilde{\mathbf{X}}_{\hat{S}^t,:}$  is different from  $(\tilde{\mathbf{X}}^\top \boldsymbol{\Sigma}^* \tilde{\mathbf{X}})_{\hat{S}^t,\hat{S}^t}$ , and captures the key sparse clustering signal in  $\boldsymbol{\beta}^*$ . This argument is justified in Appendix E.2 and numerically evaluated in Appendix H.1.

---

**Algorithm 2** Iterative SDP  $K$ -means with known covariance

---

**Require:** Data matrix  $\mathbf{X}$ , population covariance matrix  $\Sigma$ , maximum number of iteration  $T$

- 1:  $\hat{G}_1^0, \hat{G}_2^0 \leftarrow$  cluster estimates obtained by running initial clustering (i.e., spectral clustering)  
on  $\mathbf{X}$
- 2:  $\tilde{\mathbf{X}} \leftarrow \Sigma^{-1} \mathbf{X}$
- 3:  $(\omega_{11}, \dots, \omega_{pp}) \leftarrow \text{diag}(\Sigma^{-1})$
- 4: **for**  $t = 1, 2, \dots, T$  **do**
- 5:    $\hat{\boldsymbol{\beta}}^t \leftarrow \frac{1}{|\hat{G}_1^{t-1}|} \sum_{i \in \hat{G}_1^{t-1}} \tilde{\mathbf{X}}_i - \frac{1}{|\hat{G}_2^{t-1}|} \sum_{i \in \hat{G}_2^{t-1}} \tilde{\mathbf{X}}_i$
- 6:    $\hat{S}^t \leftarrow \left\{ j \in [p] : |\hat{\beta}_j^t| > \sqrt{\frac{2\omega_{jj} n \log(2p)}{|\hat{G}_1^{t-1}| \cdot |\hat{G}_2^{t-1}|}} \right\}$   $\triangleright (10)$
- 7:    $\hat{G}_1^t, \hat{G}_2^t \leftarrow \text{clust}(\tilde{\mathbf{X}}_{\hat{S}^t,:}, \Sigma_{\hat{S}^t,\hat{S}^t})$   $\triangleright$  Algorithm 1
- 8: Output  $\hat{G}_1^T, \hat{G}_2^T$

---

## 3.2 Unknown Covariance Case

We now extend Algorithm 2 to the unknown covariance scenario by adapting the estimation idea proposed in Fan and Lv (2016). The major advantage of our estimation method is that it does not require estimating the full precision matrix  $\Omega^*$ . The main idea is that, at the  $t$ -th iteration, we form an estimate of  $\tilde{\mathbf{X}}$  directly based on the current cluster assignments without estimating  $\Omega^*$ , and then calculate the estimate  $\hat{S}^t$  in (10) using the estimated  $\tilde{\mathbf{X}}$ .

The direct estimation of  $\tilde{\mathbf{X}}$  is done via the Innovated Scalable Efficient Estimation (ISEE) procedure (Fan and Lv, 2016), originally developed for high-dimensional sparse precision matrix estimation. We modify it to selectively estimate only the required quantities for our algorithm, avoiding full precision matrix recovery, and use its theory to set the threshold for feature selection. Section 3.2.1 summarizes the ISEE procedure adapted as a subroutine in our method, followed by the full algorithm in Section 3.2.2.

### 3.2.1 Innovated Scalable Efficient Estimation (ISEE) Subroutine

The ISEE procedure is motivated by two key observations. First, the transformed vector  $\tilde{\mathbf{X}}_i = \Omega^* \mathbf{X}_i \in \mathbb{R}^p$  remains Gaussian, with  $\text{Cov}(\tilde{\mathbf{X}}_i) = \Omega^* \Sigma^* \Omega^* = \Omega^*$ . Without loss of generality, assume  $p$  is an even integer, consider a subset  $A \subset [p]$  of size 2, and assume  $i \in G_1^*$ . We consider the following decomposition of  $\tilde{\mathbf{X}}_{A,i}$  as the sum of deterministic mean part and mean-zero random noise vector:

$$\tilde{\mathbf{X}}_{A,i} = (\tilde{\boldsymbol{\mu}}_1^*)_A + \tilde{\mathcal{E}}_{A,i}, \quad (12)$$

Using the the conditional distribution property of multivariate Gaussian and Shur comple-

ment, we derive the following regression relationship between sub-vectors of  $\mathbf{X}_i \sim \mathcal{N}(\boldsymbol{\mu}_1^*, \boldsymbol{\Sigma}^*)$ :

$$\underbrace{\mathbf{X}_{A,i}}_{\text{response} \in \mathbb{R}^{|A|}} = \underbrace{(\boldsymbol{\mu}_1^*)_A + (\boldsymbol{\Omega}_{A,A}^*)^{-1} \boldsymbol{\Omega}_{A,A^c}^* (\boldsymbol{\mu}_1^*)_{A^c}}_{:= (\boldsymbol{\alpha}_1)_A \in \mathbb{R}^{|A|} \text{ (intercept)}} - \underbrace{(\boldsymbol{\Omega}_{A,A}^*)^{-1} \boldsymbol{\Omega}_{A,A^c}^*}_{\text{slope} \in \mathbb{R}^{|A| \times (p-|A|)}} \underbrace{\mathbf{X}_{A^c,i}}_{\text{predictor} \in \mathbb{R}^{p-|A|}} + \underbrace{\mathbf{E}_{A,i}}_{\text{residual} \in \mathbb{R}^{|A|}}, \quad (13)$$

where  $\mathbf{E}_{A,i} \sim \mathcal{N}(0, (\boldsymbol{\Omega}_{A,A}^*)^{-1})$ . Leveraging this relationship, the quantities in (12) can be further expressed as follows (Fan and Lv, 2016):

$$(\tilde{\boldsymbol{\mu}}_1^*)_A = \boldsymbol{\Omega}_{A,A}^* (\boldsymbol{\alpha}_1)_A \quad \text{and} \quad \tilde{\mathcal{E}}_{A,i} = \boldsymbol{\Omega}_{A,A}^* \mathbf{E}_{A,i}. \quad (14)$$

Appendix F.2 provides detailed derivations for (13) and (14). Since  $p - |A|$  can be comparable or larger than  $n$ , one may want to leverage the existing regularization method for fitting the regression model (13) to obtain sample estimates of  $\boldsymbol{\Omega}_{A,A}^*$ ,  $\mathbf{E}_{A,i}$  and  $(\boldsymbol{\alpha}_1)_A$ , which further yields plug-in estimate of  $\tilde{\mathbf{X}}_{A,i}$ . This process can be repeated for all  $A \in \mathcal{A}$  with  $\mathcal{A}$  a partition set of  $[p]$  consisting of sets of size 2. By combining estimates for  $\tilde{\mathbf{X}}_{A,i}$  for all  $A \in \mathcal{A}$ , we can form an estimate of the full matrix  $\tilde{\mathbf{X}}_{G_1^*} \in \mathbb{R}^{|G_1^*| \times p}$ .

A similar expression holds for  $i \in G_2^*$ , with  $\boldsymbol{\mu}_1^*$  and  $\boldsymbol{\alpha}_1$  replaced by  $\boldsymbol{\mu}_2^*$  and  $\boldsymbol{\alpha}_2$ , respectively. Following the same steps as described above, we can obtain the estimate of the submatrix  $\tilde{\mathbf{X}}_{G_2^*} \in \mathbb{R}^{|G_2^*| \times p}$ .

Two issues remain to be addressed. First, the true cluster labels are unknown. Second, we need an implementable ISEE subroutine. Since our algorithm is iterative by nature, we use the cluster assignments in the current iteration as the proxy for true cluster labels to implement the ISEE subroutine, and then update the estimates for  $\tilde{\mathbf{X}}$  and cluster assignments in the next iteration. We next explain the ISEE subroutine for a given pair of cluster assignment  $(G_1, G_2)$ .

**ISEE Subroutine** The feature indices  $[p]$  is partitioned into non-overlapping subsets  $A_1, \dots, A_L$ , each of size 2 if  $p$  is even. For odd  $p$ , we set the size of  $A_L$  to 3. The estimation

procedure is then applied for each feature subset, and the results are aggregated. Without loss of generality, we describe the steps for the subset  $A_1$ . Given the previous cluster estimates  $\hat{G}_1^{t-1}$  and  $\hat{G}_2^{t-1}$ , we treat  $\{(\mathbf{X}_{A_1^C, i}, \mathbf{X}_{A_1, i}) : i \in \hat{G}_1^{t-1}\}$  as (predictor, response) pair and apply off-the-shelf high-dimensional regression method (for example, lasso; Tibshirani, 1996) to estimate the intercept  $(\boldsymbol{\alpha}_1)_{A_1}$  and residuals  $\{\mathbf{E}_{A_1, i}\}_{i \in \hat{G}_1^{t-1}}$ . Similarly, using  $\{(\mathbf{X}_{A_1^C, i}, \mathbf{X}_{A_1, i}) : i \in \hat{G}_2^t\}$ , we estimate the corresponding  $(\boldsymbol{\alpha}_2)_{A_1}$  and residuals  $\{\mathbf{E}_{A_1, i}\}_{i \in \hat{G}_2^t}$  for cluster 2. To estimate  $\boldsymbol{\Omega}_{A_1, A_1}^*$ , we exploit the fact that the residuals  $\mathbf{E}_{A_1, i} \sim \mathcal{N}(0, (\boldsymbol{\Omega}_{A_1, A_1}^*)^{-1})$ , and use the inverse of the estimated sample covariance matrix of  $\mathbf{E}_{A_1, i}$  as an estimator. Then applying (14), we obtain the estimates for  $(\tilde{\boldsymbol{\mu}}_1^*)_{A_1}$ ,  $(\tilde{\boldsymbol{\mu}}_2^*)_{A_1}$ , and  $\{\tilde{\mathcal{E}}_{A_1, i}\}_{i=1}^n$ . Accordingly, using (12), we can estimate  $\{\tilde{\mathbf{X}}_{A, i}\}_{i=1}^n$ . Repeating this procedure for all subsets  $A_1, \dots, A_L$  and stacking the results yields estimates of  $\tilde{\boldsymbol{\mu}}_1^*$ ,  $\tilde{\boldsymbol{\mu}}_2^*$  and  $\tilde{\mathbf{X}}$ . In summary, we have the output  $\text{isee}(\mathbf{X}, \hat{G}_1^{t-1}, \hat{G}_2^{t-1}) = (\hat{\tilde{\boldsymbol{\mu}}}_1^t, \hat{\tilde{\boldsymbol{\mu}}}_2^t, \hat{\tilde{\mathbf{X}}}^t)$  in the  $t$ -th iteration. The full procedure is detailed in Algorithm 4 in Appendix F.2.

### 3.2.2 Full Algorithm with Iterative Feature Selection via ISEE

Given the ISEE subroutine, Algorithm 3 extends Algorithm 2 to the unknown covariance scenario. In the feature selection step, we threshold  $\hat{\tilde{\boldsymbol{\mu}}}_1^t - \hat{\tilde{\boldsymbol{\mu}}}_2^t$  obtained from ISEE subroutine, instead of  $\tilde{\mathbf{X}}_{\hat{G}_1^{t-1}} - \tilde{\mathbf{X}}_{\hat{G}_2^{t-1}}$ . In the clustering step, we replace  $\tilde{\mathbf{X}}_{\hat{S}^t, \cdot}$  with the estimated transformed data matrix  $\hat{\tilde{\mathbf{X}}}^t_{\hat{S}^t, \cdot}$ . We replace  $\boldsymbol{\Sigma}_{\hat{S}^t, \hat{S}^t}$  with the pooled sample covariance, combining the sample covariances of  $\mathbf{X}_{\hat{S}^t, \hat{G}_1^{t-1}}$  and  $\mathbf{X}_{\hat{S}^t, \hat{G}_2^{t-1}}$ . We leverage the convergence rate of the ISEE procedure (Fan and Lv, 2016) to guide the choice of threshold for  $\hat{\tilde{\boldsymbol{\mu}}}_1^t - \hat{\tilde{\boldsymbol{\mu}}}_2^t$ . Specifically, for each  $k \in \{1, 2\}$  and for each subset  $A_\ell$  with  $\ell \in \{1, \dots, L\}$ , under some regularity conditions (Fan and Lv, 2016), we have:

$$\|((\hat{\tilde{\boldsymbol{\mu}}}_1)_{A_\ell} - (\hat{\tilde{\boldsymbol{\mu}}}_2)_{A_\ell}) - ((\tilde{\boldsymbol{\mu}}_1^*)_{A_\ell} - (\tilde{\boldsymbol{\mu}}_2^*)_{A_\ell})\|_2 \lesssim C_6 \max\{(J \log p)/n, \sqrt{\log p/n}\}, \quad (15)$$

---

**Algorithm 3** Iterative SDP  $K$ -means with unknown covariance

---

**Require:** Data matrix  $\mathbf{X}$ , maximum number of iteration  $T$ 

- 1:  $\hat{G}_1^0, \hat{G}_2^0 \leftarrow$  cluster estimates obtained by running initial clustering (i.e., spectral clustering) on  $\mathbf{X}$
- 2: **for**  $t = 1, 2, \dots, T$  **do**
- 3:    $\hat{\boldsymbol{\mu}}_1^t, \hat{\boldsymbol{\mu}}_2^t, \hat{\mathbf{X}}^t \leftarrow \text{isee}(\mathbf{X}, \hat{G}_1^{t-1}, \hat{G}_2^{t-1})$  ▷ Algorithm 4
- 4:    $\hat{S}^t \leftarrow \left\{ j \in [p] : |(\hat{\boldsymbol{\mu}}_1^t - \hat{\boldsymbol{\mu}}_2^t)_j| > \sqrt{\log n \log p / n} \right\}$
- 5:    $\hat{\boldsymbol{\Sigma}}_{\hat{S}^t, \hat{S}^t} \leftarrow$  pooled covariance of covariances computed from  $\mathbf{X}_{\hat{S}^t, \hat{G}_1^{t-1}}$  and  $\mathbf{X}_{\hat{S}^t, \hat{G}_2^{t-1}}$
- 6:    $\hat{G}_1^t, \hat{G}_2^t \leftarrow \text{clust}(\hat{\mathbf{X}}_{\hat{S}^t, \cdot}, \hat{\boldsymbol{\Sigma}}_{\hat{S}^t, \hat{S}^t})$  ▷ Algorithm 1
- 7: Output  $\hat{G}_1^T, \hat{G}_2^T$

---

where  $J$  is the maximum number of nonzero off-diagonal entries per row of  $\boldsymbol{\Omega}^*$ , and  $C_6 = \|\boldsymbol{\Omega}_{A_\ell, A_\ell}^*\|_2 + \|(\hat{\boldsymbol{\alpha}}_1)_{A_\ell}\|_2 + \|(\hat{\boldsymbol{\alpha}}_2)_{A_\ell}\|_2$ . This bound comes from the convergence rates of  $\|\hat{\boldsymbol{\Omega}}_{A_\ell, A_\ell} - \boldsymbol{\Omega}_{A_\ell, A_\ell}^*\|_2$  and  $\|(\hat{\boldsymbol{\alpha}}_k)_{A_\ell} - (\boldsymbol{\alpha}_k)_{A_\ell}\|_2$  proved in Fan and Lv (2016). The detailed derivation is provided in Appendix F.2. In the standard sparse high-dimensional regime of  $J\sqrt{\log p/n} = o(1)$ , the term  $\sqrt{\log p/n}$  dominates the bound. Since ISEE only involves small submatrices of size  $2 \times 2$  or  $3 \times 3$ , the terms in  $C_6$  are bounded and contribute only constant factors. To account for these constants and avoid including too many noise features, we include a slowly diverging factor  $\sqrt{\log n}$  in our threshold. Combining all the pieces, we set the feature selection threshold as  $\sqrt{(\log n \log p)/n}$ . Appendix H.2 shows numerically that this feature selection is slightly more conservative than the direct extension of (10).

Table 1: Summary of Parameter Settings for (16).  $i, j \in [p]$ .

Covariance	$p$	$n$	Separation
known ( $\Sigma^* = \mathbf{I}_p$ )	50-5000	200	$\Delta^2 = 4^2, 5^2$
unknown ( $\Omega_{i,i}^* = 1$ , $\Omega_{i,i+1}^* = \Omega_{i+1,i}^* = \rho$ , $\Omega_{i,j}^* = 0$ o.w., $\rho \in \{0.2, 0.45\}$ )	50-400	500	$\Delta_{\Sigma^*}^2 = 3^2, 4^2$

## 4 NUMERICAL STUDIES

For simulations, the data are generated from Gaussian distributions with two symmetric clusters:

$$\mathbf{X}_i \stackrel{i.i.d.}{\sim} \mathcal{N}(\boldsymbol{\mu}^*, \Sigma^*), \quad i = 1, \dots, n/2, \quad \text{and} \quad \mathbf{X}_i \stackrel{i.i.d.}{\sim} \mathcal{N}(-\boldsymbol{\mu}^*, \Sigma^*), \quad i = n/2 + 1, \dots, n. \quad (16)$$

We fix  $S_0 = [10]$  and increase the ambient dimension  $p$ . We assign equal magnitude to all entries of  $\boldsymbol{\mu}_{S_0}^*$ , with the magnitude chosen so that the signal strength, measured Mahalanobis distance  $\Delta_{\Sigma^*} = 2\sqrt{(\boldsymbol{\mu}^*)^\top \boldsymbol{\Omega}^* \boldsymbol{\mu}^*} = \sqrt{(\boldsymbol{\beta}^*)^\top \Sigma^* \boldsymbol{\beta}^*}$ , remains constant as  $p$  increases. We evaluate performance using the mis-clustering rate, averaged over 200 independent replications. We set the number of iteration as  $T = 100$ , but used early stopping criterion. The details on this criterion, code implementation, and further information required for replicating our results are provided in Appendix G.1.

**Simulation under Known Covariance** We evaluate Algorithm 2 under the setting of line 1 of Table 1. We first compare non-sparse clustering methods, including spectral clustering (Han et al., 2023), hierarchical clustering, and SDP-relaxed  $K$ -means with all features (Chen and Yang, 2021), with Algorithm 2 initialized by each of them. Here, initialization refers

to a rough cluster assignment  $\hat{G}_1^0, \hat{G}_2^0$  used to guide the first feature selection step. Results in Figures 1-(a) and 1-(b) show that while the non-sparse methods fail to adapt to sparsity, Algorithm 2, when properly initialized, is robust to high-dimensional noise and effectively adapts to sparsity. Even moderately good initializations are sufficient, as evidenced by the improved performance of Algorithm 2 when initialized with spectral or SDP  $K$ -means clustering. In contrast, poor initializations can hinder the clustering performance, as reflected in the weaker performance of Algorithm 2 initialized by hierarchical clustering. Next, Figures 1-(c) and 1-(d) highlight the competitiveness of our approach against existing two-step and iterative sparse clustering approaches: influential feature PCA (IFPCA; Jin and Wang, 2016), sparse alternate similarity clustering (SAS; Arias-Castro and Pu, 2017), sparse  $K$ -means (SKM; Witten and Tibshirani, 2010) and CHIME (Cai et al., 2019). Details of these baseline methods are provided in Appendix G.2. Appendix H.1 presents results under non-isotropic covariances.

**Simulation under Unknown Covariance** Algorithm 3 is evaluated in the setting with a chain-graph sparse precision matrix with conditional correlation  $\rho \in \{0.2, 0.4\}$ , following the setup described in line 2 of Table 1. The results in Figure 2 show that our method outperforms other sparsity-aware clustering approaches. Appendix H.2 demonstrates the effectiveness of bypassing full precision matrix estimation. It also illustrates Algorithm 3 with an alternative feature selection threshold, demonstrating that an exact threshold is unnecessary and constant factors in thresholds are not a big concern. Appendix H.3 demonstrates the convergence of the iterative algorithm and shows that slight overestimation of  $S_0$  does not affect clustering performance.

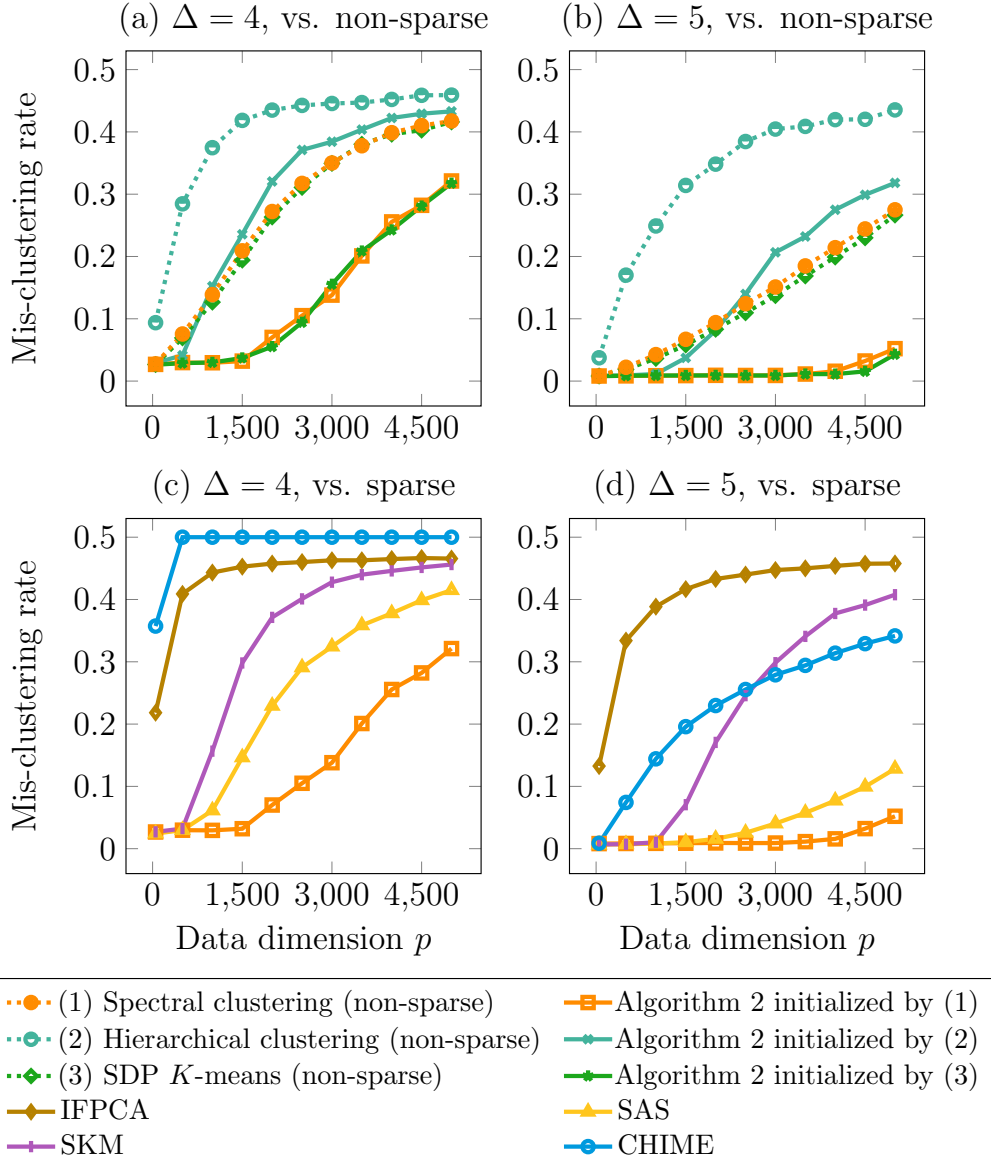


Figure 1: Mis-clustering rates of Algorithm 2 compared to non-sparse and sparse baselines.

The dotted lines (non-sparse methods) can also be interpreted as the mis-clustering rates of Algorithm 2 immediately after initialization, before any iteration. The settings are provided in line 1 of Table 1.

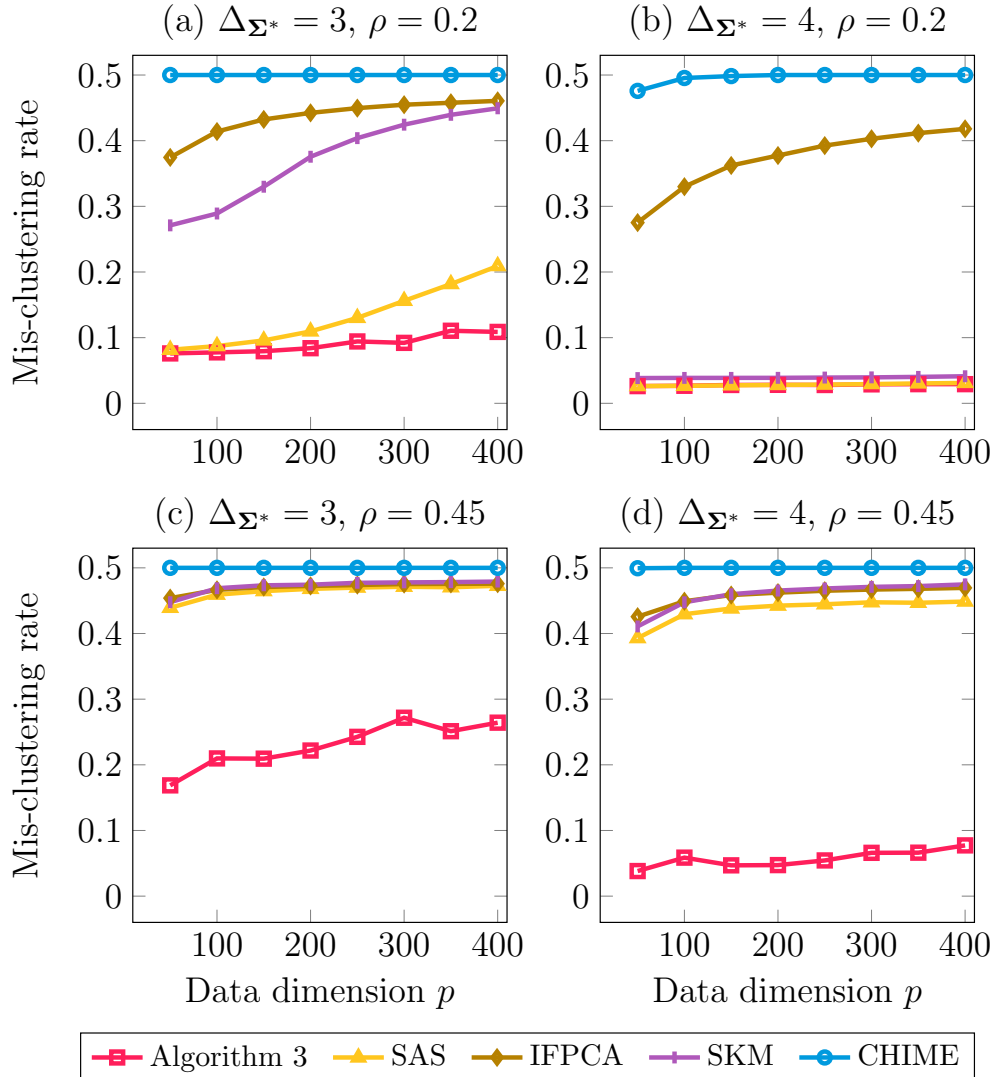


Figure 2: Mis-clustering rates of Algorithm 3, compared to other sparsity-aware baseline methods under unknown covariance scenario with varying conditional correlations. The settings follow the line 2 of Table 1.

**Application to Real Datasets** We apply Algorithm 2 to leukemia subtype clustering using gene expression data ( $n = 45$ ,  $p = 3571$ ; Golub et al., 1999) and Algorithm 3 to clustering pre-processed MNIST images of digits 1 and 7 ( $n = 1000$ ,  $p = 784$ ). The leukemia dataset, originally created by Golub et al. (1999), comprises 72 gene expression profiles of 3871 genes, obtained from bone marrow and peripheral blood samples of patients with two types of leukemia: acute myeloid leukemia (AML) and acute lymphoblastic leukemia (ALL). This dataset was previously analyzed by Jin and Wang (2016), and we used the data file available from their repository. To assess statistical performance, we performed stratified subsampling of 45 samples, repeating this procedure 100 times to compute the average clustering accuracy. The MNIST dataset consists of  $28 \times 28$  grayscale images of digits from 1 to 10. We trained a  $k$ -sparse autoencoder (Makhzani and Frey, 2013) on 30000 samples spanning all digits, using a sparsity parameter of  $k = 20$ . The trained model was then applied to 8640 test images of digits ‘1’ and ‘7’, converting them into 784-dimensional sparse representations. We applied stratified sub-sampling by selecting  $n = 1000$  images from the 8640 test samples, applied the clustering algorithms to distinguish digits ‘1’ and ‘7’, repeated the process 100 times, and reported the average clustering accuracy. We compared Algorithms 2 and 3 with Sparse  $K$ -means (SKM; Witten and Tibshirani, 2010), Influential Feature PCA (IFPCA; Jin and Wang, 2016), and Sparse Alternate Similarity clustering (SAS; Arias-Castro and Pu, 2017). We do not report the performance of CHIME (Cai et al., 2019) in this real-data analysis, as the original paper does not share the implemented code for initializing cluster centers and covariance, and unlike in simulations, there is no obvious choice of initialization for real datasets. Details of the baseline methods are provided in Appendix G.2. For the  $k$ -sparse autoencoder, we used the authors’ implementation available on their GitHub repository. The results in Table 2 show that our methods consistently outperform baseline approaches.

Table 2: Clustering accuracy on the leukemia gene expression dataset and the MNIST dataset.

	Our method	IFPCA	SKM	SAS
Leukemia	<b>0.93</b>	0.84	0.79	0.87
MNIST	<b>0.94</b>	0.61	0.57	0.56

**Additional Simulations** Appendix H.4 demonstrates that our algorithms maintain strong clustering accuracy under mild violations of the assumptions of Gaussianity, covariance homogeneity, and exact sparsity of model parameters. For scalability, while our focus is on the high-dimensional, low-sample-size regime, real-world datasets may involve much larger samples. For larger  $n$ , we recommend approximate solvers (Zhuang et al., 2022, 2024) tailored for the SDP step. Appendix H.5 demonstrates that those approximate solvers scale our algorithms up to  $n = 100,000$ . Finally, we compare our methods to subspace clustering algorithms that extracts, rather than selects, features lying in low-dimensional subspaces (Soltanolkotabi et al., 2014; Wang and Xu, 2016; Huang and Gu, 2025). Specifically, Appendix H.6 shows that our method excels the Johnson–Lindenstrauss transform-based  $K$ -means (Boutsidis et al., 2010) in sparse settings.

## 5 DISCUSSION

Under a known isotropic covariance, we derived the minimax separation required for exact cluster recovery across varying signal feature subset estimates, achieved by a modified SDP  $K$ -means. This result highlights the critical role of feature selection in sparse clustering while showing that slight overselection of features is not detrimental. Building on this

insight, we proposed iterative algorithms that integrate feature selection into SDP  $K$ -means, avoiding the need to precisely estimate nuisance parameters such as cluster centers and the covariance matrix (which may not be the identity). There are two potential directions for future research: i) establish theoretical guarantees that our algorithm can identify a subset with sufficient separation, and ii) extend our minimax framework to the general case of an unknown covariance matrix.

## References

Adamczak, R. (2008). A tail inequality for suprema of unbounded empirical processes with applications to markov chains. *Electronic Journal of Probability*, 13:1000–1034.

Arias-Castro, E. and Pu, X. (2017). A simple approach to sparse clustering. *Computational Statistics & Data Analysis*, 105:217–228.

Azizyan, M., Singh, A., and Wasserman, L. (2013). Minimax theory for high-dimensional Gaussian mixtures with sparse mean separation. In *Advances in Neural Information Processing Systems (NeurIPS)*.

Azizyan, M., Singh, A., and Wasserman, L. (2015). Efficient sparse clustering of high-dimensional non-spherical gaussian mixtures. In *International Conference on Artificial Intelligence and Statistics (AISTATS)*.

Banerjee, T., Mukherjee, G., and Radchenko, P. (2017). Feature screening in large scale cluster analysis. *Journal of Multivariate Analysis*, 161:191–212.

Bengio, Y., Lodi, A., and Prouvost, A. (2021). Machine learning for combinatorial optimi-

mization: A methodological tour d'horizon. *European Journal of Operational Research*, 290(2):405–421.

Bertsimas, D. and Kallus, N. (2020). From predictive to prescriptive analytics. *Management Science*, 66(3):1025–1044.

Bing, X., Bunea, F., and Wegkamp, M. (2020). Optimal estimation of sparse topic models. *Journal of Machine Learning Research*, 21(177):1–45.

Boucheron, S., Lugosi, G., and Massart, P. (2016). *Concentration Inequalities: A Nonasymptotic Theory of Independence*. Oxford University Press, Oxford New York, NY.

Boutsidis, C., Zouzias, A., and Drineas, P. (2010). Random projections for k-means clustering. In *Advances in Neural Information Processing Systems (NeurIPS)*.

Bouveyron, C. and Brunet-Saumard, C. (2014). Discriminative variable selection for clustering with the sparse Fisher-EM algorithm. *Computational Statistics*, 29(3):489–513.

Bouveyron, C., Girard, S., and Schmid, C. (2007). High-dimensional data clustering. *Computational Statistics & Data Analysis*, 52(1):502–519.

Brodinová, Š., Filzmoser, P., Ortner, T., Breiteneder, C., and Rohm, M. (2019). Robust and sparse k-means clustering for high-dimensional data. *Advances in Data Analysis and Classification*, 13(4):905–932.

Cai, T. T., Ma, J., and Zhang, L. (2019). CHIME: Clustering of high-dimensional Gaussian mixtures with EM algorithm and its optimality. *The Annals of Statistics*, 47(3):1234–1267.

Cai, T. T. and Zhang, L. (2019). High dimensional linear discriminant analysis: Optimality,

adaptive algorithm and missing data. *Journal of the Royal Statistical Society Series B: Statistical Methodology*, 81(4):675–705.

Chakraborty, S. and and Xu, J. (2023). Biconvex clustering. *Journal of Computational and Graphical Statistics*, 32(4):1524–1536.

Chakraborty, S., Paul, D., and Das, S. (2023). On consistent entropy-regularized k-means clustering with feature weight learning: Algorithm and statistical analyses. *IEEE Transactions on Cybernetics*, 53(8):4779–4790.

Chang, W.-C. (1983). On using principal components before separating a mixture of two multivariate normal distributions. *Journal of the Royal Statistical Society. Series C (Applied Statistics)*, 32(3):267–275.

Chen, X. and Yang, Y. (2021). Cutoff for exact recovery of gaussian mixture models. *IEEE Transactions on Information Theory*, 67(6):4223–4238.

Chen, X. and Zhang, A. Y. (2024). Achieving optimal clustering in Gaussian mixture models with anisotropic covariance structures. *Advances in Neural Information Processing Systems (NeurIPS)*.

Cunningham, J. P. and Yu, B. M. (2014). Dimensionality reduction for large-scale neural recordings. *Nature Neuroscience*, 17(11):1500–1509.

Curtis, C., Shah, S. P., Chin, S.-F., Turashvili, G., Rueda, O. M., Dunning, M. J., Speed, D., Lynch, A. G., Samarajiwa, S., Yuan, Y., Gräf, S., Ha, G., Haffari, G., Bashashati, A., Russell, R., McKinney, S., Langerød, A., Green, A., Provenzano, E., Wishart, G., Pinder, S., Watson, P., Markowetz, F., Leigh Murphy, Ellis, I., Purushotham, A., Børresen-Dale,

A.-L., Brenton, J. D., Tavaré, S., Caldas, C., and Aparicio, S. (2012). The genomic and transcriptomic architecture of 2,000 breast tumours reveals novel subgroups. *Nature*, 486(7403):346–352.

Cutler, J., Díaz, M., and Drusvyatskiy, D. (2024). Stochastic approximation with decision-dependent distributions: Asymptotic normality and optimality. *Journal of Machine Learning Research*, 25(90):1–49.

Dharamshi, A., Neufeld, A., Motwani, K., Gao, L. L., Witten, D., and Bien, J. (2025). Generalized data thinning using sufficient statistics. *Journal of the American Statistical Association*, 120(549):511–523.

Dong, W., Xu, C., Xie, J., and Tang, N. (2024). Tuning-free sparse clustering via alternating hard-thresholding. *Journal of Multivariate Analysis*, 203:105330.

Donoho, D. and Jin, J. (2004). Higher criticism for detecting sparse heterogeneous mixtures. *The Annals of Statistics*, 32(3):962–994.

Elmachtoub, A. N. and Grigas, P. (2022). Smart “Predict, then Optimize”. *Management Science*, 68(1):9–26.

Even, B., Giraud, C., and Verzelen, N. (2025). Computational lower bounds in latent models: Clustering, sparse-clustering, biclustering. *arXiv preprint arXiv:2506.13647*.

Fan, Y., Jin, J., and Yao, Z. (2013). Optimal classification in sparse Gaussian graphic model. *The Annals of Statistics*, 41(5):2537–2571.

Fan, Y., Kong, Y., Li, D., and Zheng, Z. (2015). Innovated interaction screening for high-dimensional nonlinear classification. *The Annals of Statistics*, 43(3).

Fan, Y. and Lv, J. (2016). Innovated scalable efficient estimation in ultra-large Gaussian graphical models. *The Annals of Statistics*, 44(5):2098–2126.

Fraley, C. and Raftery, A. E. (2007). Bayesian regularization for normal mixture estimation and model-based clustering. *Journal of Classification*, 24(2):155–181.

Friedman, J., Hastie, T., and Tibshirani, R. (2008). Sparse inverse covariance estimation with the graphical lasso. *Biostatistics*, 9(3):432–441.

Fu, Y., Liu, X., Sarkar, S., and Wu, T. (2021). Gaussian mixture model with feature selection: An embedded approach. *Computers & Industrial Engineering*, 152:107000.

Ghosh, D. and Chinnaian, A. M. (2002). Mixture modelling of gene expression data from microarray experiments. *Bioinformatics*, 18(2):275–286.

Giraud, C. and Verzelen, N. (2019). Partial recovery bounds for clustering with the relaxed  $K$ -means. *Mathematical Statistics and Learning*, 1(3):317–374.

Golub, T. R., Slonim, D. K., Tamayo, P., Huard, C., Gaasenbeek, M., Mesirov, J. P., Coller, H., Loh, M. L., Downing, J. R., Caligiuri, M. A., Bloomfield, C. D., and Lander, E. S. (1999). Molecular classification of cancer: Class discovery and class prediction by gene expression monitoring. *Science*, 286(5439):531–537.

Guo, J., Levina, E., Michailidis, G., and Zhu, J. (2010). Pairwise variable selection for high-dimensional model-based clustering. *Biometrics*, 66(3):793–804.

Han, X., Tong, X., and Fan, Y. (2023). Eigen selection in spectral clustering: A theory-guided practice. *Journal of the American Statistical Association*, 118(541):109–121.

He, Y., Tang, X., Huang, J., Ren, J., Zhou, H., Chen, K., Liu, A., Shi, H., Lin, Z., Li, Q., Aditham, A., Ounadjela, J., Grody, E. I., Shu, J., Liu, J., and Wang, X. (2021). ClusterMap for multi-scale clustering analysis of spatial gene expression. *Nature Communications*, 12(1):5909.

Huang, C. and Gu, Y. (2025). Minimax-optimal dimension-reduced clustering for high-dimensional nonspherical mixtures. *arXiv preprint arXiv:2502.02580*.

Huo, Z. and Tseng, G. (2017). Integrative sparse K-means with overlapping group lasso in genomic applications for disease subtype discovery. *The Annals of Applied Statistics*, 11(2):1011–1039.

James, G., Witten, D., Hastie, T., and Tibshirani, R. (2013). *An Introduction to Statistical Learning: with Applications in R*. Springer, New York, 1st ed. edition.

Javanmard, A. and Mirrokni, V. (2023). Anonymous learning via look-alike clustering: A precise analysis of model generalization. In *Advances in Neural Information Processing Systems (NeurIPS)*.

Jin, J., Ke, Z. T., and Wang, W. (2017). Phase transitions for high dimensional clustering and related problems. *The Annals of Statistics*, 45(5):2151–2189.

Jin, J. and Wang, W. (2016). Influential features pca for high dimensional clustering. *The Annals of Statistics*, 44(6):2323–2359.

Kadir, S. N., Goodman, D. F. M., and Harris, K. D. (2014). High-dimensional cluster analysis with the masked EM algorithm. *Neural Computation*, 26(11):2379–2394.

Kim, H., Kim, H., and De Veciana, G. (2024). Clustered federated learning via gradient-based partitioning. In *International Conference on Machine Learning (ICML)*.

Laurent, B. and Massart, P. (2000). Adaptive estimation of a quadratic functional by model selection. *The Annals of Statistics*, 28(5):1302–1338.

Leiner, J., Duan, B., Wasserman, L., and Ramdas, A. (2025). Data Fission: Splitting a Single Data Point. *Journal of the American Statistical Association*, 120(549):135–146.

Leung, K., Mohammadi, A., Ryu, W. S., and Nemenman, I. (2016). Stereotypical escape behavior in *caenorhabditis elegans* allows quantification of effective heat stimulus level. *PLOS Computational Biology*, 12(12):e1005262.

Li, R., Chang, X., Wang, Y., and Xu, Z. (2018). Sparse k-means with  $\ell_\infty/\ell_0$  penalty for high-dimensional data clustering. *Statistica Sinica*.

Liu, J., Zhang, J., Palumbo, M., and Lawrence, C. (2003). Bayesian clustering with variable and transformation selections. *Bayesian Statistics*, 7:249–275.

Liu, R. G. and Frank, M. J. (2022). Hierarchical clustering optimizes the tradeoff between compositionality and expressivity of task structures for flexible reinforcement learning. *Artificial Intelligence*, 312:103770.

Liu, T., Lu, Y., Zhu, B., and Zhao, H. (2023). Clustering high-dimensional data via feature selection. *Biometrics*, 79(2):940–950.

Löffler, M., Wein, A. S., and Bandeira, A. S. (2022). Computationally efficient sparse clustering. *Information and Inference: A Journal of the IMA*, 11(4):1255–1286.

Löffler, M., Zhang, A. Y., and Zhou, H. H. (2021). Optimality of spectral clustering in the Gaussian mixture model. *The Annals of Statistics*, 49(5):2506–2530.

Lu, Y. Y., Lv, J., Fuhrman, J. A., and Sun, F. (2017). Towards enhanced and interpretable clustering/classification in integrative genomics. *Nucleic Acids Research*, 45(20):e169.

Makhzani, A. and Frey, B. (2013). K-Sparse autoencoders. In *International Conference on Learning Representations (ICLR)*.

Maugis, C., Celeux, G., and Martin-Magniette, M.-L. (2009). Variable selection for clustering with gaussian mixture models. *Biometrics*, 65(3):701–709.

McIlhagga, W. (2016). Penalized: A MATLAB toolbox for fitting generalized linear models with penalties. *Journal of Statistical Software*, 72:1–21.

Mishra, S., Gordon, B. A., Su, Y., Christensen, J., Friedrichsen, K., Jackson, K., Hornbeck, R., Balota, D. A., Cairns, N. J., Morris, J. C., Ances, B. M., and Benzinger, T. L. S. (2017). AV-1451 PET imaging of tau pathology in preclinical Alzheimer disease: Defining a summary measure. *NeuroImage*, 161:171–178.

Namgung, J. Y., Mun, J., Park, Y., Kim, J., and Park, B.-y. (2024). Sex differences in autism spectrum disorder using class imbalance adjusted functional connectivity. *NeuroImage*, 304:120956.

Nystrup, P., Kolm, P. N., and Lindström, E. (2021). Feature selection in jump models. *Expert Systems with Applications*, 184:115558.

Pan, W. and Shen, X. (2007). Penalized model-based clustering with application to variable selection. *Journal of Machine Learning Research*, 8(41):1145–1164.

Park, Y.-G., Kwon, Y. W., Koh, C. S., Kim, E., Lee, D. H., Kim, S., Mun, J., Hong, Y.-M., Lee, S., Kim, J.-Y., Lee, J.-H., Jung, H. H., Cheon, J., Chang, J. W., and Park, J.-U. (2024). In-vivo integration of soft neural probes through high-resolution printing of liquid electronics on the cranium. *Nature Communications*, 15(1):1772.

Peng, J. and Wei, Y. (2007). Approximating K-means-type clustering via semidefinite programming. *SIAM Journal on Optimization*, 18(1):186–205.

Perdomo, J., Zrnic, T., Mendler-Dünner, C., and Hardt, M. (2020). Performative Prediction. In *International Conference on Machine Learning (ICML)*, pages 7599–7609. PMLR.

Raftery, A. E. and Dean, N. (2006). Variable selection for model-based clustering. *Journal of the American Statistical Association*, 101(473):168–178.

Royer, M. (2017). Adaptive clustering through semidefinite programming. In *Advances in Neural Information Processing Systems (NeurIPS)*.

Sadana, U., Chenreddy, A., Delage, E., Forel, A., Frejinger, E., and Vidal, T. (2025). A survey of contextual optimization methods for decision-making under uncertainty. *European Journal of Operational Research*, 320(2):271–289.

Soltanolkotabi, M., Elhamifar, E., and Candès, E. J. (2014). Robust subspace clustering. *The Annals of Statistics*, 42(2):669–699.

Sun, D., Toh, K.-C., Yuan, Y., and Zhao, X.-Y. (2020). SDPNAL+: A Matlab software for semidefinite programming with bound constraints (version 1.0). *Optimization Methods and Software*, 35(1):87–115.

Sun, W., Wang, J., and Fang, Y. (2012). Regularized k-means clustering of high-dimensional data and its asymptotic consistency. *Electronic Journal of Statistics*, 6:148–167.

Tadesse, M. G., , Naijun, S., and and Vannucci, M. (2005). Bayesian Variable Selection in Clustering High-Dimensional Data. *Journal of the American Statistical Association*, 100(470):602–617.

Tamayo, P., Scanfeld, D., Ebert, B. L., Gillette, M. A., Roberts, C. W. M., and Mesirov, J. P. (2007). Metagene projection for cross-platform, cross-species characterization of global transcriptional states. *Proceedings of the National Academy of Sciences*, 104(14):5959–5964.

Tibshirani, R. (1996). Regression shrinkage and selection via the lasso. *Journal of the Royal Statistical Society. Series B (Methodological)*, 58(1):267–288.

Tibshirani, R., Walther, G., and Hastie, T. (2001). Estimating the number of clusters in a data set via the gap statistic. *Journal of the Royal Statistical Society Series B: Statistical Methodology*, 63(2):411–423.

Tsai, C.-Y. and Chiu, C.-C. (2008). Developing a feature weight self-adjustment mechanism for a k-means clustering algorithm. *Computational Statistics & Data Analysis*, 52(10):4658–4672.

Van Der Vaart, A. W. and Wellner, J. A. (2023). *Weak Convergence and Empirical Processes: With Applications to Statistics*. Springer Series in Statistics. Springer International Publishing, Cham.

Vershynin, R. (2012). Introduction to the non-asymptotic analysis of random matrices. In Kutyniok, G. and Eldar, Y. C., editors, *Compressed Sensing: Theory and Applications*, pages 210–268. Cambridge University Press, Cambridge.

Vershynin, R. (2018). *High-Dimensional Probability: An Introduction with Applications in Data Science*. Cambridge University Press, Cambridge ; New York, NY, 1st edition edition.

Verzelen, N. and Arias-Castro, E. (2017). Detection and feature selection in sparse mixture models. *The Annals of Statistics*, 45(5):1920–1950.

Wang, B., Zhang, Y., Sun, W. W., and Fang, Y. (2018). Sparse convex clustering. *Journal of Computational and Graphical Statistics*, 27(2):393–403.

Wang, S. and Zhu, J. (2008). Variable selection for model-based high-dimensional clustering and its application to microarray data. *Biometrics*, 64(2):440–448.

Wang, Y.-X. and Xu, H. (2016). Noisy sparse subspace clustering. *Journal of Machine Learning Research*, 17(12):1–41.

Wilder, B., Dilkina, B., and Tambe, M. (2019). Melding the Data-Decisions Pipeline: Decision-Focused Learning for Combinatorial Optimization. In *AAAI Conference on Artificial Intelligence*.

Witten, D. M. and Tibshirani, R. (2010). A framework for feature selection in clustering. *Journal of the American Statistical Association*, 105(490):713–726.

Wu, R., Linjun, Z., and and Tony Cai, T. (2023). Sparse topic modeling: Computational efficiency, near-optimal algorithms, and statistical inference. *Journal of the American Statistical Association*, 118(543):1849–1861.

Xie, B., Pan, W., and Shen, X. (2008). Variable selection in penalized model-based clustering via regularization on grouped parameters. *Biometrics*, 64(3):921–930.

Yao, D., Xie, F., and Xu, Y. (2025). Bayesian sparse gaussian mixture model for clustering in high dimensions. *Journal of Machine Learning Research*, 26(21):1–50.

Yi, J., Zhang, L., Wang, J., Jin, R., and Jain, A. (2014). A single-pass algorithm for efficiently recovering sparse cluster centers of high-dimensional data. In *International Conference on Machine Learning (ICML)*.

Yuan, Z., Chen, J., Qiu, H., Wang, H., and Huang, Y. (2024). Adaptive sufficient sparse clustering by controlling false discovery. *Statistics and Computing*, 34(6):1–36.

Zhang, Y., Wu, W., Toll, R. T., Naparstek, S., Maron-Katz, A., Watts, M., Gordon, J., Jeong, J., Astolfi, L., Shpigel, E., Longwell, P., Sarhadi, K., El-Said, D., Li, Y., Cooper, C., Chin-Fatt, C., Arns, M., Goodkind, M. S., Trivedi, M. H., Marmar, C. R., and Etkin, A. (2021). Identification of psychiatric disorder subtypes from functional connectivity patterns in resting-state electroencephalography. *Nature Biomedical Engineering*, 5(4):309–323.

Zhang, Z., Lange, K., and Xu, J. (2020). Simple and scalable sparse k-means clustering via feature ranking. In *Advances in Neural Information Processing Systems (NeurIPS)*.

Zhou, H., Pan, W., and Shen, X. (2009). Penalized model-based clustering with unconstrained covariance matrices. *Electronic Journal of Statistics*, 3:1473–1496.

Zhuang, Y., Chen, X., and Yang, Y. (2022). Sketch-and-lift: Scalable subsampled semidefinite program for k-means clustering. In *International Conference on Artificial Intelligence and Statistics (AISTATS)*.

Zhuang, Y., Chen, X., and Yang, Y. (2023). Likelihood adjusted semidefinite programs for clustering heterogeneous data. In *International Conference on Machine Learning (ICML)*.

Zhuang, Y., Chen, X., Yang, Y., and Zhang, R. Y. (2024). Statistically optimal K-means clustering via nonnegative low-rank semidefinite programming. In *International Conference on Learning Representations (ICLR)*.

## A OVERVIEW OF APPENDIX

This supplementary material provides the technical proofs deferred in the main text, along with some additional results of interest. The content is organized as follows:

- Appendix B contains the technical lemmas and definitions used in the proof of Theorem 1.
- Appendix C provides the proof of the separation bound for exact recovery by semidefinite relaxation of  $K$ -means, as presented in Theorem 1.
- Appendix D proves the minimax lower bound for exact recovery, as presented in Theorem 2.
- Appendix E provides additional details on the SDP objectives deferred from Sections 2 and 3.1, including their derivation and how they capture the sparse clustering signal.
- Appendix F provides an omitted details for the iterative algorithms, which were deferred from Sections 3.1 and 3.2.1.
- Appendix G provides additional information on the numerical studies presented in Section 4.

## B TECHNICAL LEMMAS AND DEFINITIONS

This section presents technical lemmas and definitions that are used throughout the main proofs, beginning the tail bounds for the chi-square distribution.

**Lemma 3** (Lemma 1 of Laurent and Massart 2000). *If  $Z$  has a chi-square distribution with  $p$  degrees of freedom, then for all  $t > 0$ , we have*

$$\mathbb{P}(Z \geq p + 2\sqrt{pt} + 2t) \leq e^{-t}, \quad \text{and} \quad \mathbb{P}(Z \leq p - 2\sqrt{pt}) \leq e^{-t}.$$

Before presenting the next two lemmas, we formally define the sub-exponential norm.

**Definition 4.** *Let  $\psi_1(x) := e^x - 1$ . The sub-exponential norm of a random variable  $X$ , denoted by  $\|X\|_{\psi_1}$ , is defined as*

$$\|X\|_{\psi_1} := \inf \left\{ \lambda > 0 : \mathbb{E} \left[ \psi_1 \left( \frac{|X|}{\lambda} \right) \right] \leq 1 \right\}.$$

Using this definition, Lemma 5 provides an upper bound on the subexponential norm of a chi-square random variable.

**Lemma 5** (Lemma VIII.2 of Chen and Yang 2021). *Let  $\mathbf{X}_1, \mathbf{X}_2 \stackrel{i.i.d.}{\sim} \mathcal{N}(0, I_q)$ . Then there exists a constant  $C > 0$  such that*

$$\|\|\mathbf{X}_1\|_2^2 - q\|_{\psi_1} + \|\langle \mathbf{X}_1, \mathbf{X}_2 \rangle\|_{\psi_1} \leq C\sqrt{q}.$$

Next, Lemma 6 provides a maximal inequality for sub-exponential norm.

**Lemma 6** (Lemma 2.2.2 of Van Der Vaart and Wellner 2023). *For random variables  $X_1, \dots, X_m$ , there exists a constant  $C_{\psi_1}$  such that*

$$\left\| \max_{1 \leq i \leq m} X_i \right\|_{\psi_1} \leq C_{\psi_1} \log(m+1) \max_{1 \leq i \leq m} \|X_i\|_{\psi_1}.$$

Next, Lemma 7 provides an upper bound on the  $\ell_2$  operator norm of an  $m \times n$  random matrix with i.i.d. Gaussian entries.

**Lemma 7** (Corollary 5.35 of Vershynin 2012). *Let  $\mathbf{A} \in \mathbb{R}^{m \times n}$  have i.i.d.  $\mathcal{N}(0, \sigma^2)$  entries. Then, for any  $t > 0$ , we have*

$$\mathbb{P}(\|\mathbf{A}\|_{\text{op}} \geq \sigma(\sqrt{m} + \sqrt{n} + \sqrt{2t})) \leq e^{-t}.$$

Next, Lemma 8 provides a concentration inequality for empirical processes indexed by an unbounded function class.

**Lemma 8** (Theorem 4 of Adamczak 2008). *Let  $X_1, \dots, X_n$  be independent random variables taking values in a measurable space  $(S, \mathcal{B})$ , and let  $\mathcal{F}$  be a countable class of measurable functions  $f : S \rightarrow \mathbb{R}$ . Assume that for all  $f \in \mathcal{F}$  and all  $i = 1, \dots, n$ , it holds that  $\mathbb{E}[f(X_i)] = 0$  and*

$$\left\| \sup_{f \in \mathcal{F}} |f(X_i)| \right\|_{\psi_1} < \infty,$$

Define

$$Z := \sup_{f \in \mathcal{F}} \left| \sum_{i=1}^n f(X_i) \right|, \quad \gamma^2 := \sup_{f \in \mathcal{F}} \sum_{i=1}^n \text{Var}[f(X_i)], \quad \text{and} \quad M_{\psi_1} := \left\| \max_{i \in [n]} \sup_{f \in \mathcal{F}} |f(X_i)| \right\|_{\psi_1}$$

Then there exists a constant  $C > 0$  such that for all  $t > 0$ , we have

$$\mathbb{P}(Z \geq 2\mathbb{E}[Z] + t) \leq \exp\left(-\frac{t^2}{3\gamma^2}\right) + 3 \exp\left(-\frac{t}{CM_{\psi_1}}\right).$$

Next, Lemma 9 presents a concentration inequality for the suprema of the Gaussian process.

**Lemma 9** (Theorem 5.8 of Boucheron et al. 2016). *Let  $(X_t)_{t \in \mathcal{T}}$  be an almost surely continuous, centered Gaussian process indexed by a totally bounded set  $\mathcal{T}$ . Define*

$$\gamma^2 := \sup_{t \in \mathcal{T}} \text{Var}(X_t^2), \quad \text{and} \quad Z := \sup_{t \in \mathcal{T}} X_t.$$

Then, we have  $\text{Var}(Z) \leq \gamma^2$ . Moreover, for any  $t > 0$ ,

$$\mathbb{P}(Z - \mathbb{E}[Z] \geq t) \leq \exp\left(-\frac{t^2}{2\gamma^2}\right).$$

The next lemma, Dudley's integral inequality, bounds the expected supremum of a Gaussian process.

**Lemma 10** (Theorem 8.1.3 of Vershynin 2018). *Let  $(T, d)$  be a metric space, and let  $N(T, d, \varepsilon)$  denote the  $\varepsilon$ -covering number of  $T$  with respect to  $d$ . Let  $(X_t)_{t \in T}$  be a mean-zero random process on a metric space with sub-Gaussian increments. Then*

$$\mathbb{E} \sup_{t \in T} X_t \leq CK_{\psi_2} \int_0^\infty \sqrt{\log N(T, d, \varepsilon)} d\varepsilon,$$

where  $C$  is an absolute constant, and  $K_{\psi_2}$  is the sub-Gaussian parameter.

Finally, Lemma 11 presents the uniform Hanson-Wright inequality for Gaussian quadratic forms.

**Lemma 11** (Lemma VIII.4 of Chen and Yang 2021). *Let  $\mathbf{X} \sim \mathcal{N}(0, I_q)$  and  $\mathcal{A}$  be a bounded class of  $q \times q$  matrices. Define the random variable*

$$Z = \sup_{\mathbf{A} \in \mathcal{A}} \left( \mathbf{X}^\top \mathbf{A} \mathbf{X} - \mathbb{E}[\mathbf{X}^\top \mathbf{A} \mathbf{X}] \right),$$

which corresponds to the supremum of a centered random process. Then, there exists a constant  $C > 0$  such that for any  $t > 0$ ,

$$\mathbb{P}(|Z - \mathbb{E}[Z]| \geq t) \leq 2 \exp \left[ -C \min \left( \frac{t^2}{\|\mathbf{X}\|_{\mathcal{A}}^2}, \frac{t}{\sup_{\mathbf{A} \in \mathcal{A}} \|\mathbf{A}\|_{\text{op}}} \right) \right],$$

where  $\|\mathbf{X}\|_{\mathcal{A}} := \mathbb{E} [\sup_{\mathbf{A} \in \mathcal{A}} \|(\mathbf{A} + \mathbf{A}^T) \mathbf{X}\|_2]$ .

## C PROOF OF THEOREM 1

The proof follows the strategy of Theorem II.1 of Chen and Yang (2021), with modifications to account for the sparsity assumption. The proof proceeds in three key steps.

1. **Reformulation into high-probability bound problem (Appendix C.1):** For each  $S$ , we construct three statistics that bound a dual certificate  $\lambda^S$ , which verifies

exact cluster recovery by the SDP problem (5) corresponding to  $S$ . A nontrivial gap between these bounds guarantees the existence of such a certificate (Corollary 18).

2. **First bounds and construction of the dual variable (Appendix C.2).** Under the separation and set size conditions imposed by  $\mathcal{S}$ , we derive uniform high-probability bounds on the two statistics defined in the first step and determine the value of  $\lambda^S$  accordingly (Lemma 21).
3. **Second bounds and conclusion (Appendix C.3).** We establish a uniform high-probability bound on the third statistic and verify that the previously chosen value of  $\lambda^S$  exceeds this bound, thereby confirming the existence of a dual certificate and completing the proof.

For notational simplicity, we adopt the following matrix-based notations of our model

$$\mathbf{X}_i = \boldsymbol{\mu}_k^* + \boldsymbol{\varepsilon}_i \text{ for each } i \in G_k^*, \text{ where } \boldsymbol{\varepsilon}_i \stackrel{\text{i.i.d.}}{\sim} \mathcal{N}(0, \sigma^2 \mathbf{I}_p):$$

**Definition 12** (Matrix-based notations). *We view the data as a matrix  $\mathbf{X} \in \mathbb{R}^{p \times n}$  and write  $\mathbf{X} = \mathbf{M}^* + \mathcal{E}$ , where  $\mathbf{M}^*$  contains the cluster means column-wise, and  $\mathcal{E}$  collects the noise vectors. For any support set  $S \subset [p]$ , we denote the  $i$ th observation and its noise restricted to  $S$  by*

$$\mathbf{X}_{S,i} \quad \text{and} \quad \mathcal{E}_{S,i},$$

*respectively. Given true clusters  $G_1^*, \dots, G_K^*$ , we define the empirical mean and average noise of cluster  $k$  on support  $S$  as*

$$\overline{\mathbf{X}}_{S,k}^* := \frac{1}{|G_k^*|} \sum_{i \in G_k^*} \mathbf{X}_{S,i}, \quad \overline{\mathcal{E}}_{S,k}^* := \frac{1}{|G_k^*|} \sum_{i \in G_k^*} \mathcal{E}_{S,i}.$$

## C.1 Reformulation into high-probability bound problem

The primary goal of this section is to derive Corollary 18, which converts the optimality condition into high-probability bounds. Let  $S \subset [p]$  be a support set, and consider the primal SDP problem (17) corresponding to  $S$ , recalled below:

$$\max_{\mathbf{Z} \in \mathbb{R}^{n \times n}} \langle \mathbf{X}_{S,.}^\top \mathbf{X}_{S,.}, \mathbf{Z} \rangle \quad \text{s.t.} \quad \mathbf{Z}^\top = \mathbf{Z}, \quad \mathbf{Z} \succeq 0, \quad \text{tr}(\mathbf{Z}) = K, \quad \mathbf{Z}\mathbf{1}_n = \mathbf{1}_n, \quad \mathbf{Z} \geq 0. \quad (17)$$

Let  $\mathcal{L}(\mathbf{Z}, \mathbf{Q}^S, \lambda^S, \boldsymbol{\alpha}^S, \mathbf{B}^S)$  denote the associated Lagrangian function. Here, the Lagrange multipliers

$$\mathbf{Q}^S \in \mathbb{R}^{n \times n}, \quad \lambda^S \in \mathbb{R}, \quad \boldsymbol{\alpha}^S \in \mathbb{R}^n, \quad \text{and} \quad \mathbf{B}^S \in \mathbb{R}^{n \times n}$$

correspond to the primal constraints

$$\mathbf{Z} \succeq 0, \quad \text{tr}(\mathbf{Z}) = K, \quad \mathbf{Z}^\top = \mathbf{Z}, \quad \text{and} \quad \mathbf{Z} \geq 0,$$

respectively. Note that  $\mathbf{Q}^S \succeq 0$  and  $\mathbf{B}^S \geq 0$ . Based on this formulation, this section proceeds in three main steps to ultimately establish Corollary 18:

1. **Necessary conditions for dual certificates (Appendix C.1.1):** We formalize sufficient conditions for the existence of dual certificates (Lemma 13) and leverage them to derive necessary conditions (Lemma 14) that guide the construction of dual variables.
2. **Reduction to a single dual variable construction (Appendix C.1.2):** Leveraging the necessary conditions, we parameterize the dual variables in terms of  $\lambda^S$ , reducing the construction to a one-dimensional problem (Lemma 15).
3. **Reformulation into high-probability bound problem (Appendix C.1.3):** We derive statistics that bound the dual certificate  $\lambda^S$  from above (Lemma 16) and below (Lemma 17). This shows that a nontrivial gap between them guarantees the existence of dual variables satisfying the conditions of Lemma 13 (Corollary 18).

### C.1.1 Necessary conditions for dual certificates

Let  $S \subset [p]$  be a support set, and consider the corresponding primal SDP problem (17).

Lemma 13 provides sufficient conditions under which the dual variables  $\lambda^S$ ,  $\boldsymbol{\alpha}^S$ , and  $\mathbf{B}^S$  form a valid dual certificate (with  $\mathbf{Q}^S$  implicitly captured by the conditions). In particular, the lemma guarantees that the duality gap vanishes at the true cluster membership matrix

$$\mathbf{Z}^* = \sum_{k=1}^K \frac{1}{|G_k^*|} \mathbf{1}_{G_k^*} \mathbf{1}_{G_k^*}^\top.$$

**Lemma 13** (Optimality conditions). *Let  $S \subset [p]$  be a support set, and consider the corresponding primal SDP problem (17). The matrix  $\mathbf{Z}^*$  is the unique solution to this problem if there exist dual variables  $\lambda^S \in \mathbb{R}$ ,  $\boldsymbol{\alpha}^S \in \mathbb{R}^n$ , and  $\mathbf{B}^S \in \mathbb{R}^{n \times n}$  such that the following conditions are satisfied:*

$$(C1) \quad \mathbf{B}^S \geq 0;$$

$$(C2) \quad \mathbf{W}^S := \lambda^S \mathbf{I}_n - \mathbf{B}^S + \frac{1}{2} \mathbf{1}_n (\boldsymbol{\alpha}^S)^\top + \frac{1}{2} \boldsymbol{\alpha}^S \mathbf{1}_n^\top - \mathbf{X}_{S,\cdot}^\top \mathbf{X}_{S,\cdot} \succeq 0;$$

$$(C3) \quad \langle \mathbf{W}^S, \mathbf{Z}^* \rangle = 0;$$

$$(C4) \quad \langle \mathbf{B}^S, \mathbf{Z}^* \rangle = 0;$$

$$(C5) \quad \mathbf{B}_{\mathbf{G}_k^*, \mathbf{G}_l^*}^S > 0 \quad \text{for all } 1 \leq k \neq l \leq K.$$

In Lemma 13, conditions (C1) and (C2) ensure dual feasibility, (C3) and (C4) guarantee a zero duality gap, and (C5) ensures the uniqueness of the solution. The proof is provided in Appendix C.4.1. Building on these conditions, we now establish necessary conditions for dual certificates. Leveraging this notation, we state the necessary conditions in the following lemma.

**Lemma 14** (Necessary conditions for optimality). *Let  $S \subset [p]$  be a support set, and consider the corresponding primal SDP problem (17). Suppose dual variables  $\lambda^S \in \mathbb{R}$ ,  $\boldsymbol{\alpha}^S \in \mathbb{R}^n$ ,*

and  $\mathbf{B}^S \in \mathbb{R}^{n \times n}$  satisfy conditions (C2), (C3), and (C4) of Lemma 13. Then, for all  $1 \leq k \neq l \leq K$  and  $i \in G_k^*$ , the following statements hold:

$$\boldsymbol{\alpha}_i^S = 2\mathbf{X}_{S,i}^\top \bar{\mathbf{X}}_{S,k}^* - \frac{\lambda^S}{|G_k^*|} - \|\bar{\mathbf{X}}_{S,k}^*\|_2^2, \text{ and} \quad (18)$$

$$(\mathbf{B}_{G_k^* G_l^*}^S \mathbf{1}_{|G_l^*|})_i = -\frac{|G_k^*| + |G_l^*|}{2|G_k^*|} \lambda^S + \frac{|G_l^*|}{2} (\|\bar{\mathbf{X}}_{S,l}^* - \mathbf{X}_{S,i}\|_2^2 - \|\bar{\mathbf{X}}_{S,k}^* - \mathbf{X}_{S,i}\|_2^2), \quad (19)$$

where  $(\mathbf{B}_{G_k^* G_l^*}^S \mathbf{1}_{|G_l^*|})_i$  denotes the  $i$ th entry of the row-wise sum of  $\mathbf{B}_{G_k^* G_l^*}^S \in \mathbb{R}^{|G_k^*| \times |G_l^*|}$ , which is the  $(k, l)$ th off-diagonal block of  $\mathbf{B}^S$ .

The proof of Lemma 14 is provided in Appendix C.4.2.

### C.1.2 Reduction to a single dual variable construction

For any given  $\lambda^S \in \mathbb{R}$ , condition (18) uniquely determines the corresponding value of  $\boldsymbol{\alpha}^S$ , which we denote by  $\dot{\boldsymbol{\alpha}}^S(\lambda^S)$ . We then turn to the dual variable  $\mathbf{B}^S$  and construct  $\dot{\mathbf{B}}^S(\lambda^S)$ , designed to satisfy condition (19). The matrix  $\dot{\mathbf{B}}^S(\lambda^S)$  is structured as a block matrix, with symmetric rank-one matrices as its off-diagonal blocks and zero matrices as its diagonal blocks. These constructions follow the proof of Theorem II.1 in Chen and Yang (2021), with modifications to account for varying support sets.

We now describe the construction of  $\dot{\mathbf{B}}^S(\lambda^S)$ . Fix any value of  $\lambda^S \in \mathbb{R}$ , and for notational simplicity, we suppress the dependence on  $\lambda^S$  in what follows. For each  $k = 1, \dots, K$ , define the diagonal block  $\dot{\mathbf{B}}_{G_k^*, G_k^*}^S \in \mathbb{R}^{|G_k^*| \times |G_k^*|}$  to be the zero matrix. Next, consider the off-diagonal blocks. Given  $\lambda^S$ , the data, and the true cluster structure, condition (19) uniquely determines the row-wise sum of the  $(k, l)$  off-diagonal block of the dual certificate. Denote this unique vector by  $\mathbf{r}^{(k,l,S)} \in \mathbb{R}^{|G_k^*|}$ . Then, for each  $1 \leq k \neq l \leq K$ , we define the off-diagonal block  $\dot{\mathbf{B}}_{G_k^*, G_l^*}^S \in \mathbb{R}^{|G_k^*| \times |G_l^*|}$  as the symmetric rank-one matrix:

$$\dot{\mathbf{B}}_{G_k^*, G_l^*}^S := \frac{1}{\mathbf{1}_{|G_l^*|}^\top \mathbf{r}^{(l,k,S)}} \mathbf{r}^{(k,l,S)} (\mathbf{r}^{(l,k,S)})^\top, \quad (20)$$

This construction ensures that the row-sum condition in (19) is satisfied:

$$\begin{aligned}
\dot{\mathbf{B}}_{G_k^*, G_l^*}^S \mathbf{1}_{|G_l^*|} &= \frac{1}{\mathbf{1}_{|G_l^*|}^\top \mathbf{r}^{(l,k,S)}} \{ \mathbf{r}^{(k,l,S)} (\mathbf{r}^{(l,k,S)})^\top \} \mathbf{1}_{|G_l^*|} \\
&= \frac{1}{\mathbf{1}_{|G_l^*|}^\top \mathbf{r}^{(l,k,S)}} \mathbf{r}^{(k,l,S)} \{ (\mathbf{r}^{(l,k,S)})^\top \mathbf{1}_{|G_l^*|} \} \\
&= \mathbf{r}^{(k,l,S)}.
\end{aligned}$$

We summarize the construction of  $\dot{\alpha}^S(\lambda^S)$  and  $\dot{\mathbf{B}}^S(\lambda^S)$  in the following lemma.

**Lemma 15** (Parametrized dual certificate candidates). *Fix the data matrix  $\mathbf{X}$  and the true cluster structure  $G_1^*, \dots, G_K^*$ . Let  $S \subset [p]$  be a support set, and consider the corresponding primal SDP problem (17). Fix a value of the dual variable  $\lambda^S \in \mathbb{R}$ . Define  $\dot{\alpha}^S(\lambda^S) \in \mathbb{R}^n$  by setting, for each  $k = 1, \dots, K$ ,*

$$\dot{\alpha}_{G_k^*}^S(\lambda^S) := 2\mathbf{X}_{S,G_k^*}^\top \bar{\mathbf{X}}_{S,k}^* - \frac{\lambda^S}{|G_k^*|} \mathbf{1}_{|G_k^*|} - \|\bar{\mathbf{X}}_{S,k}^*\|_2^2 \mathbf{1}_{|G_k^*|},$$

Next, define  $\dot{\mathbf{B}}^S(\lambda^S) \in \mathbb{R}^{n \times n}$  as the block matrix:

$$\dot{\mathbf{B}}^S(\lambda^S) := \begin{bmatrix} \mathbf{0} & \dot{\mathbf{B}}_{G_1^*, G_2^*}^S(\lambda^S) & \dots & \dot{\mathbf{B}}_{G_1^*, G_K^*}^S(\lambda^S) \\ \dot{\mathbf{B}}_{G_2^*, G_1^*}^S(\lambda^S) & \mathbf{0} & \dots & \dot{\mathbf{B}}_{G_2^*, G_K^*}^S(\lambda^S) \\ \vdots & \vdots & \ddots & \vdots \\ \dot{\mathbf{B}}_{G_K^*, G_1^*}^S(\lambda^S) & \dot{\mathbf{B}}_{G_K^*, G_2^*}^S(\lambda^S) & \dots & \mathbf{0} \end{bmatrix},$$

where for each  $1 \leq k \neq l \leq K$ , the off-diagonal block  $\dot{\mathbf{B}}_{G_k^*, G_l^*}^S(\lambda^S) \in \mathbb{R}^{|G_k^*| \times |G_l^*|}$  is defined as

$$\dot{\mathbf{B}}_{G_k^*, G_l^*}^S(\lambda^S) := \frac{1}{\mathbf{1}_{|G_l^*|}^\top \mathbf{r}^{(l,k,S)}} \mathbf{r}^{(k,l,S)} (\mathbf{r}^{(l,k,S)})^\top, \quad (21)$$

with  $\mathbf{r}^{(k,l,S)} \in \mathbb{R}^{|G_k^*|}$  defined componentwise by

$$r_i^{(k,l,S)} := -\frac{|G_k^*| + |G_l^*|}{2|G_k^*|} \lambda^S + \frac{|G_l^*|}{2} (\|\bar{\mathbf{X}}_{S,l}^* - \mathbf{X}_{S,i}\|_2^2 - \|\bar{\mathbf{X}}_{S,k}^* - \mathbf{X}_{S,i}\|_2^2). \quad (22)$$

Finally, we construct

$$\dot{\mathbf{W}}^S(\lambda^S) := \lambda^S \mathbf{I}_n - \dot{\mathbf{B}}^S(\lambda^S) + \frac{1}{2} \mathbf{1}_n (\dot{\boldsymbol{\alpha}}^S(\lambda^S))^\top + \frac{1}{2} \dot{\boldsymbol{\alpha}}^S(\lambda^S) \mathbf{1}_n^\top - \mathbf{X}_{S,\cdot}^\top \mathbf{X}_{S,\cdot}$$

Constructed  $\dot{\boldsymbol{\alpha}}^S(\lambda^S)$  and  $\dot{\mathbf{B}}^S(\lambda^S)$  satisfy the conditions in Lemma 14.

### C.1.3 Reformulation into high-probability bound problem

Next, we identify conditions of  $\lambda^S$ , that ensures  $\dot{\mathbf{B}}^S(\lambda^S)$  and  $\dot{\boldsymbol{\alpha}}^S(\lambda^S)$  satisfy the conditions in Lemma 13. We begin with conditions (C1), (C3), (C4) and (C5). To this end, we introduce the following data-dependent quantities:

$$D_{kli}^S(\mathbf{X}) := \|\bar{\mathbf{X}}_{S,l}^* - \mathbf{X}_{S,i}\|_2^2 - \|\bar{\mathbf{X}}_{S,k}^* - \mathbf{X}_{S,i}\|_2^2,$$

and

$$U^S(\mathbf{X}) := \min_{1 \leq k \neq l \leq K} \left\{ \left( \frac{1}{|G_k^*|} + \frac{1}{|G_l^*|} \right)^{-1} \min_{i \in G_k^*} D_{kli}^S(\mathbf{X}) \right\}. \quad (23)$$

Based on these definitions, we now state an upper bound on  $\lambda^S$ :

**Lemma 16** (Upper bound on  $\lambda^S$ ). *Let  $S \subset [p]$  be a support set, and consider the corresponding primal SDP problem (17). For any value of  $\lambda^S$ , corresponding  $\dot{\boldsymbol{\alpha}}^S(\lambda^S)$ ,  $\dot{\mathbf{B}}^S(\lambda^S)$ , and  $\dot{\mathbf{W}}^S(\lambda^S)$  satisfy conditions (C3) and (C4) of Lemma 13. Moreover, if*

$$\lambda^S < U^S(\mathbf{X}),$$

*then  $\dot{\boldsymbol{\alpha}}^S(\lambda^S)$  and  $\dot{\mathbf{B}}^S(\lambda^S)$  also satisfy conditions (C1) and (C5) of Lemma 13.*

Proof of Lemma 16 is provided in Appendix C.4.3.

Next we move onto condition (C2) of Lemma 13. To this end, we define some notation.

We first define a linear subspace of  $\mathbb{R}^n$  as:

$$\Gamma_K := \text{span} \left( \mathbf{1}_{G_k^*} : k \in [K] \right)^\perp,$$

where  $\perp$  means orthogonal complement. For each  $\mathbf{v} \in \Gamma_K$  and support set  $S \subset [p]$ , we define a collection of data-dependent random variables. We begin with the following supremum of noise quadratic form process:

$$L_1^S(\mathbf{X}) := \sup_{\mathbf{v} \in \Gamma_K, \|\mathbf{v}\|_2=1} \|\mathcal{E}_{S,\cdot} \mathbf{v}\|_2^2, \quad (24)$$

Next, we define two fundamental components representing signal–noise and noise–noise interactions:

$$I_{kl}^S(\mathbf{v}, \mathbf{X}) := |G_l^*| \sum_{i \in G_k^*} v_i \langle (\boldsymbol{\mu}_k^* - \boldsymbol{\mu}_l^*)_{S \cap S_0}, \mathcal{E}_{S \cap S_0, i} \rangle, \text{ and} \quad (25)$$

$$N_{kl}^S(\mathbf{v}, \mathbf{X}) := |G_l^*| \sum_{i \in G_k^*} v_i \langle \bar{\mathcal{E}}_{S,k}^* - \bar{\mathcal{E}}_{S,l}^*, \mathcal{E}_{S,i} \rangle. \quad (26)$$

Note that both definitions are asymmetric with respect to the first two indices. Using these definitions, we introduce three composite random quantities:

$$T_{1,kl}^S(\mathbf{v}) := I_{kl}^S(\mathbf{v}, \mathbf{X}) \cdot I_{lk}^S(\mathbf{v}, \mathbf{X}), \quad (27)$$

$$T_{2,kl}^S(\mathbf{v}) := N_{kl}^S(\mathbf{v}, \mathbf{X}) \cdot N_{lk}^S(\mathbf{v}, \mathbf{X}), \text{ and} \quad (28)$$

$$T_{3,kl}^S(\mathbf{v}) := N_{kl}^S(\mathbf{v}, \mathbf{X}) \cdot I_{lk}^S(\mathbf{v}, \mathbf{X}) + I_{kl}^S(\mathbf{v}, \mathbf{X}) \cdot N_{lk}^S(\mathbf{v}, \mathbf{X}). \quad (29)$$

Next, the following quantity represents the sum of all elements of  $\dot{\mathbf{B}}_{G_l^*, G_k^*}^S$ ,  $(l, k)$ th off-diagonal block of  $\dot{\mathbf{B}}^S(\lambda^S)$ :

$$t_{lk}^S(\lambda^S) := \sum_{j \in G_l^*} r_j^{(l,k,S)} = \sum_{j \in G_l^*} \left\{ \frac{|G_k^*|}{2} D_{lkj}(\mathbf{X}, S) - \frac{|G_k^*| + |G_l^*|}{2|G_l^*|} \lambda^S \right\}. \quad (30)$$

Leveraging all these notations, we finally define:

$$L_2^S(\mathbf{X}, \lambda^S) := \sup_{\mathbf{v} \in \Gamma_K, \|\mathbf{v}\|_2=1} \left\{ \sum_{1 \leq k \neq l \leq K} \frac{1}{t_{lk}^S(\lambda^S)} \left( T_{1,kl}^S(\mathbf{v}) + T_{2,kl}^S(\mathbf{v}) + T_{3,kl}^S(\mathbf{v}) \right) \right\}, \quad (31)$$

Using this quantity, Lemma 17 states the lower bound condition on  $\lambda_S$  that guarantees condition (C2) of Lemma 13 is satisfied.

**Lemma 17** (Lower bound on  $\lambda_S$ ). *Let  $S \subset [p]$  be a support set, and consider the corresponding primal SDP problem (17). If*

$$\lambda^S > L_1^S(\mathbf{X}) + L_2^S(\mathbf{X}, \lambda^S),$$

*then the constructed dual variables  $\dot{\alpha}^S(\lambda^S)$  and  $\dot{\mathbf{B}}^S(\lambda^S)$  satisfy condition (C2) of Lemma 13.*

Proof of Lemma 17 is provided in Appendix C.4.4. Combining Lemmas 16 and 17, we finally arrive at the following corollary:

**Corollary 18** (Problem reformulation). *Let  $S \subset [p]$  be a support set, and consider the corresponding primal SDP problem (17). If there exists  $\lambda^S$  such that*

$$L_1^S(\mathbf{X}) + L_2^S(\mathbf{X}, \lambda^S) < \lambda^S < U^S(\mathbf{X}),$$

*then the dual variables constructed with this  $\lambda^S$  via Lemma 15 yield a valid certificate that satisfies all conditions of Lemma 13, verifying that  $\mathbf{Z}^*$  is the unique optimal point of the primal problem.*

## C.2 First Bounds and Construction of the Dual Variable

This section is devoted to the derivation of Lemma 21, which establishes that, under the separation condition, there exists a  $\lambda^S$  that partially satisfies the condition stated in Corollary 18. We proceed in two main steps:

1. **High-probability bounds (Appendix C.2.1)** : We derive a lower bound for  $U^S(\mathbf{X})$  (Lemma 19) and an upper bound for  $L_1^S(\mathbf{X})$  (Lemma 20), under the separation and set size condition of  $S$ .

2. **Specifying the value of the dual variable (Appendix C.2.2):** We set the value of  $\lambda^S$  to lie between the bounds established in the previous step (Lemma 21).

### C.2.1 High-probability Bounds

Recall from (23) that  $U^S(\mathbf{X})$  is defined as

$$U^S(\mathbf{X}) = \min_{1 \leq k \neq l \leq K} \left\{ \left( \frac{1}{|G_k^*|} + \frac{1}{|G_l^*|} \right)^{-1} \min_{i \in G_k^*} D_{kli}^S(\mathbf{X}) \right\},$$

where

$$D_{kli}^S(\mathbf{X}) = \|\bar{\mathbf{X}}_{S,l}^* - \mathbf{X}_{S,i}\|_2^2 - \|\bar{\mathbf{X}}_{S,k}^* - \mathbf{X}_{S,i}\|_2^2.$$

Recall from (9) that we define  $\mathcal{S}$  as

$$\mathcal{S} := \left\{ S : S \subset [p], S \cap S_0 \neq \emptyset, |S| \leq \sqrt{p}, \Delta_{S \cap S_0}^2 \gtrsim \sigma^2 \left( \log n + \frac{|S| \log p}{m} + \sqrt{\frac{|S| \log p}{m}} \right) \right\},$$

where

$$\Delta_{S \cap S_0}^2 = \min_{1 \leq k \neq l \leq K} \|(\boldsymbol{\mu}_l^* - \boldsymbol{\mu}_k^*)_{S \cap S_0}\|_2^2,$$

and

$$m = \min_{1 \leq k \neq l \leq K} \left( \frac{2|G_l^*||G_k^*|}{|G_l^*| + |G_k^*|} \right) \geq C_1 \frac{n}{\log n}.$$

The following lemma establishes a high-probability lower bound for  $D_{kli}^S(\mathbf{X})$ .

**Lemma 19.** *Uniformly across all index  $(k, l, i)$  ranging over all pairs  $1 \leq k \neq l \leq K$  and*

*$i \in G_k^*$ , and all  $S \in \mathcal{S}$ , with probability at least  $1 - C_7/n$ , it holds that*

$$D_{kli}^S(\mathbf{X}) \gtrsim \|(\boldsymbol{\mu}_k^* - \boldsymbol{\mu}_l^*)_{S \cap S_0}\|_2^2 + \left( \frac{1}{|G_k^*|} + \frac{1}{|G_l^*|} \right) |S| - R_{kl}^S.$$

where  $C_7 > 0$  is a constant and

$$R_{kl}^S := \sqrt{\frac{\xi^S}{|G_l^*|}} \|(\boldsymbol{\mu}_l^* - \boldsymbol{\mu}_k^*)_{S \cap S_0}\|_2 + \left( \frac{1}{|G_k^*|} + \frac{1}{|G_l^*|} \right) \sqrt{|S|\xi^S} + \frac{1}{|G_k^*|} \zeta^S,$$

and  $\zeta^S := \log(n^2|S|^2 \binom{p}{|S|})$ .

The proof of Lemma 19 is presented in Appendix C.4.5.

Next, Lemma 20 establishes a high-probability upper bound for  $L_1^S(\mathbf{X})$ , where we recall from (24):

$$L_1^S(\mathbf{X}) = \sup_{\mathbf{v} \in \Gamma_K, \|\mathbf{v}\|_2=1} \|\mathcal{E}_{S,\cdot} \mathbf{v}\|_2^2,$$

and  $\mathcal{E}_{S,\cdot}$  is a submatrix of  $\mathcal{E} \in \mathbb{R}^{p \times n}$ , whose entries are i.i.d. Gaussian random variables.

**Lemma 20.** *Uniformly across all  $S \subset [p]$  such that  $|S| \leq \sqrt{p}$ , with probability at least  $1 - C_8/n$ , where  $C_8 > 0$  is a constant, it holds that*

$$L_1^S(\mathbf{X}) \lesssim \sigma^2(n + \log n + |S| \log p).$$

The proof of Lemma 20 is provided in Appendix C.4.6.

### C.2.2 Specifying the Value of the Dual Variable

Since  $L_2^S(\mathbf{X}, \lambda^S)$  in (31) depends on  $\lambda^S$ , we first specify a value which lies between  $L_1^S(\mathbf{X})$  and  $U^S(\mathbf{X})$  with high probability, uniformly over  $S \in \mathcal{S}$ .

**Lemma 21.** *Let  $\dot{\lambda}^S := \sigma^2|S| + m\Delta_{S \cap S_0}^2/4$ . Then Uniformly over  $S \in \mathcal{S}$ , with probability at least  $1 - C_9/n$ , where  $C_9 > 0$  is a constant, it holds that*

$$L_1^S(\mathbf{X}) \lesssim \dot{\lambda}^S \lesssim U^S(\mathbf{X}).$$

Proof of Lemma 21 is provided in Appendix C.4.7.

## C.3 Second high-probability bounds and conclusion

This section completes the proof by showing that, with high probability,  $L_2^S(\mathbf{X}, \dot{\lambda}^S) \lesssim \dot{\lambda}^S$ . As defined in equation (31),  $L_2^S(\mathbf{X}, \dot{\lambda}^S)$  is the supremum of an empirical process involving statistics

$t_{lk}^S$  (30),  $I_{kl}^S(\mathbf{v}, \mathbf{X})$   $I_{lk}^S(\mathbf{v}, \mathbf{X})$  (25),  $N_{kl}^S(\mathbf{v}, \mathbf{X})$ , and  $N_{lk}^S(\mathbf{v}, \mathbf{X})$  (26). Therefore, the bound on  $L_2^S(\mathbf{X}, \dot{\lambda}^S)$  follows directly from bounds on the  $t_{lk}^S$ ,  $I_{kl}^S(\mathbf{v}, \mathbf{X})$  and  $N_{kl}^S(\mathbf{v}, \mathbf{X})$ . Accordingly, the remainder of this section proceeds as follows:

1. **Bounding the off-diagonal block sum of the dual variable matrix (Appendix C.3.1):** We derive a high-probability lower bound for  $t_{lk}^S$  (Lemma 22).
2. **Bounding the signal–noise interaction term (Appendix C.3.2):** We derive a high-probability upper bound for  $I_{kl}^S(\mathbf{v}, \mathbf{X})$  (Lemma 23) and show that the corresponding component of  $L_2^S(\mathbf{X}, \dot{\lambda}^S)$  is dominated by  $\dot{\lambda}^S$  (Lemma 24).
3. **Bounding the noise–noise interaction term (Appendix C.3.3):** We derive a high-probability upper bound for  $N_{kl}^S(\mathbf{v}, \mathbf{X})$  (Lemmas 25 and 26), and show that the corresponding component of  $L_2^S(\mathbf{X}, \dot{\lambda}^S)$  is dominated by  $\dot{\lambda}^S$  (Lemma 27).
4. **Conclusion (Appendix C.3.4).**

### C.3.1 Bounding the off-diagonal block sum of the dual variable matrix

With the value of  $\dot{\lambda}^S$  set in Lemma 21, we provide a high-probability lower bound of  $t_{lk}^S(\dot{\lambda}^S)$  defined in (30).

**Lemma 22.** *For any  $1 \leq l \neq k \leq K$ , if  $|G_l^*| \geq 2$  and  $|G_k^*| \geq 2$ , uniformly over  $S \in \mathcal{S}$ , with probability at least  $1 - C_7/n$ , where  $C_0$  is the constant used in Lemma 19, it holds that*

$$t_{lk}^S(\dot{\lambda}^S) \gtrsim |G_l^*| |G_k^*| \left( \|(\boldsymbol{\mu}_k^* - \boldsymbol{\mu}_l^*)_{S \cap S_0}\|_2^2 + |S| \right).$$

The proof of Lemma 22 is provided in Appendix C.4.8.

### C.3.2 Bounding the signal-noise interaction term

We first provide a high-probability upper bound of  $I_{kl}^S(\mathbf{v}, \mathbf{X}) = |G_l^*| \sum_{i \in G_k^*} v_i \langle (\boldsymbol{\mu}_k^* - \boldsymbol{\mu}_l^*)_{S \cap S_0}, \mathcal{E}_{S \cap S_0, i} \rangle$ , defined in (25).

**Lemma 23.** *Uniformly across  $S \in \mathcal{S}$  and  $(k, l)$  such that  $1 \leq k \neq l \leq K$ , with probability at least  $1 - C_{10}/n$ , where  $C_{10} > 0$  is a constant, it holds that*

$$\begin{aligned} & \sup_{\mathbf{v} \in \Gamma_K, \|\mathbf{v}\|_2=1} I_{kl}^S(\mathbf{v}, \mathbf{X}) \\ & \lesssim |G_l^*| \|(\boldsymbol{\mu}_k^* - \boldsymbol{\mu}_l^*)_{S \cap S_0}\|_2 \left( |G_k^*| + \sqrt{|G_k^*| \log n} + \sqrt{|G_k^*| |S| \log p} + \log n + |S| \log p \right)^{1/2}. \end{aligned}$$

The proof of Lemma 23 is provided in Appendix C.4.9. Building on this result, we establish the first partial upper bound for  $L_2^S(\mathbf{X}, \dot{\lambda}^S)$ , corresponding to the term  $T_{1,kl}^S(\mathbf{v}) = I_{kl}^S(\mathbf{v}, \mathbf{X}) \cdot I_{lk}^S(\mathbf{v}, \mathbf{X})$ , defined in (27).

**Lemma 24.** *Uniformly across  $S \in \mathcal{S}$ , with probability at least  $1 - C_{11}/n$ , where  $C_{11} > 0$  is a constant, it holds that*

$$\sup_{\mathbf{v} \in \Gamma_K, \|\mathbf{v}\|_2=1} \sum_{1 \leq k \neq l \leq K} \frac{T_{1,kl}^S(\mathbf{v})}{t_{lk}^S(\dot{\lambda}^S)} \lesssim \dot{\lambda}^S.$$

Proof of Lemma 24 is provided in Appendix C.4.10.

### C.3.3 Bounding the noise-noise interaction term

Since  $N_{kl}^S(\mathbf{v}, \mathbf{X})$ , defined in (26), is an inner product of dependent Gaussian variables, we decompose it into a sum of inner products between independent Gaussian variables.

$$\begin{aligned} N_{kl}^S(\mathbf{v}, \mathbf{X}) &= |G_l^*| \sum_{i \in G_k^*} v_i \langle \bar{\mathcal{E}}_{S,k}^* - \bar{\mathcal{E}}_{S,l}^*, \mathcal{E}_{S,i} \rangle \\ &= |G_l^*| \sum_{i \in G_k^*} v_i \langle \bar{\mathcal{E}}_{S,k}^*, \mathcal{E}_{S,i} \rangle - |G_l^*| \sum_{i \in G_k^*} v_i \langle \bar{\mathcal{E}}_{S,l}^*, \mathcal{E}_{S,i} \rangle \end{aligned}$$

$$= \underbrace{\frac{|G_l^*|}{|G_k^*|} \sum_{\{(i,j) \in G_k^*\}} v_i \langle \mathcal{E}_{S,i}, \mathcal{E}_{S,j} \rangle}_{:= G_{1,kl}^S(\mathbf{v})} - |G_l^*| \sum_{i \in G_k^*} v_i \langle \bar{\mathcal{E}}_{S,l}^*, \mathcal{E}_{S,i} \rangle, \underbrace{\sum_{i \in G_k^*} v_i \langle \bar{\mathcal{E}}_{S,l}^*, \mathcal{E}_{S,i} \rangle}_{:= G_{2,kl}^S(\mathbf{v})}$$

We now present high-probability upper bounds for  $G_{1,kl}^S(\mathbf{v})$  and  $G_{2,kl}^S(\mathbf{v})$  in order. Since all terms consist purely of noise random variables, no separation condition is needed in this case.

**Lemma 25.** *Uniformly across  $S \in [p]$  such that  $|S| \leq \sqrt{p}$  and  $(k, l)$  such that  $1 \leq k \neq l \leq K$ , with probability at least  $1 - C_{11}/n$ , where  $C_{11} > 0$  is a constant, it holds that*

$$\sup_{\mathbf{v} \in \Gamma_K, \|\mathbf{v}\|_2=1} G_{1,kl}^S(\mathbf{v}) \lesssim |G_l^*| \sqrt{|S|(\log n + |S| \log p)}.$$

The proof of Lemma 25 is provided in Appendix C.4.11.

**Lemma 26.** *Uniformly across  $S \in [p]$  such that  $|S| \leq \sqrt{p}$  and  $(k, l)$  such that  $1 \leq k \neq l \leq K$ , with probability at least  $1 - C_{12}/n$ , where  $C_{12} > 0$  is a constant, it holds that*

$$\sup_{\mathbf{v} \in \Gamma_K, \|\mathbf{v}\|_2=1} |G_{2,kl}^S(\mathbf{v})| \lesssim \sqrt{|G_l^*|} \sqrt{|S| + 2\sqrt{|S|\xi^S} + 2\xi^S} \sqrt{|G_k^*| + \sqrt{\xi^S}},$$

where  $\xi^S = \log(n|S|^2 \binom{p}{|S|})$ .

The proof of Lemma 26 is provided in Appendix C.4.12.

**Lemma 27.** *Uniformly across  $S \in \mathcal{S}$  and  $(k, l)$  such that  $1 \leq k \neq l \leq K$ , with probability at least  $1 - C_{13}/n$ , where  $C_{13} > 0$  is a constant, it holds that*

$$\sup_{\mathbf{v} \in \Gamma_K, \|\mathbf{v}\|_2=1} \sum_{1 \leq k \neq l \leq K} \frac{T_{2,kl}^S(\mathbf{v})}{t_{lk}^S(\dot{\lambda}^S)} \lesssim \dot{\lambda}^S.$$

Proof of Lemma 27 is provided in Appendix C.4.13.

### C.3.4 Conclusion

The inequality regarding  $T_{3,kl}^S(\mathbf{v})$  is a direct consequence of Lemmas 24, and 27, by the Cauchy-Schwarz inequality. Therefore, by combining Lemmas 21, 24, and 27, we conclude that, uniformly over  $S \in \mathcal{S}$ , with probability at least  $1 - C_{14}/n$ , where  $C_{14} > 0$  is a constant, the quantity  $\dot{\lambda}^S$  constructed in Lemma 20 satisfies

$$L_1^S(\mathbf{X}) + L_2^S(\mathbf{X}, \dot{\lambda}^S) \lesssim \dot{\lambda}^S \lesssim U^S(\mathbf{X}).$$

Therefore, by Corollary 18, the dual variables constructed in Lemma 15 serve as dual certificates verifying that  $\mathbf{Z}^*$  is the unique optimal solution to the primal SDP problem corresponding to  $S$ , stated in (17). This completes the proof of Theorem 1.

## C.4 Proof of Supporting Lemmas

This section presents omitted proof of lemmas presented in the proof of Theorem 1.

### C.4.1 Proof of Lemma 13

The proof proceeds in three steps:

1. Conditions (C1) and (C2) from dual feasibility,
2. Conditions (C3) and (C4) from zero dual gap,
3. Condition (C5) from the block-diagonal structure of  $\mathbf{Z}^* = \sum_{k=1}^K |G_k^*|^{-1} \mathbf{1}_{G_k^*} \mathbf{1}_{G_k^*}^\top$ .

*Proof.* We proceed by following the steps outlined above in sequence.

**1. Conditions (C1) and (C2) from dual feasibility.** After simplification, the Lagrangian function becomes an affine function of  $\mathbf{Z}$ :

$$\begin{aligned}\mathcal{L}(\mathbf{Z}, \mathbf{Q}^S, \lambda^S, \boldsymbol{\alpha}^S, \mathbf{B}^S) \\ := \langle \mathbf{X}_{S,\cdot}^\top \mathbf{X}_{S,\cdot}, \mathbf{Z} \rangle + \langle \mathbf{Q}^S, \mathbf{Z} \rangle + \lambda^S(K - \text{tr}(\mathbf{Z})) + (\boldsymbol{\alpha}^S)^\top \left( \mathbf{1}_n - \frac{1}{2}(\mathbf{Z} + \mathbf{Z}^\top) \mathbf{1}_n \right) + \langle \mathbf{B}^S, \mathbf{Z} \rangle \\ = \lambda^S K + (\boldsymbol{\alpha}^S)^\top \mathbf{1}_n + \langle \mathbf{Q}^S - \mathbf{W}^S, \mathbf{Z} \rangle,\end{aligned}$$

where we use  $\text{tr}(\mathbf{Z}) = \langle \mathbf{I}_n, \mathbf{Z} \rangle$  and recall from Lemma 13 that

$$\mathbf{W}^S = \lambda^S \mathbf{I}_n - \mathbf{B}^S + \frac{1}{2} \mathbf{1}_n (\boldsymbol{\alpha}^S)^\top + \frac{1}{2} \boldsymbol{\alpha}^S \mathbf{1}_n^\top - \mathbf{X}_{S,\cdot}^\top \mathbf{X}_{S,\cdot}.$$

Therefore, the Lagrange dual function, shown below, can be derived analytically, as a linear function is bounded only when the slope part is zero.

$$\begin{aligned}g(\mathbf{Q}^S, \lambda^S, \boldsymbol{\alpha}^S, \mathbf{B}^S) &:= \sup_{\mathbf{Z} \in \mathbb{R}^{n \times n}} \mathcal{L}(\mathbf{Z}, \mathbf{Q}^S, \lambda^S, \boldsymbol{\alpha}^S, \mathbf{B}^S) \\ &= \lambda^S K + (\boldsymbol{\alpha}^S)^\top \mathbf{1}_n + \sup_{\mathbf{Z} \in \mathbb{R}^{n \times n}} \langle \mathbf{Q}^S - \mathbf{W}^S, \mathbf{Z} \rangle,\end{aligned}$$

As a result, we have:

$$g(\mathbf{Q}^S, \lambda^S, \boldsymbol{\alpha}^S, \mathbf{B}^S) = \begin{cases} \lambda^S K + (\boldsymbol{\alpha}^S)^\top \mathbf{1}_n, & \mathbf{Q}^S = \mathbf{W}^S \text{ (slope is 0)} \\ \infty, & \text{otherwise.} \end{cases}$$

Making the following domain of the dual function as an explicit linear equality constraint, and combining it with  $\mathbf{Q}^S \succeq 0$  and  $\mathbf{B}^S \geq 0$ , with some abuse of terminology, we refer to the following problem as the Lagrange dual problem associated with the primal SDP problem

$$\min_{\lambda^S \in \mathbb{R}, \boldsymbol{\alpha}^S \in \mathbb{R}^n, \mathbf{B}^S \in \mathbb{R}^{n \times n}} \lambda^S K + (\boldsymbol{\alpha}^S)^\top \mathbf{1}_n, \quad \text{s.t.} \quad \mathbf{B}^S \geq 0, \mathbf{W}^S \succeq 0.$$

The constraints in this optimization problem correspond to conditions (C1) and (C2).

**2. Conditions (C3) and (C4) from zero dual gap.** The duality gap is simply the difference between the dual and primal objective function:

$$\begin{aligned}
& \lambda^S K + (\boldsymbol{\alpha}^S)^\top \mathbf{1}_n - \langle \mathbf{X}_{S,\cdot}^\top \mathbf{X}_{S,\cdot}, \mathbf{Z} \rangle \\
& \stackrel{(i)}{=} \lambda^S \text{tr}(\mathbf{Z}) + \frac{1}{2} (\boldsymbol{\alpha}^S)^\top (\mathbf{Z} + \mathbf{Z}^\top) \mathbf{1}_n - \langle \mathbf{X}_{S,\cdot}^\top \mathbf{X}_{S,\cdot}, \mathbf{Z} \rangle \\
& \stackrel{(ii)}{=} \left\langle \lambda^S \mathbf{I}_n + \frac{1}{2} \mathbf{1}_n (\boldsymbol{\alpha}^S)^\top + \frac{1}{2} \boldsymbol{\alpha}^S \mathbf{1}_n^\top - \mathbf{X}_{S,\cdot}^\top \mathbf{X}_{S,\cdot} - \mathbf{B}^S, \mathbf{Z} \right\rangle + \langle \mathbf{B}^S, \mathbf{Z} \rangle \\
& = \langle \mathbf{W}^S, \mathbf{Z} \rangle + \langle \mathbf{B}^S, \mathbf{Z} \rangle
\end{aligned}$$

where step (i) uses primal constraints  $\text{tr}(\mathbf{Z}) = K$ ,  $\mathbf{Z}^\top = \mathbf{Z}$  and  $\mathbf{Z}\mathbf{1}_n = \mathbf{1}_n$ , step (ii) uses  $\text{tr}(\mathbf{Z}) = \langle \mathbf{I}_n, \mathbf{Z} \rangle$ , and added and subtracted  $\langle \mathbf{B}^S, \mathbf{Z} \rangle$ . This duality gap is zero if  $\langle \mathbf{W}^S, \mathbf{Z} \rangle = 0$  (C3) and  $\langle \mathbf{B}^S, \mathbf{Z} \rangle = 0$  (C4).

**3. Condition (C5) from the block-diagonal structure.** Finally, we derive condition (C5), which ensures that  $\mathbf{Z}^*$  is the unique solution to the primal SDP. To this end, we first show that it is the only primal feasible point with the following block-diagonal structure: where  $\mathbf{Z}_{G_k^*, G_l^*} = 0$  for all  $1 \leq k \neq l \leq K$ :

$$\mathbf{Z} = \begin{bmatrix} \mathbf{Z}^{(1)} & \mathbf{0} & \cdots & \mathbf{0} \\ \mathbf{0} & \mathbf{Z}^{(2)} & \cdots & \mathbf{0} \\ \vdots & \vdots & \ddots & \vdots \\ \mathbf{0} & \mathbf{0} & \cdots & \mathbf{Z}^{(K)} \end{bmatrix}.$$

We use proof by contradiction. Suppose there exists a primal feasible  $\mathbf{Z} \neq \mathbf{Z}^*$  with the block diagonal structure described above. By the primal constraint  $\mathbf{Z}\mathbf{1}_n = \mathbf{1}_n$ , each block  $\mathbf{Z}^{(k)}$  satisfies  $\mathbf{Z}^{(k)}\mathbf{1}_{|G_k^*|} = \mathbf{1}_{|G_k^*|}$ , which implies that  $(1, n_k^{-1/2}\mathbf{1}_{|G_k^*|})$  is an eigenvalue-eigenvector pair of  $\mathbf{Z}^{(k)}$ . Since the trace of a matrix equals the sum of its eigenvalues, this implies  $\text{tr}(\mathbf{Z}^{(k)}) \geq 1$  for every  $k$ . Combining this with the overall trace constraint  $\text{tr}(\mathbf{Z}) = \sum_{k=1}^K \text{tr}(\mathbf{Z}^{(k)}) = K$ , we

deduce that  $\text{tr}(\mathbf{Z}^{(k)}) = 1$  for every  $k$ . Additionally, each  $\mathbf{Z}^{(k)}$  is positive semidefinite, due to the primal constraint  $\mathbf{Z} \succeq 0$ , along with the Schur complement condition for the positive semidefiniteness of block matrices. Then  $\mathbf{Z}^{(k)}$  must take the form  $n_k^{-1} \mathbf{1}_{|G_k^*|} \mathbf{1}_{|G_k^*|}^\top$ , since 1 is the only nonzero eigenvalue of  $\mathbf{Z}^{(k)}$ , corresponding to the eigenvector  $n_k^{-1/2} \mathbf{1}_{|G_k^*|}$ . Consequently,  $\mathbf{Z} = \mathbf{Z}^*$ , a contradiction.

Given this block diagonal structure and the condition  $\text{tr}(\mathbf{B}^S \mathbf{Z}^*) = 0$ , we conclude that  $\mathbf{Z}^*$  is the unique solution to the primal SDP problem if (C1)-(C4) is satisfied and  $\mathbf{B}_{G_k^*, G_l^*}^S > 0$  for all  $1 \leq k \neq l \leq K$ . This corresponds to condition (C5) and completes the proof of Lemma 13.  $\square$

#### C.4.2 Proof of Lemma 14

The proof proceeds in three steps:

1. Preliminary computations,
2. Necessary condition for  $\boldsymbol{\alpha}^S$ ,
3. Necessary condition for  $\mathbf{B}^S$ .

*Proof.* Throughout the proof, we assume that conditions (C1)–(C5) from 13 are satisfied. Recall that true cluster membership matrix is defined as  $\mathbf{Z}^* = \sum_{k=1}^K |G_k^*|^{-1} \mathbf{1}_{G_k^*} \mathbf{1}_{G_k^*}^\top$ , where  $\mathbf{1}_{G_k^*}$ , as defined in Section 1, is the indicator vector for membership in  $G_k^*$ .

**1. Preliminary computations.** We first summarize the results for reference. The derivations will follow.

$$((\mathbf{X}_{S,\cdot}^\top \mathbf{X}_{S,\cdot}) \mathbf{1}_{G_l^*})_{G_k^*} = |G_l^*| \mathbf{X}_{S,G_k^*}^\top \bar{\mathbf{X}}_{S,l}^*, \text{ for } (k, l) \in [K]^2 \text{ (no condition required)}, \quad (32)$$

$$\mathbf{1}_{G_k^*}^\top \mathbf{W}^S \mathbf{1}_{G_k^*} = 0 \text{ for } k \in [K] \text{ (by (C2) and (C3))}, \quad (33)$$

$$\mathbf{W}^S \mathbf{1}_{G_k^*} = \mathbf{0} \text{ for } k \in [K] \text{ (by (C2) and (C3))}, \quad (34)$$

$$\mathbf{B}_{G_k^*, G_k^*}^S = \mathbf{0} \text{ for } k \in [K] \text{ (by (C4))} \quad (35)$$

$$(\mathbf{B}^S \mathbf{1}_{G_k^*})_{G_k^*} = 0 \text{ for } k \in [K] \text{ (by (C4))}, \text{ and} \quad (36)$$

$$(\mathbf{B}^S \mathbf{1}_{G_l^*})_{G_k^*} = \mathbf{B}_{G_k^*, G_l^*}^S \mathbf{1}_{|G_l^*|} \text{ for } 1 \leq k \neq l \leq K \text{ (no condition required)}. \quad (37)$$

We start with (32). For  $1 \leq k \leq K$  and  $1 \leq l \leq K$ , using only the definition of  $\mathbf{1}_{G_k^*}$  and  $\mathbf{1}_{G_l^*}$  given in Section 1, we have

$$\begin{aligned} ((\mathbf{X}_{S,\cdot}^\top \mathbf{X}_{S,\cdot}) \mathbf{1}_{G_l^*})_{G_k^*} &= (\mathbf{X}_{S,\cdot}^\top \mathbf{X}_{S,\cdot})_{G_k^*, G_k^*} (\mathbf{1}_{G_l^*})_{G_k^*} + (\mathbf{X}_{S,\cdot}^\top \mathbf{X}_{S,\cdot})_{G_k^*, (G_k^*)^C} (\mathbf{1}_{G_l^*})_{(G_k^*)^C} \\ &\stackrel{(i)}{=} (\mathbf{X}_{S,\cdot}^\top \mathbf{X}_{S,\cdot})_{G_k^*, (G_k^*)^C} (\mathbf{1}_{G_l^*})_{(G_k^*)^C} \\ &= (\mathbf{X}_{S,\cdot}^\top \mathbf{X}_{S,\cdot})_{G_k^*, G_l^*} \mathbf{1}_{|G_l^*|} \\ &= (\mathbf{X}_{S,G_k^*})^\top \mathbf{X}_{S,G_l^*} \mathbf{1}_{|G_l^*|} \\ &= |G_l^*| \mathbf{X}_{S,G_k^*}^\top \bar{\mathbf{X}}_{S,l}^*, \end{aligned}$$

where step (i) uses  $(\mathbf{1}_{G_l^*})_{G_k^*} = 0$ .

Using the definition of  $\mathbf{Z}^*$  and condition (C3), which states that  $\langle \mathbf{W}^S, \mathbf{Z}^* \rangle = 0$ , we obtain:

$$\langle \mathbf{W}^S, \mathbf{Z}^* \rangle = \sum_{k=1}^K \frac{1}{|G_k^*|} \langle \mathbf{W}^S, \mathbf{1}_{G_k^*} \mathbf{1}_{G_k^*}^\top \rangle = \sum_{k=1}^K \frac{1}{|G_k^*|} \mathbf{1}_{G_k^*}^\top \mathbf{W}^S \mathbf{1}_{G_k^*} = 0.$$

By the condition (C2), which states that  $\mathbf{W}^S \succeq 0$ , we have  $\mathbf{1}_{G_k^*}^\top \mathbf{W}^S \mathbf{1}_{G_k^*} \geq 0$  for all  $k = 1, \dots, K$ . This along with the equality above implies (33):

$$\mathbf{1}_{G_k^*}^\top \mathbf{W}^S \mathbf{1}_{G_k^*} = 0 \text{ for all } k = 1, \dots, K.$$

Given that  $\mathbf{W}^S \succeq 0$ , the function  $\mathbf{v} \mapsto \mathbf{v}^\top \mathbf{W}^S \mathbf{v}$  is convex and bounded below by 0. Therefore,

$\mathbf{1}_{G_k^*}^\top \mathbf{W}^S \mathbf{1}_{G_k^*} = 0$  implies that  $\mathbf{1}_{G_k^*}$  minimizes  $\mathbf{v}^\top \mathbf{W}^S \mathbf{v}$ . By the first order condition, we obtain (34)

$$\mathbf{W}^S \mathbf{1}_{G_k^*} = \mathbf{0} \text{ for all } k = 1, \dots, K.$$

By condition (C4), which states that  $\langle \mathbf{B}^S, \mathbf{Z}^* \rangle = 0$ , and the block-diagonal structure of  $\mathbf{Z}^*$ , we obtain (35):

$$\mathbf{B}_{G_k^*, G_k^*}^S = \mathbf{0},$$

which implies (36):

$$(\mathbf{B}^S \mathbf{1}_{G_k^*})_{G_k^*} = \mathbf{B}_{G_k^*, G_k^*}^S (\mathbf{1}_{G_k^*})_{G_k^*} + \mathbf{B}_{G_k^*, G_k^* C}^S (\mathbf{1}_{G_k^*})_{G_k^* C} = 0.$$

On the other hand, since the off-diagonal block  $\mathbf{B}_{G_k^*, G_l^*}^S$  may be nonzero for  $k \neq l$ , we can only conclude as (37):

$$(\mathbf{B}^S \mathbf{1}_{G_l^*})_{G_k^*} = \mathbf{B}_{G_k^*, G_l^*}^S \mathbf{1}_{|G_l^*|}.$$

**2. Necessary condition for  $\boldsymbol{\alpha}^S$ .** Our goal is to derive condition (18). Only using the definition of  $\mathbf{W}^S$  given in Lemma 13, we compute:

$$\begin{aligned} \mathbf{W}^S \mathbf{1}_{G_k^*} &= \lambda^S \mathbf{1}_{G_k^*} + \frac{1}{2} \mathbf{1}_n (\boldsymbol{\alpha}^S)^\top \mathbf{1}_{G_k^*} + \frac{1}{2} \boldsymbol{\alpha}^S \mathbf{1}_n^\top \mathbf{1}_{G_k^*} - (\mathbf{X}_{S,\cdot}^\top \mathbf{X}_{S,\cdot}) \mathbf{1}_{G_k^*} - \mathbf{B}^S \mathbf{1}_{G_k^*} \\ &= \lambda^S \mathbf{1}_{G_k^*} + \frac{1}{2} \left( \sum_{i \in G_k^*} \boldsymbol{\alpha}_i^S \right) \mathbf{1}_n + \frac{|G_k^*|}{2} \boldsymbol{\alpha}^S - (\mathbf{X}_{S,\cdot}^\top \mathbf{X}_{S,\cdot}) \mathbf{1}_{G_k^*} - \mathbf{B}^S \mathbf{1}_{G_k^*}. \end{aligned} \quad (38)$$

Then the restriction of  $\mathbf{W}^S \mathbf{1}_{G_k^*}$  to the indices in  $G_k^*$  is given by:

$$(\mathbf{W}^S \mathbf{1}_{G_k^*})_{G_k^*} \stackrel{(i)}{=} \lambda^S \mathbf{1}_{|G_k^*|} + \frac{1}{2} \left( \sum_{i \in G_k^*} \boldsymbol{\alpha}_i^S \right) \mathbf{1}_{|G_k^*|} + \frac{|G_k^*|}{2} \boldsymbol{\alpha}_{G_k^*}^S - |G_k^*| \mathbf{X}_{S,G_k^*}^\top \bar{\mathbf{X}}_{S,k}^* \stackrel{(ii)}{=} 0, \quad (39)$$

where step (i) uses (32) and (36), which require (C4), and step (ii) uses (34), which requires (C2) and (C3). Rearranging the terms, this computation implies:

$$\boldsymbol{\alpha}_{G_k^*}^S = 2 \mathbf{X}_{S,G_k^*}^\top \bar{\mathbf{X}}_{S,k}^* - \left\{ \frac{2\lambda^S}{|G_k^*|} + \frac{1}{|G_k^*|} \left( \sum_{i \in G_k^*} \boldsymbol{\alpha}_i^S \right) \right\} \mathbf{1}_{|G_k^*|}. \quad (40)$$

It remains to express  $\sum_{i \in G_k^*} \boldsymbol{\alpha}_i^S$  on the right-hand side solely in terms of the data and  $\lambda^S$ .

To this end, we compute:

$$\mathbf{1}_{G_k^*}^\top \mathbf{W}^S \mathbf{1}_{G_k^*} \stackrel{(i)}{=} \mathbf{1}_{G_k^*}^\top \left\{ \lambda^S \mathbf{1}_{G_k^*} + \frac{1}{2} \left( \sum_{i \in G_k^*} \boldsymbol{\alpha}_i^S \right) \mathbf{1}_n + \frac{|G_k^*|}{2} \boldsymbol{\alpha}^S - (\mathbf{X}_{S,\cdot}^\top \mathbf{X}_{S,\cdot}) \mathbf{1}_{G_k^*} - \mathbf{B}^S \mathbf{1}_{G_k^*} \right\}$$

$$\begin{aligned}
&\stackrel{(ii)}{=} \lambda^S |G_k^*| + |G_k^*| \sum_{i \in G_k^*} \boldsymbol{\alpha}_i^S - |G_k^*|^2 \|\bar{\mathbf{X}}_{S,k}^*\|_2^2 \\
&\stackrel{(iii)}{=} 0,
\end{aligned} \tag{41}$$

where step (i) uses (38) step (ii) uses (35), which require (C4), and step (iii) uses (33), which require (C2) and (C3). Rearranging the terms, this computation implies:

$$\sum_{i \in G_k^*} \boldsymbol{\alpha}_i^S = |G_k^*| \|\bar{\mathbf{X}}_{S,k}^*\|_2^2 - \lambda^S. \tag{42}$$

This with (40) implies:

$$\boldsymbol{\alpha}_{G_k^*}^S = 2\mathbf{X}_{S,G_k^*}^\top \bar{\mathbf{X}}_{S,k}^* - \left\{ \frac{\lambda^S}{|G_k^*|} + \|\bar{\mathbf{X}}_{S,k}^*\|_2^2 \right\} \mathbf{1}_{|G_k^*|}.$$

This corresponds precisely to condition 18.

**3. Necessary condition for  $\mathbf{B}^S$ .** Our goal is to derive condition (19). Fix  $1 \leq k \neq l \leq K$ .

Similar to (38), only using the definition of  $\mathbf{W}^S$  given in Lemma 13, we compute:

$$\mathbf{W}^S \mathbf{1}_{G_l^*} = \lambda^S \mathbf{1}_{G_l^*} + \frac{1}{2} \left( \sum_{i \in G_l^*} \boldsymbol{\alpha}_i^S \right) \mathbf{1}_n + \frac{|G_l^*|}{2} \boldsymbol{\alpha}^S - (\mathbf{X}_{S,\cdot}^\top \mathbf{X}_{S,\cdot}) \mathbf{1}_{G_l^*} - \mathbf{B}^S \mathbf{1}_{G_l^*}.$$

Then, the restriction of  $\mathbf{W}^S \mathbf{1}_{G_l^*}$  to the indices in  $G_k^*$  is given by:

$$(\mathbf{W}^S \mathbf{1}_{G_l^*})_{G_k^*} \stackrel{(i)}{=} \frac{1}{2} \left( \sum_{i \in G_l^*} \boldsymbol{\alpha}_i^S \right) \mathbf{1}_{|G_k^*|} + \frac{|G_l^*|}{2} \boldsymbol{\alpha}_{G_k^*}^S - |G_l^*| \mathbf{X}_{S,G_k^*}^\top \bar{\mathbf{X}}_{S,l}^* - \mathbf{B}_{G_k^*, G_l^*}^S \mathbf{1}_{|G_l^*|} \stackrel{(ii)}{=} 0, \tag{43}$$

where step (i) uses  $(\mathbf{1}_{G_l^*})_{G_k^*} = 0$ , (32), and (37), and step (ii) uses (34), which requires (C2) and (C3). Rearranging the terms, this computation implies:

$$\mathbf{B}_{G_k^*, G_l^*}^S \mathbf{1}_{|G_l^*|} = \frac{1}{2} \left( \sum_{i \in G_l^*} \boldsymbol{\alpha}_i^S \right) \mathbf{1}_{|G_k^*|} + \frac{|G_l^*|}{2} \boldsymbol{\alpha}_{G_k^*}^S - |G_l^*| \mathbf{X}_{S,G_k^*}^\top \bar{\mathbf{X}}_{S,l}^*. \tag{44}$$

Using (42) with  $k$  replaced by  $l$ , and (40), which require (C2) and (C3), this computation implies:

$$\mathbf{B}_{G_k^*, G_l^*}^S \mathbf{1}_{|G_l^*|} = \left\{ \frac{|G_l^*|}{2} \|\bar{\mathbf{X}}_{S,l}^*\|_2^2 - \frac{|G_k^*| + |G_l^*|}{2|G_k^*|} \lambda^S - \frac{|G_l^*|}{2} \|\bar{\mathbf{X}}_{S,k}^*\|_2^2 \right\} \mathbf{1}_{|G_k^*|}$$

$$+ |G_l^*| \mathbf{X}_{S, G_k^*}^\top \bar{\mathbf{X}}_{S, k}^* - |G_l^*| \mathbf{X}_{S, G_k^*}^\top \bar{\mathbf{X}}_{S, l}^*.$$

This implies that, for  $i \in G_k^*$ , the  $i$ th row sum of  $\mathbf{B}_{G_k^* G_l^*}^S$  is expressed as:

$$\begin{aligned} (\mathbf{B}_{G_k^* G_l^*}^S \mathbf{1}_{|G_l^*|})_i &\stackrel{(i)}{=} -\frac{|G_k^*| + |G_l^*|}{2|G_k^*|} \lambda^S + \frac{|G_l^*|}{2} (\|\bar{\mathbf{X}}_{S, l}^*\|_2^2 - 2\mathbf{X}_{S, i}^\top \bar{\mathbf{X}}_{S, l}^* + \|\mathbf{X}_{S, i}\|_2^2) \\ &\quad - \frac{|G_l^*|}{2} (\|\bar{\mathbf{X}}_{S, k}^*\|_2^2 - 2\mathbf{X}_{S, i}^\top \bar{\mathbf{X}}_{S, k}^* + \|\mathbf{X}_{S, i}\|_2^2), \\ &= -\frac{|G_k^*| + |G_l^*|}{2|G_k^*|} \lambda^S + \frac{|G_l^*|}{2} (\|\bar{\mathbf{X}}_{S, l}^* - \mathbf{X}_{S, i}\|_2^2 - \|\bar{\mathbf{X}}_{S, k}^* - \mathbf{X}_{S, i}\|_2^2), \end{aligned}$$

where step (i) adds and subtracts  $\frac{|G_l^*|}{2} \|\mathbf{X}_{S, i}\|_2^2$ . This concludes the derivation of condition (19) and completes the proof of Lemma 14.  $\square$

**Remark 28.** If we construct  $\boldsymbol{\alpha}^S$  and  $\mathbf{B}_{G_k^* G_l^*}^S$  according to conditions (18) and (19), then step (ii) in (39) and (43) hold without requiring conditions (C2) and (C3), as the construction is explicitly designed to satisfy these equalities. This observation is useful in the proof of Lemma 17, presented in Appendix C.4.4.

### C.4.3 Proof of Lemma 16

Let  $S \subset [p]$  be a support set, and consider the corresponding primal SDP problem (17). We show that constructing  $\dot{\boldsymbol{\alpha}}^S(\lambda^S)$ ,  $\dot{\mathbf{B}}^S(\lambda^S)$  and  $\dot{\mathbf{W}}^S(\lambda^S)$  as in Lemma 15 guarantees the following:

1. Conditions (C3) and (C4) in Lemma 13 are satisfied for any  $\lambda^S$ ,
2. Conditions (C1) and (C5) are satisfied for  $\lambda^S < U^S(\mathbf{X})$ .

*Proof.* For notational simplicity, we omit the notation  $\lambda^S$  from  $\dot{\boldsymbol{\alpha}}^S(\lambda^S)$ ,  $\dot{\mathbf{B}}^S(\lambda^S)$ , and  $\dot{\mathbf{W}}^S(\lambda^S)$  and denote them  $\dot{\boldsymbol{\alpha}}^S$ ,  $\dot{\mathbf{B}}^S$ , and  $\dot{\mathbf{W}}^S$ , respectively.

**1. Conditions (C3) and (C4).** Condition (C4) follows directly from the block-diagonal structure of both  $\mathbf{Z}^* = \sum_{k=1}^K |G_k^*|^{-1} \mathbf{1}_{G_k^*} \mathbf{1}_{G_k^*}^\top$  and  $\dot{\mathbf{B}}^S$ . To verify condition (C3), which requires that  $\langle \dot{\mathbf{W}}^S, \mathbf{Z}^* \rangle = 0$ , we use the definition  $\mathbf{Z}^* = \sum_{k=1}^K |G_k^*|^{-1} \mathbf{1}_{G_k^*} \mathbf{1}_{G_k^*}^\top$  to expand the inner product as

$$\langle \dot{\mathbf{W}}^S, \mathbf{Z}^* \rangle = \frac{1}{|G_k^*|} \sum_{k=1}^K \mathbf{1}_{G_k^*}^\top \dot{\mathbf{W}}^S \mathbf{1}_{G_k^*}.$$

Thus, it suffices to verify that  $\mathbf{1}_{G_k^*}^\top \dot{\mathbf{W}}^S \mathbf{1}_{G_k^*} = 0$  for all  $k = 1, \dots, K$ . Since our construction sets  $\dot{\mathbf{B}}_{G_k^*, G_k^*}^S = \mathbf{0}$ , we can invoke (41) to state that

$$\mathbf{1}_{G_k^*}^\top \dot{\mathbf{W}}^S \mathbf{1}_{G_k^*} = \lambda^S |G_k^*| + |G_k^*| \sum_{i \in G_k^*} (\dot{\alpha}^S(\lambda_S))_i - |G_k^*|^2 \|\bar{\mathbf{X}}_{S,k}^*\|_2^2.$$

Now using our construction of  $\dot{\alpha}^S(\lambda_S)$ , recalled below:

$$\dot{\alpha}_{G_k^*}^S = 2\mathbf{X}_{S,G_k^*}^\top \bar{\mathbf{X}}_{S,k}^* - \frac{\lambda^S}{|G_k^*|} \mathbf{1}_{|G_k^*|} - \|\bar{\mathbf{X}}_{S,k}^*\|_2^2 \mathbf{1}_{|G_k^*|},$$

we can conclude:

$$\mathbf{1}_{G_k^*}^\top \dot{\mathbf{W}}^S \mathbf{1}_{G_k^*} = \lambda^S |G_k^*| + 2|G_k^*|^2 \|\bar{\mathbf{X}}_{S,k}^*\|_2^2 - \lambda^S |G_k^*| - |G_k^*|^2 \|\bar{\mathbf{X}}_{S,k}^*\|_2^2 - |G_k^*|^2 \|\bar{\mathbf{X}}_{S,k}^*\|_2^2 = 0.$$

This concludes the verification of condition (C3).

**2. Conditions (C1) and (C5).** We now show that the condition  $\lambda^S < U^S(\mathbf{X})$  ensures conditions (C1) and (C5). Since our construction sets the diagonal block  $\dot{\mathbf{B}}_{G_k^*, G_k^*}^S$  as a zero matrix, it suffices to show that if  $\lambda^S < U^S(\mathbf{X})$ , then  $\dot{\mathbf{B}}_{G_k^*, G_l^*}^S > 0$  for all  $1 \leq k \neq l \leq K$ . By our construction in (21), for  $i \in G_k^*$  and  $j \in G_l^*$ , the  $(i, j)$ th element of  $\dot{\mathbf{B}}_{G_k^*, G_l^*}^S$  is

$$\frac{r_i^{(k,l,S)} r_j^{(l,k,S)}}{\sum_{j \in G_l^*} r_j^{(l,k,S)}}. \quad (45)$$

where

$$r_i^{(k,l,S)} = -\frac{|G_k^*| + |G_l^*|}{2|G_k^*|} \lambda^S + \frac{|G_l^*|}{2} (\|\bar{\mathbf{X}}_{S,l}^* - \mathbf{X}_{S,i}\|_2^2 - \|\bar{\mathbf{X}}_{S,k}^* - \mathbf{X}_{S,i}\|_2^2),$$

and

$$r_j^{(l,k,S)} = -\frac{|G_l^*| + |G_k^*|}{2|G_l^*|} \lambda^S + \frac{|G_k^*|}{2} (\|\bar{\mathbf{X}}_{S,k}^* - \mathbf{X}_{S,j}\|_2^2 - \|\bar{\mathbf{X}}_{S,l}^* - \mathbf{X}_{S,j}\|_2^2).$$

Therefore, all elements of  $\dot{\mathbf{B}}_{G_k^*, G_k^*}^S$  for all  $1 \leq k \neq l \leq K$  are strictly positive if, for all  $1 \leq k \neq l \leq K$  and  $i \in G_k^*$ , the inequality  $r_i^{(k,l,S)} > 0$  holds, or equivalently,

$$\lambda^S < \frac{|G_l^*||G_k^*|}{|G_k^*| + |G_l^*|} (\|\bar{\mathbf{X}}_{S,l}^* - \mathbf{X}_i\|_2^2 - \|\bar{\mathbf{X}}_{S,k}^* - \mathbf{X}_i\|_2^2).$$

This condition is precisely  $\lambda^S < U^S(\mathbf{X})$ , completing the proof of Lemma 16.  $\square$

#### C.4.4 Proof of Lemma 17

The proof proceeds in four steps:

1. Reduction to uniform control of a quadratic form over a subspace (equation (46)),
2. Derivation of  $L_1^S(\mathbf{X})$  (equation (48)),
3. Derivation of  $t_{lk}^S(\lambda^S)$  (equation (49)),
4. Derivation of  $T_{1,kl}^S$ ,  $T_{2,kl}^S$ , and  $T_{3,kl}^S$  (equation 50).

*Proof.* Given  $\lambda_S$ , we construct  $\dot{\mathbf{B}}(\lambda_S)$ ,  $\dot{\boldsymbol{\alpha}}^S(\lambda_S)$ , and  $\dot{\mathbf{W}}^S(\lambda_S)$  according to Lemma 15 and denote them by  $\dot{\boldsymbol{\alpha}}^S$ ,  $\dot{\mathbf{B}}^S$ , and  $\dot{\mathbf{W}}^S$ , respectively, for notational simplicity.

**1. Reduction to uniform control of a quadratic form over a subspace.** By Lemma 16, these constructed dual variables satisfy condition (C4) of Lemma 13. Therefore, by Remark 28, for any  $k = 1, \dots, K$ , we have  $(\dot{\mathbf{W}}^S \mathbf{1}_{G_k^*})_{G_k^*} = \mathbf{0}$ , from (18), and for all  $l \neq k$ , we have  $(\dot{\mathbf{W}}^S \mathbf{1}_{G_k^*})_{G_l^*} = \mathbf{0}$  by (19). Therefore, we have  $\dot{\mathbf{W}}^S \mathbf{1}_{G_k^*} = \mathbf{0}$  for  $k = 1, \dots, K$ . This implies that  $\mathbf{1}_{G_1^*}, \dots, \mathbf{1}_{G_K^*}$  are eigenvectors of  $\dot{\mathbf{W}}^S$  corresponding to zero eigenvalues. Since any vector

in  $\mathbb{R}^n$  can be decomposed into the sum of its projections onto  $\text{span}(\mathbf{1}_{G_k^*} : k \in [K])$  and its orthogonal complement, denoted as  $\Gamma_K$ , to show that  $\dot{\mathbf{W}}^S \succeq 0$ , it suffices to prove that

$$\mathbf{v}^\top \dot{\mathbf{W}}^S \mathbf{v} \geq 0 \quad \text{for all } \mathbf{v} \in \Gamma_K \text{ such that } \|\mathbf{v}\|_2 = 1. \quad (46)$$

**2. Derivation of  $L_1^S(\mathbf{X})$ .** By the definition of  $\Gamma_k$ ,  $\mathbf{v} \in \Gamma_k$  implies  $\mathbf{v}^\top \mathbf{1}_{G_1^*} = \mathbf{v}^\top \mathbf{1}_{G_2^*} = \dots = \mathbf{v}^\top \mathbf{1}_{G_K^*} = 0$ , which implies

$$\sum_{j \in G_k^*} v_j = \sum_{i=1}^n v_i = 0 \text{ for all } k = 1, \dots, K. \quad (47)$$

Now we compute the quadratic form  $\mathbf{v}^\top \dot{\mathbf{W}}^S \mathbf{v}$  for  $\mathbf{v} \in \Gamma_K$  such that  $\|\mathbf{v}\|_2 = 1$ :

$$\begin{aligned} \mathbf{v}^\top \dot{\mathbf{W}}^S \mathbf{v} &\stackrel{(i)}{=} \lambda^S \mathbf{v}^\top \mathbf{I}_n \mathbf{v} + \frac{1}{2} \mathbf{v}^\top \mathbf{1}_n (\boldsymbol{\alpha}^S)^\top \mathbf{v} + \frac{1}{2} \mathbf{v}^\top \boldsymbol{\alpha}^S \mathbf{1}_n^\top \mathbf{v} - \mathbf{v}^\top \mathbf{X}_{S,\cdot}^\top \mathbf{X}_{S,\cdot} \mathbf{v} - \mathbf{v}^\top \dot{\mathbf{B}}^S \mathbf{v} \\ &\stackrel{(ii)}{=} \lambda^S + (\mathbf{v}^\top \boldsymbol{\alpha}_S) \sum_{i=1}^n v_i - \|\mathbf{X}_{S,\cdot} \mathbf{v}\|_2^2 - \mathbf{v}^\top \dot{\mathbf{B}}^S \mathbf{v} \\ &\stackrel{(ii)}{=} \lambda^S - \|\mathbf{X}_{S,\cdot} \mathbf{v}\|_2^2 - \mathbf{v}^\top \dot{\mathbf{B}}^S \mathbf{v}, \end{aligned}$$

where step (i) uses the construction  $\dot{\mathbf{W}}^S = \lambda^S \mathbf{I}_n + \frac{1}{2} \mathbf{1}_n (\dot{\boldsymbol{\alpha}}^S)^\top + \frac{1}{2} \dot{\boldsymbol{\alpha}}^S \mathbf{1}_n^\top - \mathbf{X}_{S,\cdot}^\top \mathbf{X}_{S,\cdot} - \dot{\mathbf{B}}^S$ , step (ii) uses  $\mathbf{v}^\top \mathbf{I}_n \mathbf{v} = \|\mathbf{v}\|^2 = 1$ , and step (ii) uses (47). Using our model and notation in Definition 12,

$$\mathbf{X}_{S,\cdot} \mathbf{v} = \sum_{i=1}^n v_i \mathbf{X}_{S,i} = \sum_{k=1}^K \left( \sum_{i \in G_k^*} v_i (\boldsymbol{\mu}_k)_S + \sum_{i=1}^n v_i \mathcal{E}_{S,i} \right) \stackrel{(i)}{=} \sum_{i=1}^n v_i \mathcal{E}_{S,i} = \mathcal{E}_{S,\cdot} \mathbf{v},$$

where step (i) uses (47). Therefore, a sufficient condition for (46) is:

$$\lambda^S \geq \underbrace{\sup_{\mathbf{v} \in \Gamma_K, \|\mathbf{v}\|_2=1} \|\mathcal{E}_{S,\cdot} \mathbf{v}\|_2^2}_{L_1^S(\mathbf{X})} + \sup_{\mathbf{v} \in \Gamma_K, \|\mathbf{v}\|_2=1} \mathbf{v}^\top \dot{\mathbf{B}}^S \mathbf{v}. \quad (48)$$

This completes the derivation of  $L_1^S(\mathbf{X})$ .

**3. Derivation of  $t_{lk}^S(\lambda^S)$ .** Now we start to derive  $L_2^S(\mathbf{X}, \lambda^S)$ . Recall from Lemma 15 that given  $\lambda^S$ , we construct  $\dot{\mathbf{B}}$  as a block-diagonal matrix, where the diagonal blocks are zero matrices and for  $1 \leq k \neq l \leq K$ , the  $(k, l)$ th off-diagonal block is defined as:

$$\dot{\mathbf{B}}_{G_k^*, G_l^*}^S = \frac{1}{\mathbf{1}_{|G_l^*|}^\top \mathbf{r}^{(l,k,S)}} \mathbf{r}^{(k,l,S)} (\mathbf{r}^{(l,k,S)})^\top,$$

with  $\mathbf{r}^{(k,l,S)} \in \mathbb{R}^{|G_k^*|}$  defined componentwise by

$$r_i^{(k,l,S)} = -\frac{|G_k^*| + |G_l^*|}{2|G_k^*|} \lambda^S + \frac{|G_l^*|}{2} (\|\bar{\mathbf{X}}_{S,l}^* - \mathbf{X}_{S,i}\|_2^2 - \|\bar{\mathbf{X}}_{S,k}^* - \mathbf{X}_{S,i}\|_2^2).$$

Using this definition, we compute  $\mathbf{v}^\top \dot{\mathbf{B}}^S \mathbf{v}$  in (48):

$$\mathbf{v}^\top \dot{\mathbf{B}}^S \mathbf{v} \stackrel{(i)}{=} \sum_{1 \leq k \neq l \leq K} \mathbf{v}_{G_k^*}^\top \dot{\mathbf{B}}_{G_k^*, G_l^*}^S \mathbf{v}_{G_l^*} \stackrel{(ii)}{=} \sum_{1 \leq k \neq l \leq K} \sum_{i \in G_k^*} \sum_{j \in G_l^*} \underbrace{\frac{(\mathbf{v}_{G_k^*}^\top \mathbf{r}^{(k,l,S)})(\mathbf{v}_{G_l^*}^\top \mathbf{r}^{(l,k,S)})}{\mathbf{1}_{|G_l^*|}^\top \mathbf{r}^{(l,k,S)}}}_{=t_{lk}^S(\lambda^S)}, \quad (49)$$

where step (i) uses  $\dot{\mathbf{B}}_{G_k^*, G_k^*}^S = \mathbf{0}$  for  $k = 1, \dots, K$ , and step (ii) uses our construction of  $\dot{\mathbf{B}}_{G_k^*, G_l^*}^S$ .

**4. Derivation of  $T_{1,kl}^S$ ,  $T_{2,kl}^S$ , and  $T_{3,kl}^S$ .** From (49), we analyze one term in the numerator:

$$\begin{aligned} & \mathbf{v}_{G_k^*}^\top \mathbf{r}^{(k,l,S)} \\ &= \sum_{i \in G_k^*} v_i r_i^{(k,l,S)} \\ &= \sum_{i \in G_k^*} v_i \left\{ -\frac{|G_k^*| + |G_l^*|}{2|G_k^*|} \lambda^S + \frac{|G_l^*|}{2} (\|\bar{\mathbf{X}}_{S,l}^* - \mathbf{X}_{S,i}\|_2^2 - \|\bar{\mathbf{X}}_{S,k}^* - \mathbf{X}_{S,i}\|_2^2) \right\} \\ &\stackrel{(i)}{=} \frac{|G_l^*|}{2} \sum_{i \in G_k^*} v_i (\|\bar{\mathbf{X}}_{S,l}^* - \mathbf{X}_{S,i}\|_2^2 - \|\bar{\mathbf{X}}_{S,k}^* - \mathbf{X}_{S,i}\|_2^2) \\ &= \frac{|G_l^*|}{2} \sum_{i \in G_k^*} v_i (\|\bar{\mathbf{X}}_{S,l}^*\|_2^2 + \|\mathbf{X}_{S,i}\|_2^2 - 2\langle \bar{\mathbf{X}}_{S,l}^*, \mathbf{X}_{S,i} \rangle - \|\bar{\mathbf{X}}_{S,k}^*\|_2^2 - \|\mathbf{X}_{S,i}\|_2^2 + 2\langle \bar{\mathbf{X}}_{S,k}^*, \mathbf{X}_{S,i} \rangle) \\ &\stackrel{(ii)}{=} |G_l^*| \sum_{i \in G_k^*} v_i \langle \bar{\mathbf{X}}_{S,k}^* - \bar{\mathbf{X}}_{S,l}^*, \mathbf{X}_{S,i} \rangle \end{aligned}$$

$$\begin{aligned}
&\stackrel{(iii)}{=} |G_l^*| \sum_{i \in G_k^*} v_i \langle (\boldsymbol{\mu}_k^* - \boldsymbol{\mu}_l^*)_S + \bar{\mathcal{E}}_{S,k}^* - \bar{\mathcal{E}}_{S,l}^*, \mathcal{E}_{S,i} \rangle \\
&= |G_l^*| \sum_{i \in G_k^*} v_i \langle (\boldsymbol{\mu}_k^* - \boldsymbol{\mu}_l^*)_{S \cap S_0}, \mathcal{E}_{S \cap S_0, i} \rangle + |G_l^*| \sum_{i \in G_k^*} v_i \langle \bar{\mathcal{E}}_{S,k}^* - \bar{\mathcal{E}}_{S,l}^*, \mathcal{E}_{S,i} \rangle \\
&= I_{kl}^S(\mathbf{v}, \mathbf{X}) + N_{kl}^S(\mathbf{v}, \mathbf{X})
\end{aligned}$$

where step (i) and (ii) use  $\sum_{i \in G_k^*} v_i = 0$  for  $k = 1, \dots, K$ , and step (iii) comes from our model and notation in Definition 12. Similarly, we have

$$\mathbf{v}_{G_l^*}^\top \mathbf{r}^{(l,k,S)} = I_{lk}^S(\mathbf{v}, \mathbf{X}) + N_{lk}^S(\mathbf{v}, \mathbf{X}).$$

Therefore, we have

$$\begin{aligned}
\mathbf{v}^\top \dot{\mathbf{B}}^S \mathbf{v} &= \sum_{1 \leq k \neq l \leq K} \sum_{i \in G_k^*} \sum_{j \in G_l^*} \frac{1}{t_{lk}^S(\lambda^S)} (I_{kl}^S(\mathbf{v}, \mathbf{X}) + N_{kl}^S(\mathbf{v}, \mathbf{X})) (I_{lk}^S(\mathbf{v}, \mathbf{X}) + N_{lk}^S(\mathbf{v}, \mathbf{X})) \\
&= \sum_{1 \leq k \neq l \leq K} \sum_{i \in G_k^*} \sum_{j \in G_l^*} \frac{1}{t_{lk}^S(\lambda^S)} (T_{1,kl}^S(\mathbf{v}) + T_{2,kl}^S(\mathbf{v}) + T_{3,kl}^S(\mathbf{v})).
\end{aligned} \tag{50}$$

Plugging this into (48) completes the proof of Lemma 17. □

#### C.4.5 Proof of Lemma 19

For notational simplicity, we assume  $\sigma^2 = 1$  here. The proof proceeds in the following steps:

1. Decomposition of  $D_{kli}^S(\mathbf{X})$  into Chi-squares, Gaussian and inner product of Gaussians,
2. Bounding the Gaussian and Chi-squares using the tail bounds,
3. Bounding the Gaussian inner product using conditioning, Gaussian tail bounds and separation condition,
4. Defining the uniform bound event,

5. Bounding the probability of the uniform bound event.

*Proof.* We proceed by following the steps outlined above in sequence.

**1. Decomposition of  $D_{kli}^S(\mathbf{X})$  into Chi-squares, Gaussian and inner product of Gaussians.** Fix indices  $1 \leq k \neq l \leq K$  and choose  $i \in G_k^*$ . Based on our model and notation in Definition 12, we consider the following decomposition of  $D_{kli}^S(\mathbf{X})$ :

$$\begin{aligned}
D_{kli}^S(\mathbf{X}) &= \|\mathbf{X}_{S,i} - \bar{\mathbf{X}}_{S,l}^*\|_2^2 - \|\mathbf{X}_{S,i} - \bar{\mathbf{X}}_{S,k}^*\|_2^2 \\
&= \|(\boldsymbol{\mu}_k^* - \boldsymbol{\mu}_l^*)_S + \mathcal{E}_{S,i} - \bar{\mathcal{E}}_{S,l}^*\|_2^2 - \|\mathcal{E}_{S,i} - \bar{\mathcal{E}}_{S,k}^*\|_2^2 \\
&= \|(\boldsymbol{\mu}_k^* - \boldsymbol{\mu}_l^*)_S + \mathcal{E}_{S,i} - \bar{\mathcal{E}}_{S,l}^*\|_2^2 - \left(\frac{|G_k^*| - 1}{|G_k^*|}\right)^2 \|\mathcal{E}_{S,i} - \bar{\mathcal{E}}_{S,k \setminus \{i\}}^*\|_2^2 \\
&\stackrel{(i)}{=} \|(\boldsymbol{\mu}_k^* - \boldsymbol{\mu}_l^*)_{S \cap S_0}\|_2^2 + \|\mathcal{E}_{S,i}\|_2^2 + \|\bar{\mathcal{E}}_{S,l}^*\|_2^2 + 2 \langle (\boldsymbol{\mu}_k^* - \boldsymbol{\mu}_l^*)_S, \mathcal{E}_{S,i} \rangle \\
&\quad - 2 \langle (\boldsymbol{\mu}_k^* - \boldsymbol{\mu}_l^*)_{S \cap S_0}, \bar{\mathcal{E}}_{S \cap S_0, l}^* \rangle - 2 \langle \bar{\mathcal{E}}_{S,l}^*, \mathcal{E}_{S,i} \rangle \\
&\quad - \left(\frac{|G_k^*| - 1}{|G_k^*|}\right)^2 \left( \|\mathcal{E}_{S,i}\|_2^2 + \|\bar{\mathcal{E}}_{S,k \setminus \{i\}}^*\|_2^2 - 2 \langle \mathcal{E}_{S,i}, \bar{\mathcal{E}}_{S,k \setminus \{i\}}^* \rangle \right) \\
&= \|(\boldsymbol{\mu}_k^* - \boldsymbol{\mu}_l^*)_{S \cap S_0}\|_2^2 + \|\bar{\mathcal{E}}_{S,l}^*\|_2^2 + \frac{2|G_k^*| - 1}{|G_k^*|^2} \|\mathcal{E}_{S,i}\|_2^2 \\
&\quad - \left(\frac{|G_k^*| - 1}{|G_k^*|}\right)^2 \|\bar{\mathcal{E}}_{S,k \setminus \{i\}}^*\|_2^2 - 2 \langle (\boldsymbol{\mu}_k^* - \boldsymbol{\mu}_l^*)_{S \cap S_0}, \bar{\mathcal{E}}_{S \cap S_0, l}^* \rangle \\
&\quad + 2 \left\langle (\boldsymbol{\mu}_k^* - \boldsymbol{\mu}_l^*)_S - \bar{\mathcal{E}}_{S,l}^* + \left(\frac{|G_k^*| - 1}{|G_k^*|}\right)^2 \bar{\mathcal{E}}_{S,k \setminus \{i\}}^*, \mathcal{E}_{S,i} \right\rangle, \tag{51}
\end{aligned}$$

where step (i) uses the sparsity assumption on cluster center difference.

The six terms in this decomposition are classified into the following categories:

- Signal:  $\|(\boldsymbol{\mu}_k^* - \boldsymbol{\mu}_l^*)_{S \cap S_0}\|_2^2$

- Chi-square noise:

$$\text{CN}_l^S := \|\bar{\mathcal{E}}_{S,l}^*\|_2^2,$$

$$\begin{aligned} \text{CN}_i^S &:= \frac{2|G_k^*| - 1}{|G_k^*|^2} \|\mathcal{E}_{S,i}\|_2^2, \text{ and} \\ \text{CN}_{ki}^S &:= - \left( \frac{|G_k^*| - 1}{|G_k^*|} \right)^2 \|\bar{\mathcal{E}}_{S,k \setminus \{i\}}\|_2^2 \end{aligned}$$

- Gaussian signal-noise interaction:

$$\text{GSN}_{kl}^S := -2\langle (\boldsymbol{\mu}_k^* - \boldsymbol{\mu}_l^*)_{S \cap S_0}, \bar{\mathcal{E}}_{S \cap S_0, l}^* \rangle$$

- Inner product of Gaussians:

$$\text{IP}_{kli}^S := 2 \left\langle (\boldsymbol{\mu}_k^* - \boldsymbol{\mu}_l^*)_S - \bar{\mathcal{E}}_{S,l}^* + \left( \frac{|G_k^*| - 1}{|G_k^*|} \right)^2 \bar{\mathcal{E}}_{S,k \setminus \{i\}}^*, \mathcal{E}_{S,i} \right\rangle,$$

In summary, we have:

$$D_{kli}^S(\mathbf{X}) = \|(\boldsymbol{\mu}_k^* - \boldsymbol{\mu}_l^*)_{S \cap S_0}\|_2^2 + \text{CN}_l^S + \text{CN}_i^S + \text{CN}_{ki}^S + \text{GSN}_{kl}^S + \text{IP}_{kli}^S. \quad (52)$$

**2. Bounding the Gaussian and Chi-squares using the tail inequalities.** Chi-square noise and Gaussian signal-noise interaction terms ( $\text{CN}_l^S$ ,  $\text{CN}_i^S$ ,  $\text{CN}_{ki}^S$ , and  $\text{GSN}_{kl}^S$ ) in (52) are straightforward to bound from below. Define the following lower bound events:

$$\mathcal{B}_{kl,S}^{(i,1)} := \left\{ \text{CN}_l^S \geq \frac{|S| - 2\sqrt{|S|\zeta^S}}{|G_l^*|} \right\}, \quad (53)$$

$$\mathcal{B}_{kl,S}^{(i,2)} := \left\{ \text{CN}_i^S \geq \frac{2|G_k^*| - 1}{|G_k^*|^2} (|S| - 2\sqrt{|S|\zeta^S}) \right\}, \quad (54)$$

$$\mathcal{B}_{kl,S}^{(i,3)} := \left\{ \text{CN}_{ki}^S \geq \frac{1 - |G_k^*|}{|G_k^*|^2} (|S| + 2\sqrt{|S|\zeta^S} + 2\zeta^S) \right\}, \quad (55)$$

$$\mathcal{B}_{kl,S}^{(i,4)} := \left\{ \text{GSN}_{kl}^S \geq -2\sqrt{\frac{2\zeta^S}{|G_l^*|}} \|(\boldsymbol{\mu}_k^* - \boldsymbol{\mu}_l^*)_{S \cap S_0}\|_2 \right\}, \quad (56)$$

By setting  $\zeta^S = \log(n^2|S|^2 \binom{p}{|S|})$ , Lemma 3 implies that each event has a probability of at least  $1 - 1/(n^2 K^2 |S|^2 \binom{p}{|S|})$ , for any  $S \in \mathcal{S}$ .

### 3. Bounding the Gaussian inner product using conditioning, Gaussian tail bounds

**and separation condition.** Here, we use the separation condition to bound the term. If we condition on  $\bar{\mathcal{E}}_{S,l}^*$  and  $\bar{\mathcal{E}}_{S,k \setminus \{i\}}^*$ , then  $-\text{IP}_{kli}^S$  has a univariate Gaussian distribution with mean zero and variance as the following:

$$\begin{aligned} \text{Var}(-\text{IP}_{kli}^S \mid \bar{\mathcal{E}}_{S,l}^*, \bar{\mathcal{E}}_{S,k \setminus \{i\}}^*) &= \left\| (\boldsymbol{\mu}_k^* - \boldsymbol{\mu}_l^*)_S - \bar{\mathcal{E}}_{S,l}^* + (1 - |G_k^*|^{-1})^2 \bar{\mathcal{E}}_{S,k \setminus \{i\}}^* \right\|_2^2 \\ &\stackrel{(i)}{=} \|(\boldsymbol{\mu}_k^* - \boldsymbol{\mu}_l^*)_{S \cap S_0}\|_2^2 + \underbrace{\left\| \bar{\mathcal{E}}_{S,l}^* - (1 - |G_k^*|^{-1})^2 \bar{\mathcal{E}}_{S,k \setminus \{i\}}^* \right\|_2^2}_{:= \text{CN}_{kli}^S} \\ &\quad + \underbrace{2 \langle (\boldsymbol{\mu}_k^* - \boldsymbol{\mu}_l^*)_{S \cap S_0}, (1 - |G_k^*|^{-1})^2 \bar{\mathcal{E}}_{S \cap S_0, k \setminus \{i\}}^* - \bar{\mathcal{E}}_{S \cap S_0, l}^* \rangle}_{:= \text{GN}_{kli}^S}, \end{aligned}$$

where step (i) uses our sparsity assumption on cluster center difference.

Next, we define events that bound this variance from above:

$$\begin{aligned} \mathcal{B}_{kl,S}^{(i,5)} &:= \left\{ \text{CN}_{kli}^S \leq (|G_l^*|^{-1} + |G_k^*|^{-1})(|S| + 2\sqrt{|S|\zeta^S} + 2\zeta^S) \right\}, \\ \mathcal{B}_{kl,S}^{(i,6)} &:= \left\{ \text{GN}_{kli}^S \leq 2\sqrt{2(|G_l^*|^{-1} + |G_k^*|^{-1})\zeta^S} \|(\boldsymbol{\mu}_k^* - \boldsymbol{\mu}_l^*)_{S \cap S_0}\|_2 \right\}. \end{aligned}$$

By setting  $\zeta^S = \log(n^2|S|^2 \binom{p}{|S|})$ , Lemma 3 implies that each event has a probability of at least  $1 - 1/(n^2|S|^2 \binom{p}{|S|})$ , uniformly overall all  $S \in \mathcal{S}$ .

Thus, conditioned on events  $\mathcal{B}_{kl,S}^{(i,5)}$  and  $\mathcal{B}_{kl,S}^{(i,6)}$ , the variance can be bounded as

$$\begin{aligned} \text{Var}(-\text{IP}_{kli}^S \mid \bar{\mathcal{E}}_{S,l}^*, \bar{\mathcal{E}}_{S,k \setminus \{i\}}^*) &\leq \|(\boldsymbol{\mu}_k^* - \boldsymbol{\mu}_l^*)_{S \cap S_0}\|_2^2 + (|G_l^*|^{-1} + |G_k^*|^{-1})(|S| + 2\sqrt{|S|\zeta^S} + 2\zeta^S) \\ &\quad + 2\sigma^2 \sqrt{2(|G_l^*|^{-1} + |G_k^*|^{-1})\zeta^S} \|(\boldsymbol{\mu}_k^* - \boldsymbol{\mu}_l^*)_{S \cap S_0}\|_2. \end{aligned}$$

To further bound this variance, it is convenient to remove the first-order signal term  $\|(\boldsymbol{\mu}_k^* - \boldsymbol{\mu}_l^*)_{S \cap S_0}\|_2$ . To this end, we collect some conditions. First, recall from Theorem 1 that

$$m = 2 \min_{1 \leq k \neq l \leq K} (|G_l^*|^{-1} + |G_k^*|^{-1})^{-1}.$$

From (9), recall that for  $S \in \mathcal{S}$ , we have

$$\min_{1 \leq k \neq l \leq K} \|(\boldsymbol{\mu}_k^* - \boldsymbol{\mu}_l^*)_{S \cap S_0}\|_2^2 \gtrsim \sigma^2 \left( \log n + \frac{|S| \log p}{m} + \sqrt{\frac{|S| \log p}{m}} \right), \quad (57)$$

and  $|S| \leq \sqrt{p}$ . Under these conditions, by treating  $K$  as a constant, we have

$$\zeta^S = \log(n^2 |S|^2 \binom{p}{|S|}) \lesssim |S| \log p + \log n,$$

which implies

$$2\sqrt{2(|G_l^*|^{-1} + |G_k^*|^{-1})\zeta^S} \|(\boldsymbol{\mu}_k^* - \boldsymbol{\mu}_l^*)_{S \cap S_0}\|_2 \leq 2\sqrt{\frac{\zeta^S}{m}} \|(\boldsymbol{\mu}_k^* - \boldsymbol{\mu}_l^*)_{S \cap S_0}\|_2 \lesssim \|(\boldsymbol{\mu}_k^* - \boldsymbol{\mu}_l^*)_{S \cap S_0}\|_2^2.$$

Therefore, we can further bound the variance as

$$\text{Var}(-\text{IP}_{kli}^S) \lesssim \|(\boldsymbol{\mu}_k^* - \boldsymbol{\mu}_l^*)_{S \cap S_0}\|_2^2 + (|G_l^*|^{-1} + |G_k^*|^{-1})(|S| + 2\sqrt{|S|\zeta^S} + 2\zeta^S).$$

Therefore, by the Gaussian tail inequality, we have

$$\begin{aligned} \text{CP}_{kli}^S &:= \mathbb{P} \left( -\text{IP}_{kli}^S > \|(\boldsymbol{\mu}_k^* - \boldsymbol{\mu}_l^*)_{S \cap S_0}\|_2^2 \mid \bar{\mathcal{E}}_{S,l}^*, \bar{\mathcal{E}}_{S,k \setminus \{i\}}^* \right) \\ &\leq \exp \left( \frac{-\|(\boldsymbol{\mu}_k^* - \boldsymbol{\mu}_l^*)_{S \cap S_0}\|_2^4}{2\text{Var}(-\text{IP}_{kli}^S \mid \bar{\mathcal{E}}_{S,l}^*, \bar{\mathcal{E}}_{S,k \setminus \{i\}}^*)} \right) \\ &\lesssim \exp \left( \frac{-\|(\boldsymbol{\mu}_k^* - \boldsymbol{\mu}_l^*)_{S \cap S_0}\|_2^4}{\|(\boldsymbol{\mu}_k^* - \boldsymbol{\mu}_l^*)_{S \cap S_0}\|_2^2 + 2(|G_l^*|^{-1} + |G_k^*|^{-1})(|S| + 2\sqrt{|S|\zeta^S} + 2\zeta^S)} \right), \end{aligned} \quad (58)$$

where the last step uses the variance bound. We want to bound the last term by  $C/n^2$ , with

$C$  a constant. To this end, it suffices to show

$$\frac{\|(\boldsymbol{\mu}_k^* - \boldsymbol{\mu}_l^*)_{S \cap S_0}\|_2^4}{\|(\boldsymbol{\mu}_k^* - \boldsymbol{\mu}_l^*)_{S \cap S_0}\|_2^2 + 2(|G_l^*|^{-1} + |G_k^*|^{-1})(|S| + 2\sqrt{|S|\zeta^S} + 2\zeta^S)} \gtrsim \log n,$$

which is indeed satisfied under our separation condition in (57).

**4. Defining the uniform bound event.** We collect the bounds in (53), (54), (55), (56), and (58). From (52), recalled below,

$$D_{kli}^S(\mathbf{X}) = \|(\boldsymbol{\mu}_k^* - \boldsymbol{\mu}_l^*)_{S \cap S_0}\|_2^2 + \text{CN}_l^S + \text{CN}_i^S + \text{CN}_{ki}^S + \text{GSN}_{kl}^S + \text{IP}_{kli}^S.$$

we can say

$$\begin{aligned}
D_{kli}^S(\mathbf{X}) &\gtrsim \|(\boldsymbol{\mu}_l^* - \boldsymbol{\mu}_k^*)_{S \cap S_0}\|_2^2 + \frac{|S| - 2\sqrt{|S|\zeta^S}}{|G_l^*|} + \frac{2|G_k^*| - 1}{|G_k^*|^2}(|S| - 2\sqrt{|S|\zeta^S}) \\
&\quad + \frac{1 - |G_k^*|}{|G_k^*|^2}(|S| + 2\sqrt{|S|\zeta^S} + 2\zeta^S) - 2\sqrt{\frac{2\zeta^S}{|G_l^*|}}\|(\boldsymbol{\mu}_k^* - \boldsymbol{\mu}_l^*)_{S \cap S_0}\|_2 \\
&\quad + \|(\boldsymbol{\mu}_k^* - \boldsymbol{\mu}_l^*)_{S \cap S_0}\|_2^2, \\
&\gtrsim \|(\boldsymbol{\mu}_l^* - \boldsymbol{\mu}_k^*)_{S \cap S_0}\|_2^2 - \sqrt{\frac{\zeta^S}{|G_l^*|}}\|(\boldsymbol{\mu}_k^* - \boldsymbol{\mu}_l^*)_{S \cap S_0}\|_2 \\
&\quad - \left(\frac{1}{|G_k^*|} + \frac{1}{|G_l^*|}\right)|S| - \left(\frac{1}{|G_k^*|} + \frac{1}{|G_l^*|}\right)\sqrt{|S|\zeta^S} - \frac{1}{|G_k^*|}\zeta^S \\
&= \|(\boldsymbol{\mu}_l^* - \boldsymbol{\mu}_k^*)_{S \cap S_0}\|_2^2 - \left(\frac{1}{|G_k^*|} + \frac{1}{|G_l^*|}\right)|S| - R_{kl}^S,
\end{aligned}$$

where

$$R_{kl}^S = \sqrt{\frac{\zeta^S}{|G_l^*|}}\|(\boldsymbol{\mu}_l^* - \boldsymbol{\mu}_k^*)_{S \cap S_0}\|_2 + \left(\frac{1}{|G_k^*|} + \frac{1}{|G_l^*|}\right)\sqrt{|S|\zeta^S} + \frac{1}{|G_k^*|}\zeta^S.$$

As a result, we define an event

$$\mathcal{A}_{kli}^S := \left\{ D_{kli}^S(\mathbf{X}) \gtrsim \|(\boldsymbol{\mu}_k^* - \boldsymbol{\mu}_l^*)_{S \cap S_0}\|_2^2 + \left(\frac{1}{|G_k^*|} + \frac{1}{|G_l^*|}\right)|S| - R_{kl}^S \right\}, \quad (59)$$

with the index  $(k, l, i)$  ranging  $1 \leq k \neq l \leq K$  and all  $i \in G_k^*$ , and  $S$  ranging over  $\mathcal{S}$ . The proof is complete once we show that the intersection event

$$\bigcap_{1 \leq k \neq l \leq K} \bigcap_{i \in G_k^*} \bigcap_{S \in \mathcal{S}} \mathcal{A}_{kli}^S$$

holds with high probability.

**5. Bounding the probability of the uniform bound event.** To prove the lemma, it suffices to show that

$$\mathbb{P} \left( \bigcup_{1 \leq k \neq l \leq K} \bigcup_{i \in G_k^*} \bigcup_{S \in \mathcal{S}} (\mathcal{A}_{kli}^S)^C \right) \lesssim \frac{1}{n}.$$

To show this, first denote

$$\mathcal{B}_{kl,S}^{(i)} := \bigcap_{\ell=1}^6 \mathcal{B}_{kl,S}^{(i,\ell)}.$$

Then, we have

$$\begin{aligned} & \mathbb{P} \left( \bigcup_{1 \leq k \neq l \leq K} \bigcup_{i \in G_k^*} \bigcup_{S \in \mathcal{S}} (\mathcal{A}_{kli}^S)^C \right) \\ & \leq \sum_{1 \leq k \neq l \leq K} \sum_{i \in G_k^*} \sum_{S \in \mathcal{S}} \mathbb{P}((\mathcal{A}_{kli}^S)^C) \\ & = \sum_{1 \leq k \neq l \leq K} \sum_{i \in G_k^*} \sum_{S \in \mathcal{S}} \mathbb{E} [\mathbb{P}((\mathcal{A}_{kli}^S)^C \mid \bar{\mathcal{E}}_{S,l}^*, \mathcal{E}_{S,i}, \bar{\mathcal{E}}_{S,k \setminus \{i\}})] \\ & \leq \sum_{1 \leq k \neq l \leq K} \sum_{i \in G_k^*} \sum_{S \in \mathcal{S}} \mathbb{E} [\mathbb{P}((\mathcal{A}_{kli}^S)^C \mid \bar{\mathcal{E}}_{S,l}^*, \mathcal{E}_{S,i}, \bar{\mathcal{E}}_{S,k \setminus \{i\}}) \mathbb{1}(\mathcal{B}_{kl,S}^{(i)}) + \mathbb{1}(\mathcal{B}_{kl,S}^{(i)})^C] \\ & \stackrel{(i)}{\leq} \left( \sum_{1 \leq k \neq l \leq K} \sum_{i \in G_k^*} \sum_{q=1}^{\lfloor \sqrt{p} \rfloor} \sum_{S \in \mathcal{S}, |S|=q} \mathbb{E} [\text{CP}_{kli}^S \mathbb{1}(\mathcal{B}_{kl,S}^{(i)})] \right) + \frac{\pi^2}{n} \\ & \stackrel{(ii)}{\lesssim} \frac{K^2 \pi^2}{6n} + \frac{K^2 \pi^2}{n}, \end{aligned}$$

where step (i) uses  $\sum_{q=1}^{\infty} (1/q^2) = \pi^2/6$ , and step (ii) uses (58). Treating  $K$  as a constant, we conclude that

$$D_{kli}^S(\mathbf{X}) \gtrsim \|(\boldsymbol{\mu}_k^* - \boldsymbol{\mu}_l^*)_{S \cap S_0}\|_2^2 + \left( \frac{1}{|G_k^*|} + \frac{1}{|G_l^*|} \right) |S| - R_{kl}^S.$$

uniformly over  $S \in \mathcal{S}$ , with probability at least  $1 - C/n$ , where  $C > 0$  is a constant. This completes the proof of Lemma 19. □

#### C.4.6 Proof of Lemma 20

*Proof.* Given a support set  $S \subset [p]$  with  $|S| \leq \sqrt{p}$ , we have

$$L_1^S(\mathbf{X}) = \sup_{\mathbf{v} \in \Gamma_K, \|\mathbf{v}\|_2=1} \|\mathcal{E}_{S,\cdot} \mathbf{v}\|_2^2 \leq \sup_{\mathbf{v} \in \mathbb{R}^n, \|\mathbf{v}\|_2=1} \|\mathcal{E}_{S,\cdot} \mathbf{v}\|_2^2 = \|\mathcal{E}_{S,\cdot}\|_{\text{op}}^2.$$

Here,  $\mathcal{E}_{S,\cdot}$  is a  $|S| \times n$  random matrix with i.i.d. Gaussian entries distributed as  $\mathcal{N}(0, \sigma^2)$ .

Therefore, by Lemma 7, if we define an event

$$\mathcal{C}_L^S := \{L_1^S(\mathbf{X}) \leq \sigma^2(n + |S| + \xi^S)\}, \quad (60)$$

where  $\xi^S = \log(n|S|^2 \binom{p}{|S|})$ , then we have  $\mathbb{P}(\mathcal{C}_L^S) \geq 1 - 1/(n|S|^2 \binom{p}{|S|})$ . Now we show that the event  $\mathcal{C}_L^S$  holds uniformly across all  $S \subset [p]$  such that  $|S| \leq \sqrt{p}$ , with probability at least  $1 - C_8/n$ , where  $C_8 > 0$  is a constant.

$$\mathbb{P}\left(\bigcup_{S \subset [p], |S| \leq \sqrt{p}} (\mathcal{C}_L^S)^C\right) \leq \sum_{q=1}^{\lfloor \sqrt{p} \rfloor} \sum_{|S|=q} \mathbb{P}((\mathcal{C}_L^S)^C) \leq \sum_{q=1}^{\lfloor \sqrt{p} \rfloor} \sum_{|S|=q} \frac{1}{n|S|^2 \binom{p}{|S|}} = \sum_{q=1}^{\lfloor \sqrt{p} \rfloor} \frac{1}{nq^2} \leq \frac{\pi^2}{6n},$$

where the last step uses  $\sum_{q=1}^{\infty} \frac{1}{q^2} = \pi^2/6$ . Since  $|S| \leq \sqrt{p}$ ,  $|S| \log p$  dominates  $\log |S|$ . Therefore, we conclude that uniformly across  $S \in [p]$  such that  $|S| \leq \sqrt{p}$ , with probability at least  $1 - C_8/n$ , it holds that

$$L_1^S(\mathbf{X}) \lesssim \sigma^2(n + \log n + |S| \log p).$$

This completes the proof of Lemma 20.  $\square$

#### C.4.7 Proof of Lemma 21

The proof proceeds in the following steps:

1. The first inequality  $L_1^S(\mathbf{X}) \lesssim \dot{\lambda}^S$ .
2. The second inequality  $\dot{\lambda}^S \lesssim U^S(\mathbf{X})$ .

*Proof.* For simplicity, we assume  $\sigma^2 = 1$  here.

**1. The first inequality.** We aim to show  $L_1^S(\mathbf{X}) \lesssim \dot{\lambda}^S$ . From (9), recall that for  $S \in \mathcal{S}$ , we have

$$\Delta_{S \cap S_0}^2 = \min_{1 \leq k \neq l \leq K} \|(\boldsymbol{\mu}_l^* - \boldsymbol{\mu}_k^*)_{S \cap S_0}\|_2^2 \gtrsim \sigma^2 \left( \log n + \frac{|S| \log p}{m} + \sqrt{\frac{|S| \log p}{m}} \right), \quad (61)$$

where

$$m = 2 \min_{1 \leq k \neq l \leq K} \left\{ \left( \frac{1}{|G_k^*|} + \frac{1}{|G_l^*|} \right)^{-1} \right\}.$$

Therefore, with probability at least  $1 - C_8/n$  uniformly across all  $S \in \mathcal{S}$ , where  $C_8 > 0$  is a constant from Lemma 20, it holds that

$$\begin{aligned} L_1^S(\mathbf{X}) &\lesssim (n + \log n + |S| \log p) \\ &\stackrel{(i)}{\lesssim} |S| + \frac{1}{4} (m \log n + |S| \log p + \sqrt{m|S| \log p}) \\ &\lesssim |S| + \frac{m}{4} \Delta_{S \cap S_0}^2 \\ &= \dot{\lambda}^S, \end{aligned}$$

where step (i) uses Lemma 20. This completes the derivation of the first inequality.

**2. The second inequality.** We aim to show  $\dot{\lambda}^S \lesssim U^S(\mathbf{X})$ . Recall from (23) that

$$U^S(\mathbf{X}) = \min_{1 \leq k \neq l \leq K} \left\{ \left( \frac{1}{|G_k^*|} + \frac{1}{|G_l^*|} \right)^{-1} \min_{i \in G_k^*} D_{kli}^S(\mathbf{X}) \right\}.$$

By Lemma 19, with probability at least  $1 - C_7/n$  uniformly across  $S \in \mathcal{S}$  and uniformly over  $(k, l, i)$  where  $1 \leq k \neq l \leq K$  and  $i \in G_k^*$ , we have

$$\left( \frac{1}{|G_k^*|} + \frac{1}{|G_l^*|} \right)^{-1} D_{kli}^S(\mathbf{X}) \gtrsim \underbrace{\left( \frac{1}{|G_k^*|} + \frac{1}{|G_l^*|} \right)^{-1} \|(\boldsymbol{\mu}_k^* - \boldsymbol{\mu}_l^*)_{S \cap S_0}\|_2^2 + |S|}_{\text{Part A}} - \underbrace{\left( \frac{1}{|G_k^*|} + \frac{1}{|G_l^*|} \right)^{-1} R_{kl}^S}_{\text{Part B}},$$

where

$$R_{kl}^S = \sqrt{\frac{\xi^S}{|G_l^*|}} \|(\boldsymbol{\mu}_l^* - \boldsymbol{\mu}_k^*)_{S \cap S_0}\|_2 + \left( \frac{1}{|G_k^*|} + \frac{1}{|G_l^*|} \right) \sqrt{|S|\xi^S} + \frac{1}{|G_k^*|} \xi^S,$$

and  $\xi^S = \log(n^2 K^2 |S|^2 \binom{p}{|S|})$ . Under the separation condition for  $\mathcal{S}$ , recalled in (61), and noting that  $|S| \leq \sqrt{p}$  for all  $S \in \mathcal{S}$ , Part A dominates Part B in the inequality above.

Therefore, we have

$$\min_{1 \leq k \neq l \leq K} \left\{ \left( \frac{1}{|G_k^*|} + \frac{1}{|G_l^*|} \right)^{-1} D_{kli}^S(\mathbf{X}) \right\} \gtrsim \min_{1 \leq k \neq l \leq K} \left( \frac{1}{|G_k^*|} + \frac{1}{|G_l^*|} \right)^{-1} \|(\boldsymbol{\mu}_k^* - \boldsymbol{\mu}_l^*)_{S \cap S_0}\|_2^2 + |S|$$

$$\begin{aligned} &\gtrsim |S| + \frac{m}{4} \Delta_{S \cap S_0}^2 \\ &= \dot{\lambda}^S. \end{aligned}$$

This concludes the derivation of the second inequality and thereby completes the proof.  $\square$

#### C.4.8 Proof of Lemma 22

*Proof.* For notational simplicity, let  $\sigma^2 = 1$ . Fix  $S \in \mathcal{S}$  and  $(l, k)$  with  $1 \leq l \neq k \leq K$ .

Condition on the high-probability event in Lemma 19. Then we have

$$\begin{aligned} t_{lk}^S(\dot{\lambda}^S) &\stackrel{(i)}{=} \sum_{j \in G_l^*} \left\{ \frac{|G_k^*|}{2} D_{lkj}(\mathbf{X}, S) - \frac{|G_k^*| + |G_l^*|}{2|G_l^*|} \dot{\lambda}^S \right\} \\ &\stackrel{(ii)}{=} \sum_{j \in G_l^*} \left\{ \frac{|G_k^*|}{2} D_{lkj}(\mathbf{X}, S) - \frac{|G_k^*| + |G_l^*|}{2|G_l^*|} \left( |S| + \frac{m}{4} \Delta_{S \cap S_0}^2 \right) \right\} \\ &\stackrel{(iii)}{\gtrsim} \sum_{j \in G_l^*} \left\{ \frac{|G_k^*|}{2} \left( |S| + \|(\boldsymbol{\mu}_l^* - \boldsymbol{\mu}_k^*)_{S \cap S_0}\|_2^2 \right) - \frac{|G_k^*| + |G_l^*|}{2|G_l^*|} \left( |S| + \frac{m}{4} \Delta_{S \cap S_0}^2 \right) \right\} \\ &\stackrel{(iii)}{\geq} \sum_{j \in G_l^*} \left( \frac{|G_k^*|}{2} |S| + \frac{|G_k^*|}{2} \|(\boldsymbol{\mu}_k^* - \boldsymbol{\mu}_l^*)_{S \cap S_0}\|_2^2 \right. \\ &\quad \left. - \frac{|G_k^*| + |G_l^*|}{2|G_l^*|} |S| - \frac{|G_k^*| + |G_l^*|}{2|G_l^*|} \frac{m}{4} \|(\boldsymbol{\mu}_l^* - \boldsymbol{\mu}_k^*)_{S \cap S_0}\|_2^2 \right) \\ &\stackrel{(iv)}{\geq} \sum_{j \in G_l^*} \left\{ \left( \frac{|G_k^*|}{2} - \frac{|G_k^*| + |G_l^*|}{2|G_l^*|} \right) |S| + \frac{|G_k^*|}{4} \|(\boldsymbol{\mu}_l^* - \boldsymbol{\mu}_k^*)_{S \cap S_0}\|_2^2 \right\} \\ &= \frac{|G_l^*| |G_k^*|}{4} \|\boldsymbol{\mu}_k^* - \boldsymbol{\mu}_l^*\|_2^2 + \frac{|G_l^*| |G_k^*|}{2} |S| - \frac{|G_k^*| + |G_l^*|}{2} |S|. \\ &\stackrel{(v)}{\gtrsim} |G_l^*| |G_k^*| (\|\boldsymbol{\mu}_k^* - \boldsymbol{\mu}_l^*\|_2^2 + |S|) \end{aligned}$$

where step (i) follows from the definition of  $t_{lk}^S(\lambda^S)$  in (30), step (ii) follows from the definition of  $\dot{\lambda}_S$  in Lemma 21, step (iii) uses  $-\Delta_{S \cap S_0}^2 > -\|(\boldsymbol{\mu}_k^* - \boldsymbol{\mu}_l^*)_{S \cap S_0}\|_2^2$ , step (iv) uses

$$-m \geq -2 \left\{ \frac{|G_k^*| \cdot |G_l^*|}{|G_k^*| + |G_l^*|} \right\},$$

and step (v) uses  $|G_k^*| \geq 2$  and  $|G_l^*| \geq 2$ . This completes the proof of Lemma 22.  $\square$

### C.4.9 Proof of Lemma 23

the proof proceeds in the following steps.

1. Individual bound by Chi-square tail bound,
2. Uniform bound.

*Proof.* For notational simplicity, let  $\sigma^2 = 1$ .

**1. Individual bound by Chi-square tail bound.** Fix  $(k, l)$  such that  $1 \leq k \neq l \leq K$  and  $S \in \mathcal{S}$ . Then we have

$$\begin{aligned} \sup_{\mathbf{v} \in \Gamma_K, \|\mathbf{v}\|_2=1} I_{kl}^S(\mathbf{v}, \mathbf{X}) &= \sup_{\mathbf{v} \in \Gamma_K, \|\mathbf{v}\|_2=1} |G_l^*| \sum_{i \in G_k^*} v_i \langle (\boldsymbol{\mu}_k^* - \boldsymbol{\mu}_l^*)_{S \cap S_0}, \mathcal{E}_{S \cap S_0, i} \rangle \\ &\leq \sup_{\mathbf{v} \in \Gamma_K, \|\mathbf{v}\|_2=1} |G_l^*| \left| \sum_{i \in G_k^*} v_i \langle (\boldsymbol{\mu}_k^* - \boldsymbol{\mu}_l^*)_{S \cap S_0}, \mathcal{E}_{S \cap S_0, i} \rangle \right| \\ &\stackrel{(i)}{\leq} \sup_{\mathbf{v} \in \Gamma_K, \|\mathbf{v}\|_2=1} |G_l^*| \left( \sum_{i \in G_k^*} v_i^2 \right)^{1/2} \left( \sum_{i \in G_k^*} \langle (\boldsymbol{\mu}_k^* - \boldsymbol{\mu}_l^*)_{S \cap S_0}, \mathcal{E}_{S \cap S_0, i} \rangle^2 \right)^{1/2} \\ &\leq |G_l^*| \left( \sum_{i \in G_k^*} \langle (\boldsymbol{\mu}_k^* - \boldsymbol{\mu}_l^*)_{S \cap S_0}, \mathcal{E}_{S \cap S_0, i} \rangle^2 \right)^{1/2}, \end{aligned}$$

where step (i) uses the Cauchy-Schwarz inequality.

Now we derive an inequality for  $\sum_{i \in G_k^*} \langle (\boldsymbol{\mu}_k^* - \boldsymbol{\mu}_l^*)_{S \cap S_0}, \mathcal{E}_{S \cap S_0, i} \rangle^2$ . Since

$$\frac{1}{\|(\boldsymbol{\mu}_k^* - \boldsymbol{\mu}_l^*)_{S \cap S_0}\|_2} \langle (\boldsymbol{\mu}_k^* - \boldsymbol{\mu}_l^*)_{S \cap S_0}, \mathcal{E}_{S \cap S_0, i} \rangle \stackrel{\text{i.i.d.}}{\sim} \mathcal{N}(0, 1), \quad i = 1, \dots, |G_k^*|,$$

the square of this quantity follows a chi-square distribution with  $|G_k^*|$  degrees of freedom, provided that  $S$  is nonempty. Applying the chi-square tail inequality (Lemma 3), if we define

$$\mathcal{C}_{Ikl}^S := \left\{ \sup_{\mathbf{v} \in \Gamma_K, \|\mathbf{v}\|_2=1} I_{kl}^S(\mathbf{v}, \mathbf{X}) \leq \|(\boldsymbol{\mu}_k^* - \boldsymbol{\mu}_l^*)_{S \cap S_0}\|_2 (|G_k^*| + 2\sqrt{|G_k^*| \zeta_I^S} + 2\zeta_I^S)^{1/2} \right\}, \quad (62)$$

where  $\zeta_I^S = \log(nK^2|S|^2 \binom{p}{|S|})$ , then we have  $\mathbb{P}(\mathcal{C}_{Ikl}^S) \geq 1 - 1/(n^2 K^2 |S|^2 \binom{p}{|S|})$ .

**2. Uniform bound.** Now we show that the event  $\mathcal{C}_{Ikl}^S$  holds uniformly across all  $S \subset \mathcal{S}$

and  $1 \leq k \neq l \leq K$ , with probability at least  $1 - C_{10}/n$ , where  $C_{10} > 0$  is a constant.

$$\mathbb{P}\left(\bigcup_{1 \leq k \neq l \leq K} \bigcup_{S \in \mathcal{S}} (\mathcal{C}_{Ikl}^S)^C\right) \leq \sum_{1 \leq k \neq l \leq K} \sum_{q=1}^{\lfloor \sqrt{p} \rfloor} \sum_{|S|=q} \mathbb{P}((\mathcal{C}_{Ikl}^S)^C) \stackrel{(i)}{\leq} \sum_{q=1}^{\lfloor \sqrt{p} \rfloor} \sum_{|S|=q} \frac{1}{n|S|^2 \binom{p}{|S|}} = \sum_{q=1}^{\lfloor \sqrt{p} \rfloor} \frac{1}{nq^2} \leq \frac{\pi^2}{6n},$$

where the last step uses  $\sum_{q=1}^{\infty} \frac{1}{q^2} = \pi^2/6$ . Since  $|S| \leq \sqrt{p}$ ,  $|S| \log p$  dominates  $\log |S|$ . Therefore, we conclude that uniformly across  $S \in \mathcal{S}$  and  $(k, l)$  such that  $1 \leq k \neq l \leq K$ , with probability at least  $1 - C_{10}/n$ , it holds that

$$\begin{aligned} & \sup_{\mathbf{v} \in \Gamma_K, \|\mathbf{v}\|_2=1} I_{kl}^S(\mathbf{v}, \mathbf{X}) \\ & \lesssim |G_l^*| \|(\boldsymbol{\mu}_k^* - \boldsymbol{\mu}_l^*)_{S \cap S_0}\|_2 \left( |G_k^*| + \sqrt{|G_k^*| \log n} + \sqrt{|G_k^*| |S| \log p} + \log n + |S| \log p \right)^{1/2}. \end{aligned}$$

This completes the proof of Lemma 23.  $\square$

#### C.4.10 Proof of Lemma 24

*Proof.* For notational simplicity, let  $\sigma^2 = 1$  and for  $k = 1, \dots, K$ , denote

$$\text{IB}_k := \left( |G_k^*| + \sqrt{|G_k^*| \log n} + \sqrt{|G_k^*| |S| \log p} + \log n + |S| \log p \right)^{1/2}.$$

Then we have

$$\begin{aligned} & \sup_{\mathbf{v} \in \Gamma_K, \|\mathbf{v}\|_2=1} \sum_{1 \leq k \neq l \leq K} \frac{T_{1,kl}^S(\mathbf{v})}{t_{lk}^S(\lambda^S)} \stackrel{(i)}{\lesssim} \sup_{\mathbf{v} \in \Gamma_K, \|\mathbf{v}\|_2=1} \sum_{1 \leq k \neq l \leq K} \frac{I_{kl}^S(\mathbf{v}, \mathbf{X}) \times I_{lk}^S(\mathbf{v}, \mathbf{X})}{|G_l^*| \cdot |G_k^*| \cdot \|(\boldsymbol{\mu}_k^* - \boldsymbol{\mu}_l^*)_{S \cap S_0}\|_2^2 + |S|} \\ & \leq \sup_{\mathbf{v} \in \Gamma_K, \|\mathbf{v}\|_2=1} \sum_{1 \leq k \neq l \leq K} \frac{I_{kl}^S(\mathbf{v}, \mathbf{X}) \times I_{lk}^S(\mathbf{v}, \mathbf{X})}{|G_l^*| \cdot |G_k^*| \cdot \|(\boldsymbol{\mu}_k^* - \boldsymbol{\mu}_l^*)_{S \cap S_0}\|_2^2} \\ & \stackrel{(ii)}{\lesssim} \sum_{1 \leq k \neq l \leq K} \text{IB}_k^S \times \text{IB}_l^S \\ & \leq \sum_{k=1}^K \text{IB}_k^S \sum_{l=1}^K \text{IB}_l^S \\ & \stackrel{(iii)}{\lesssim} n + \sqrt{n \log n} + \sqrt{n|S| \log p} + \log n + |S| \log p \end{aligned}$$

$$\begin{aligned}
&\stackrel{(iv)}{\lesssim} |S| + m \log n + \sqrt{m|S|\log p} + |S|\log p \\
&\stackrel{(v)}{\lesssim} |S| + \frac{m}{4}\Delta_{S \cap S_0}^2 = \lambda^S,
\end{aligned}$$

where step (i) uses Lemma 22 and definition  $T_{1,kl}^S(\mathbf{v}) = I_{kl}^S(\mathbf{v}, \mathbf{X}) \times I_{lk}^S(\mathbf{v}, \mathbf{X})$  presented in (27), step (ii) uses Lemma 23, step (iii) uses the identity  $\sum_{k=1}^K |G_k^*| = n$  and inequality  $\sum_{k=1}^K \sqrt{|G_k^*|} \leq \sqrt{K \sum_{k=1}^K |G_k^*|} \lesssim \sqrt{n}$ , step (iv) uses the condition  $m \gtrsim n/\log n$  of Theorem 1, and step (v) uses the separation condition of  $\mathcal{S}$ , presented in (9). This completes the proof of Lemma 24.  $\square$

#### C.4.11 Proof of Lemma 25

With appropriate algebraic manipulation, the problem reduces to an application of the concentration inequality for an unbounded empirical process developed by Adamczak (2008) (Lemma 8). This requires estimating the expectation, variance, and sub-exponential norm of the empirical process. Accordingly, the proof proceeds in the following steps.

1. Reformulation into a quadratic form,
2. Bounding the operator norm dependent terms,
3. Bounding the expectation of the supremum,
4. Individual bound using Hanson-wright inequality,
5. Uniform bound.

*Proof.* For notational simplicity, we set  $\sigma^2 = 1$  and assume, without loss of generality, that  $G_k^* = 1, \dots, |G_k^*|$  throughout the proof.

**1. Transformation into a quadratic form.** Fix  $(k, l)$  such that  $1 \leq k \neq l \leq K$  and

$S \subset [p]$  such that  $|S| \leq \sqrt{p}$ . We can express  $G_{3,kl}^S(\mathbf{v})$  as a scaled quadratic form:

$$\begin{aligned} G_{1,kl}^S(\mathbf{v}) &= \frac{|G_l^*|}{|G_k^*|} \sum_{\{(i,j) \in G_k^*\}} v_i \langle \mathcal{E}_{S,i}, \mathcal{E}_{S,j} \rangle \\ &= \frac{|G_l^*|}{|G_k^*|} \sum_{\{(i,j) \in G_k^*\}} \frac{1}{2} (v_i + v_j) \langle \mathcal{E}_{S,i}, \mathcal{E}_{S,j} \rangle \\ &= \frac{|G_l^*|}{|G_k^*|} \underbrace{\text{vec}(\mathcal{E}_{S,G_k^*})^\top (\mathbf{A}^{\mathbf{v}} \otimes \mathbf{I}_{|S|}) \text{vec}(\mathcal{E}_{S,G_k^*})}_{\text{QF}_{kl}^S(\mathbf{A}^{\mathbf{v}} \otimes \mathbf{I}_{|S|}, \mathbf{X})}, \end{aligned} \quad (63)$$

Here, the  $(i, j)$ th element of the matrix  $\mathbf{A}^{\mathbf{v}} \in \mathbb{R}^{|G_k^*| \times |G_k^*|}$  is defined as  $A_{i,j}^{\mathbf{v}} := (v_i + v_j)/2$ , and  $\text{vec}(\mathcal{E}_{S,G_k^*})$  denotes the  $|S| \cdot |G_k^*|$ -dimensional vector obtained by stacking the columns of  $\mathcal{E}_{S,G_k^*}$  in order, with the first column at the top and the last column at the bottom, and  $\mathbf{A}^{\mathbf{v}} \otimes \mathbf{I}_{|S|}$  denotes the tensor product:

$$\mathbf{A}^{\mathbf{v}} \otimes \mathbf{I}_{|S|} = \begin{bmatrix} A_{1,1}^{\mathbf{v}} \mathbf{I}_{|S|} & \cdots & A_{1,|G_k^*|}^{\mathbf{v}} \mathbf{I}_{|S|} \\ \vdots & \ddots & \vdots \\ A_{|G_k^*|,1}^{\mathbf{v}} \mathbf{I}_{|S|} & \cdots & A_{|G_k^*|,|G_k^*|}^{\mathbf{v}} \mathbf{I}_{|S|} \end{bmatrix}.$$

The quadratic form  $\text{QF}_{kl}^S(\mathbf{A}^{\mathbf{v}} \otimes \mathbf{I}_{|S|}, \mathbf{X})$  is centered because

$$\mathbb{E}[\text{QF}_{kl}^S(\mathbf{A}^{\mathbf{v}} \otimes \mathbf{I}_{|S|}, \mathbf{X})] = \mathbb{E} \sum_{\{(i,j) \in G_k^*\}} v_i \mathbb{E}[\langle \mathcal{E}_{S,i}, \mathcal{E}_{S,j} \rangle] = \sum_{i \in G_k^*} v_i \mathbb{E}[\|\mathcal{E}_{S,i}\|_2^2] \stackrel{(i)}{=} |S| \sum_{i \in G_k^*} v_i = 0,$$

where step (i) uses  $\sum_{i=1}^n v_i = 0$ , shown in (47), and indexed by

$$\mathcal{M}_{kl}^S = \{\mathbf{A}^{\mathbf{v}} \otimes \mathbf{I}_{|S|} \mid \mathbf{v} \in \Gamma_K, \|\mathbf{v}\|_2 = 1\}.$$

To derive the uniform bound, we apply the uniform Hanson-Wright inequality (Lemma 11) to obtain the concentration inequality for

$$\sup_{\mathbf{M} \in \mathcal{M}_{kl}^S} \text{QF}_{kl}^S(\mathbf{M}, \mathbf{X}) - \mathbb{E} \left[ \sup_{\mathbf{M} \in \mathcal{M}_{kl}^S} \text{QF}_{kl}^S(\mathbf{M}, \mathbf{X}) \right].$$

To apply Lemma 11, we need to bound the following two quantities:

$$\sup_{\mathbf{M} \in \mathcal{A}_{kl}^S} \|\mathbf{M}\|_{\text{op}} \quad \text{and} \quad \|\text{vec}(\mathcal{E}_{S,G_k^*})\|_{\mathcal{A}_{kl}^S} := \mathbb{E} \left[ \sup_{\mathbf{M} \in \mathcal{A}_{kl}^S} \|(\mathbf{M} + \mathbf{M}^\top) \text{vec}(\mathcal{E}_{S,G_k^*})\|_2 \right],$$

where bounding both terms critically depends on  $\|\mathbf{A}^{\mathbf{v}}\|_{\text{op}}$ , and the expectation of supremum

$$\mathbb{E} \left[ \sup_{\mathbf{M} \in \mathcal{M}_{kl}^S} \text{QF}_{kl}^S(\mathbf{M}, \mathbf{X}) \right].$$

We present the bounds in order.

**2. Bounding the operator norm dependent terms.** We start by bounding  $\sup_{\mathbf{M} \in \mathcal{A}_{kl}^S} \|\mathbf{M}\|_{\text{op}}$ .

First note that for  $\mathbf{M} \in \mathcal{A}_{kl}^S$ , its operator norm can be simplified into:

$$\|\mathbf{M}\|_{\text{op}} = \|\mathbf{A}^{\mathbf{v}} \otimes \mathbf{I}_{|S|}\|_{\text{op}} = \|\mathbf{A}^{\mathbf{v}}\|_{\text{op}} \|\mathbf{I}_{|S|}\|_{\text{op}} = \|\mathbf{A}^{\mathbf{v}}\|_{\text{op}}.$$

Therefore it suffices to bound the supremum of  $\|\mathbf{A}^{\mathbf{v}}\|_{\text{op}}$ :

$$\begin{aligned} \|\mathbf{A}^{\mathbf{v}}\|_{\text{op}} &= \max_{\|\mathbf{u}\|_2=1, \mathbf{u} \in \mathbb{R}^{|G_k^*|}} \mathbf{u}^T \mathbf{A}^{\mathbf{v}} \mathbf{u} \\ &= \max_{\|\mathbf{u}\|_2=1, \mathbf{u} \in \mathbb{R}^{|G_k^*|}} \sum_{\{(i,j) \in G_k^*\}} u_i u_j \frac{v_i + v_j}{2} \\ &= \max_{\|\mathbf{u}\|_2=1, \mathbf{u} \in \mathbb{R}^{|G_k^*|}} \left( \sum_{i=1}^{|G_k^*|} u_i v_i \right) \left( \sum_{j=1}^{|G_k^*|} u_j \right) \\ &\stackrel{(i)}{\leq} \max_{\|\mathbf{u}\|_2=1, \mathbf{u} \in \mathbb{R}^{|G_k^*|}} \left( \sum_{i=1}^{|G_k^*|} u_i^2 \right)^{1/2} \left( \sum_{i=1}^{|G_k^*|} v_i^2 \right)^{1/2} \left( \sum_{j=1}^{|G_k^*|} u_j^2 \right)^{1/2} \sqrt{|G_k^*|} \\ &\stackrel{(ii)}{\leq} \sqrt{|G_k^*|}, \end{aligned}$$

where step (i) uses Cauchy-Schwarz inequality, and step (ii) uses  $\|\mathbf{v}\|_2 \leq 1$  for  $\mathbf{v} \in \mathbb{V}_k$ . Since the last term do not depend on  $\mathbf{v}$ , we have

$$\sup_{\mathbf{M} \in \mathcal{A}_{kl}^S} \|\mathbf{M}\|_{\text{op}} \leq \sqrt{|G_k^*|}. \quad (64)$$

Next, we bound  $\|\text{vec}(\mathcal{E}_{S,G_k^*})\|_{\mathcal{A}_{kl}^S}^2$ :

$$\begin{aligned}
\|\text{vec}(\mathcal{E}_{S,G_k^*})\|_{\mathcal{A}_{kl}^S}^2 &= (\mathbb{E} \left[ \sup_{\mathbf{M} \in \mathcal{A}_{kl}^S} \|(\mathbf{M} + \mathbf{M}^\top) \text{vec}(\mathcal{E}_{S,G_k^*})\|_2 \right])^2 \\
&\leq (\mathbb{E} \left[ \sup_{\mathbf{M} \in \mathcal{A}_{kl}^S} \|(\mathbf{M} + \mathbf{M}^\top)\|_{\text{op}} \|\text{vec}(\mathcal{E}_{S,G_k^*})\|_2 \right])^2 \\
&\stackrel{(i)}{\leq} (\mathbb{E} \left[ 2|G_k^*|^{1/2} \|\text{vec}(\mathcal{E}_{S,G_k^*})\|_2 \right])^2 \\
&\stackrel{(ii)}{\leq} 4|G_k^*| \mathbb{E} \left[ \|\text{vec}(\mathcal{E}_{S,G_k^*})\|_2^2 \right] \\
&= 4|G_k^*| \sum_{i \in G_k^*} \mathbb{E} \left[ \|\mathcal{E}_{S,i}\|_2^2 \right] \\
&= 4|G_k^*|^2 |S|,
\end{aligned}$$

where step (i) uses (64), step (ii) applies Jensen's inequality to a convex function  $x \mapsto x^2$ .

**3. Bounding the expectation of the supremum.** It is more convenient to start from (63) and decompose the quadratic form  $\text{QF}_{kl}^S(\mathbf{A}^{\mathbf{v}}, \mathbf{X})$  into the following two terms:

$$\text{QF}_{kl}^S(\mathbf{A}^{\mathbf{v}}, \mathbf{X}) = \sum_{\{(i,j) \in G_k^*: i \neq j\}} v_j \langle \mathcal{E}_{S,i}, \mathcal{E}_{S,j} \rangle + \sum_{i \in G_k^*} v_i \|\mathcal{E}_{S,i}\|_2^2.$$

For these two terms, the index set  $\mathcal{A}_{kl}^S$ , which indexes the quadratic form, is more suitably represented by

$$\mathbb{V}_k := \left\{ \mathbf{v}_{G_k^*} : \mathbf{v} \in \Gamma_K, \|\mathbf{v}\|_2 = 1 \right\}.$$

We provide the bound for each of these two terms, starting with the first one. First note that given  $\mathbf{v} \in \mathbb{V}_k$ , we have

$$\begin{aligned}
\sup_{\mathbf{v} \in \mathbb{V}_k} \sum_{\{(i,j) \in G_k^*: i \neq j\}} v_j \langle \mathcal{E}_{S,i}, \mathcal{E}_{S,j} \rangle &= \sup_{\mathbf{v} \in \mathbb{V}_k} \left| \sum_{\{(i,j) \in G_k^*: i \neq j\}} v_j \langle \mathcal{E}_{S,i}, \mathcal{E}_{S,j} \rangle \right| \\
&= \sup_{\mathbf{v} \in \mathbb{V}_k} \left| \sum_{j \in G_k^*} v_j \langle \mathcal{E}_{S,j}, \sum_{i \in G_k^*, i \neq j} \mathcal{E}_{S,i} \rangle \right|
\end{aligned}$$

$$\begin{aligned}
&\stackrel{(i)}{\leq} \sup_{\mathbf{v} \in \mathbb{V}_k} \left( \sum_{j \in G_k^*} v_j^2 \right)^{1/2} \left( \sum_{j \in G_k^*} \left\langle \mathcal{E}_{S,j}, \sum_{i \in G_k^*, i \neq j} \mathcal{E}_{S,i} \right\rangle^2 \right)^{1/2} \\
&\stackrel{(ii)}{\leq} \left( \sum_{j \in G_k^*} \left\langle \mathcal{E}_{S,j}, \sum_{i \in G_k^*, i \neq j} \mathcal{E}_{S,i} \right\rangle^2 \right)^{1/2},
\end{aligned}$$

where step (i) uses Cauchy-Schwarz inequality and step (ii) uses  $\|\mathbf{v}\|_2 \leq 1$  for  $\mathbf{v} \in \mathbb{V}_k$ . Using this bound, we can upper bound the expectation as follows:

$$\begin{aligned}
\mathbb{E} \left[ \sup_{\mathbf{v} \in \mathbb{V}_k} \sum_{\{(i,j) \in G_k^*: i \neq j\}} v_j \langle \mathcal{E}_{S,i}, \mathcal{E}_{S,j} \rangle \right] &\leq \mathbb{E} \left[ \left( \sum_{j \in G_k^*} \left\langle \mathcal{E}_{S,j}, \sum_{i \in G_k^*, i \neq j} \mathcal{E}_{S,i} \right\rangle^2 \right)^{1/2} \right] \\
&\stackrel{(i)}{\leq} \left( \sum_{j \in G_k^*} \mathbb{E} \left[ \left\langle (\mathcal{E}_j)_S, \sum_{i \neq j, i \in [n_k]} \mathcal{E}_{S,i} \right\rangle^2 \right] \right)^{1/2} \\
&\stackrel{(ii)}{=} \left( \sum_{j \in G_k^*} \mathbb{E} \left\| \sum_{i \in G_k^*, i \neq j} \mathcal{E}_{S,i} \right\|_2^2 \right)^{1/2} \\
&\stackrel{(iii)}{\leq} \left( |G_k^*| (|G_k^*| - 1) |S| \right)^{1/2} \\
&\leq |G_k^*| \sqrt{|S|}, \tag{65}
\end{aligned}$$

where step (i) uses Jensen's inequality to a concave function  $x \mapsto x^{1/2}$ , step (ii) the independence and zero-mean assumption, and step (iii) uses isotropic Gaussian assumption.

Next, we bound the expectation of the supremum of  $\sum_{i \in G_k^*} v_i \|\mathcal{E}_{S,i}\|_2^2$ .

$$\begin{aligned}
\mathbb{E} \sup_{\mathbf{v} \in \mathbb{V}_k} \left| \sum_{i \in G_k^*} v_i \|\mathcal{E}_{S,i}\|_2^2 \right| &\stackrel{(i)}{=} \mathbb{E} \sup_{\mathbf{v} \in \mathbb{V}_k} \left| \sum_{i \in G_k^*} v_i (\|\mathcal{E}_{S,i}\|_2^2 - |S|) \right| \\
&\stackrel{(ii)}{\leq} \mathbb{E} \sup_{\mathbf{v} \in \mathbb{V}_k} \left( \sum_{i \in G_k^*} v_i^2 \right)^{1/2} \left\{ \sum_{i \in G_k^*} (\|\mathcal{E}_{S,i}\|_2^2 - |S|)^2 \right\}^{1/2} \\
&\stackrel{(iii)}{\leq} \mathbb{E} \left\{ \sum_{i \in G_k^*} (\|\mathcal{E}_{S,i}\|_2^2 - |S|)^2 \right\}^{1/2} \\
&\stackrel{(iv)}{\leq} \left\{ \sum_{i \in G_k^*} \mathbb{E} (\|\mathcal{E}_{S,i}\|_2^2 - |S|)^2 \right\}^{1/2} \\
&= \left( \sum_{i \in G_k^*} \text{Var} \|\mathcal{E}_{S,i}\|_2^2 \right)^{1/2} \\
&\stackrel{(v)}{=} \sqrt{2|G_k^*||S|}, \tag{66}
\end{aligned}$$

where step (i) uses  $\sum_{i \in G_k^*} v_i = 0$ , which follows from the fact that  $\Gamma_k$  is orthogonal to  $\mathbb{1}_{G_k^*}$ , step (ii) uses Cauchy-Schwarz inequality, step (iii) uses  $\|\mathbf{v}\|_2 \leq 1$ , step (iv) uses Jensen's inequality to a concave function  $x \mapsto x^{1/2}$ , and step (v) uses our Gaussian noise assumption and the variance formula for Chi-square random variables.

Combining (65) and (66), we conclude that

$$\mathbb{E} \left[ \sup_{\mathbf{M} \in \mathcal{M}_{kl}^S} \text{QF}_{kl}^S(\mathbf{M}, \mathbf{X}) \right] \lesssim |G_k^*| \sqrt{|S|}.$$

**4. Individual bound using Hanson-wright inequality.** Applying Lemma 11 with the bounds established in the previous steps and using the formulation (63) of  $G_{1,kl}^S(\mathbf{v})$ , we define an event

$$\mathcal{C}_{N,kl}^S := \left\{ \sup_{\mathbf{v} \in \mathbb{V}_k} \frac{|G_l^*|}{|G_k^*|} \sum_{\{(i,j) \in G_k^*\}} v_i \langle \mathcal{E}_{S,i}, \mathcal{E}_{S,j} \rangle \lesssim \frac{|G_l^*|}{|G_k^*|} \underbrace{|G_k^*| \sqrt{|S|}}_{\mathbb{E} \left[ \sup_{\mathbf{M} \in \mathcal{M}_{kl}^S} \text{QF}_{kl}^S(\mathbf{M}, \mathbf{X}) \right]} + \frac{|G_l^*|}{|G_k^*|} \zeta_{N,kl}^S \right\},$$

where  $\zeta_{N,kl}^S := |G_k^*| \sqrt{|S|} (\log n + 2 \log |S| + \log \binom{p}{|S|})$ , then we have

$$\begin{aligned} \mathbb{P} \left( (\mathcal{C}_{N,kl}^S)^C \right) &\lesssim \exp \left[ - \min \left( \frac{(\zeta_{N,kl}^S)^2}{|G_k^*|^2 |S|}, \underbrace{\frac{\zeta_{N,kl}^S}{\sqrt{|G_k^*|}}}_{\|\text{vec}(\mathcal{E}_{S,G_k^*})\|_{\mathcal{A}_{kl}^S}^2 \lesssim \sup_{\mathbf{M} \in \mathcal{A}_{kl}^S} \|\mathbf{M}\|_{\text{op}} \lesssim} \right) \right] \\ &\lesssim \frac{1}{n |S|^2 \binom{p}{|S|}}. \end{aligned}$$

The proof is complete once we show that the intersection event

$$\bigcap_{S \in [p], |S| \leq \sqrt{p}} \bigcap_{1 \leq k \neq l \leq K} \mathcal{C}_{N,kl}^S$$

holds with high probability.

**5. Uniform bound.** Now we show that the event  $\mathcal{C}_{N,kl}^S$  holds uniformly across all  $S \in [p]$  such that  $|S| \leq \sqrt{p}$  and  $1 \leq k \neq l \leq K$ , with probability at least  $1 - C_{11}/n$ , where  $C_{11} > 0$

is a constant.

$$\begin{aligned}
\mathbb{P}\left(\bigcup_{S \in [p], |S| \leq \sqrt{p}} \bigcup_{1 \leq k \neq l \leq K} (\mathcal{C}_{N,kl}^S)^C\right) &\leq \sum_{1 \leq k \neq l \leq K} \sum_{q=1}^{\lfloor \sqrt{p} \rfloor} \sum_{|S|=q} \mathbb{P}((\mathcal{C}_{N,kl}^S)^C) \\
&\lesssim \sum_{q=1}^{\lfloor \sqrt{p} \rfloor} \sum_{|S|=q} \frac{K^2}{n|S|^2 \binom{p}{|S|}} \\
&= \sum_{q=1}^{\lfloor \sqrt{p} \rfloor} \frac{K^2}{nq^2} \\
&\leq \frac{K^2 \pi^2}{6n},
\end{aligned}$$

where the last step uses  $\sum_{q=1}^{\infty} = \pi^2/6$ . Since  $|S| \leq \sqrt{p}$ ,  $|S| \log p$  dominates  $\log |S|$ . Also, we treat  $K$  as a constant. Therefore, we conclude we conclude that uniformly across  $S \in \mathcal{S}$  and  $(k, l)$  such that  $1 \leq k \neq l \leq K$ , with probability at least  $1 - C_{11}/n$ , it holds that

$$\sup_{\mathbf{v} \in \Gamma_K, \|\mathbf{v}\|_2=1} G_{1,kl}^S(\mathbf{v}) \lesssim |G_l^*| \sqrt{|S|(\log n + |S| \log p)}$$

This completes the proof of Lemma 25. □

#### C.4.12 Proof of Lemma 26

The proof proceeds in the following steps.

1. Conditional analysis using a concentration inequality for the supremum of a Gaussian process,
2. Individual bound by Chi-square tail bound,
3. Uniform bound

*Proof.* For notational simplicity, let  $\sigma^2 = 1$ .

**1. Conditional analysis.** Since the sum of inner products of Gaussian random vectors is challenging to analyze directly, we first condition on  $\bar{\mathcal{E}}_{S,l}^*$  and then apply the concentration inequality for the supremum of a Gaussian process (Lemma 9). Fix  $(k, l)$  such that  $1 \leq k \neq l \leq K$  and  $S \subset [p]$  such that  $|S| \leq \sqrt{p}$ . Conditioned on  $\bar{\mathcal{E}}_{S,l}^*$ ,  $G_{2,kl}^S(\mathbf{v})$  can be viewed as a canonical Gaussian process  $\langle G, \mathbf{w} \rangle$ , where  $G \sim \mathcal{N}(0, \mathbf{I}_{|G_k^*|})$  and  $\mathbf{w} \in \mathbb{W}_k$ , with

$$\mathbb{W}_k := \left\{ \|\bar{\mathcal{E}}_{S,l}^*\|_2 \mathbf{v}_{|G_k^*} : \mathbf{v} \in \Gamma_K, \|\mathbf{v}\|_2 = 1 \right\},$$

where  $\mathbf{v}_{|G_k^*}$  is the restriction of  $\mathbf{v} \in \Gamma_K$  onto  $G_k^*$ , and the canonical metric on  $\mathbb{W}_k$  is the  $\ell_2$ -metric.

To apply Lemma 9, we have to bound

$$\text{EC}_{kl}^S(\bar{\mathcal{E}}_{S,l}^*) := \mathbb{E} \left[ \sup_{\mathbf{v} \in \Gamma_K, \|\mathbf{v}\|_2=1} \sum_{i \in G_k^*} v_i \langle \bar{\mathcal{E}}_{S,l}^*, \mathcal{E}_{S,i} \rangle \mid \bar{\mathcal{E}}_{S,l}^* \right] = \mathbb{E} \left[ \sup_{\mathbf{w} \in \mathbb{W}_k} \langle G, \mathbf{w} \rangle \mid \bar{\mathcal{E}}_{S,l}^* \right], \text{ and}$$

$$\text{SVC}_{kl}^S(\bar{\mathcal{E}}_{S,l}^*) := \sup_{\mathbf{v} \in \Gamma_k, \|\mathbf{v}\|_2=1} \text{Var} \left( \sum_{i \in G_k^*} v_i \langle \bar{\mathcal{E}}_{S,l}^*, \mathcal{E}_{S,i} \rangle \mid \bar{\mathcal{E}}_{S,l}^* \right) = \sup_{\mathbf{w} \in \mathbb{W}_k} \text{Var} \left( \langle G, \mathbf{w} \rangle \mid \bar{\mathcal{E}}_{S,l}^* \right).$$

We bound  $\text{EC}_{kl}^S(\bar{\mathcal{E}}_{S,l}^*)$  using Dudley's integral inequality (Lemma 10):

$$\text{EC}_{kl}^S(\bar{\mathcal{E}}_{S,l}^*) \lesssim \int_0^\infty \sqrt{\log N(\mathbb{W}_k, \epsilon)} d\epsilon \stackrel{(i)}{\lesssim} \|\bar{\mathcal{E}}_{S,l}^*\|_2 \int_0^\infty \sqrt{|G_k^*| \log(1/\epsilon)} d\epsilon = \|\bar{\mathcal{E}}_{S,l}^*\|_2 \sqrt{|G_k^*|},$$

where step (i) uses the fact that the  $\epsilon$ -covering entropy of the unit sphere in  $\mathbb{R}^{|G_k^*|}$  is at most  $|G_k^*| \log(1/\epsilon)$ , up to a constant factor, for any  $\epsilon \in (0, 1)$ .

Next, we bound  $\text{SVC}_{kl}^S(\bar{\mathcal{E}}_{S,l}^*)$ :

$$\text{SVC}_{kl}^S(\bar{\mathcal{E}}_{S,l}^*) = \sup_{\mathbf{w} \in \mathbb{W}_k} \text{Var} \left( \langle G, \mathbf{w} \rangle \mid \bar{\mathcal{E}}_{S,l}^* \right) = \sup_{\mathbf{w} \in \mathbb{W}_k} \|\bar{\mathcal{E}}_{S,l}^*\|_2^2 \sum_{i \in G_k^*} v_i^2 \leq \|\bar{\mathcal{E}}_{S,l}^*\|_2^2,$$

where the last inequality follows from  $\|\mathbf{v}\|_2 = 1$  for  $\mathbf{v} \in \Gamma_K$ . Let us denote  $\xi^S = \log(n|S|^2 \binom{p}{|S|})$ .

Define the following conditional probability as follows:

$$\text{CP}_{N,kl}^S := \mathbb{P} \left( \sup_{\mathbf{v} \in \Gamma_K, \|\mathbf{v}\|_2=1} |G_{2,kl}^S(\mathbf{v})| \gtrsim |G_l^*| \underbrace{\|\bar{\mathcal{E}}_{S,l}^*\|_2 \sqrt{|G_k^*|} + |G_l^*|}_{\gtrsim \text{EC}_{kl}^S(\bar{\mathcal{E}}_{S,l}^*)} \underbrace{\|\bar{\mathcal{E}}_{S,l}^*\|_2}_{\gtrsim \sqrt{\text{SVC}_{kl}^S(\bar{\mathcal{E}}_{S,l}^*)}} \sqrt{\xi^S} \mid \bar{\mathcal{E}}_{S,l}^* \right),$$

Then by Lemma 9, we have

$$\text{CP}_{N,kl}^S \leq \frac{1}{n|S|^2 \binom{p}{|S|}}. \quad (67)$$

**2. Chi-square tail bound** Now we use the Chi-square tail inequality to further bound

$\|\bar{\mathcal{E}}_{S,l}^*\|_2$  and  $\|\bar{\mathcal{E}}_{S,l}^*\|_2^2$ . If we define the following event:

$$\mathcal{B}_{N,kl}^S := \left\{ \|\bar{\mathcal{E}}_{S,l}^*\|_2^2 \leq \frac{1}{|G_l^*|} \left( |S| + 2\sqrt{|S|\xi^S} + 2\xi^S \right) \right\}.$$

By Lemma 3, we have

$$\mathbb{P}((\mathcal{B}_{N,kl}^S)^C) \leq \frac{1}{n|S|^2 \binom{p}{|S|}}.$$

Combining the bounds in  $\text{CP}_{N,kl}^S$  and  $\mathcal{B}_{N,kl}^S$ , we define an event:

$$\mathcal{A}_{N,kl}^S := \left\{ \sup_{\mathbf{v} \in \Gamma_K, \|\mathbf{v}\|_2=1} |G_{2,kl}^S(\mathbf{v})| \lesssim \sqrt{|G_l^*|} \sqrt{|S| + 2\sqrt{|S|\xi^S} + 2\xi^S} (\sqrt{|G_k^*|} + \sqrt{\xi^S}) \right\}.$$

The proof is complete once we show that the intersection event

$$\bigcap_{1 \leq k \neq l \leq K} \bigcap_{S \in [p], |S| \leq \sqrt{p}} \mathcal{A}_{N,kl}^S$$

holds with high probability.

**3. Uniform bound.** We have

$$\begin{aligned} & \mathbb{P} \left( \bigcup_{1 \leq k \neq l \leq K} \bigcup_{S \in [p], |S| \leq \sqrt{p}} (\mathcal{A}_{N,kl}^S)^C \right) \\ & \leq \sum_{1 \leq k \neq l \leq K} \sum_{q=1}^{\lfloor \sqrt{p} \rfloor} \sum_{|S|=q} \mathbb{P}((\mathcal{A}_{N,kl}^S)^C) \\ & = \sum_{1 \leq k \neq l \leq K} \sum_{q=1}^{\lfloor \sqrt{p} \rfloor} \sum_{|S|=q} \mathbb{E} [\mathbb{P}((\mathcal{A}_{N,kl}^S)^C \mid \bar{\mathcal{E}}_{S,l}^*)] \\ & \leq \sum_{1 \leq k \neq l \leq K} \sum_{q=1}^{\lfloor \sqrt{p} \rfloor} \sum_{|S|=q} \mathbb{E} [\mathbb{P}((\mathcal{A}_{N,kl}^S)^C \mid \bar{\mathcal{E}}_{S,l}^*) \mathbb{1}(\mathcal{B}_{N,kl}^S) + \mathbb{1}((\mathcal{B}_{N,kl}^S)^C)] \end{aligned}$$

$$\begin{aligned}
&\stackrel{(i)}{\leq} \left( \sum_{1 \leq k \neq l \leq K} \sum_{q=1}^{\lfloor \sqrt{p} \rfloor} \sum_{|S|=q} \mathbb{E}[\text{CP}_{N,kl}^S \mathbb{1}(\mathcal{B}_{N,kl}^S)] \right) + \frac{K^2 \pi^2}{6n} \\
&\stackrel{(ii)}{\lesssim} \frac{K^2 \pi^2}{6n} + \frac{K^2 \pi^2}{6n},
\end{aligned}$$

where step (i) uses  $\sum_{q=1}^{\infty} (1/q^2) = \pi^2/6$ , and step (ii) also uses it and additionally uses (67).

Treating  $K$  as a constant, we conclude that uniformly across  $S \in \mathcal{S}$  and  $(k, l)$  such that  $1 \leq k \neq l \leq K$ , with probability at least  $1 - C_{12}/n$ , where  $C_{12} > 0$  is a constant, it holds that

$$\sup_{\mathbf{v} \in \Gamma_K, \|\mathbf{v}\|_2=1} |G_{2,kl}^S(\mathbf{v})| \lesssim \sqrt{|G_l^*|} \sqrt{|S| + 2\sqrt{|S|\xi^S} + 2\xi^S} \sqrt{|G_k^*| + \sqrt{\xi^S}}.$$

This completes the proof of Lemma 26.  $\square$

#### C.4.13 Proof of Lemma 27

Leveraging the decomposition of  $T_{2,kl}^S$  into  $G_{1,kl}^S$  and  $G_{2,kl}^S$  given in Appendix C.3.3, the proof proceeds in the following intermediate steps:

1. Problem decomposition
2. Inequality for the  $G_1 \times G_1$  term
3. Inequality for the  $G_2 \times G_2$  term
4. Conclusion

*Proof.* For notational simplicity, let  $\sigma^2 = 1$ .

**1. Problem decomposition.** Recall that we defined  $\Delta_{S \cap S_0}^2 = \min_{1 \leq k \neq l \leq K} \|(\boldsymbol{\mu}_l^* - \boldsymbol{\mu}_k^*)_{S \cap S_0}\|_2^2$  in Theorem 1, and  $\dot{\lambda}^S = |S| + m\Delta_{S \cap S_0}^2/4$  in Lemma 21.

$$\sup_{\mathbf{v} \in \Gamma_K, \|\mathbf{v}\|_2=1} \sum_{1 \leq k \neq l \leq K} \frac{T_{2,kl}^S(\mathbf{v})}{t_{lk}^S(\dot{\lambda}^S)}$$

$$\begin{aligned}
&\stackrel{(i)}{=} \sum_{1 \leq k \neq l \leq K} \sup_{\mathbf{v} \in \Gamma_K, \|\mathbf{v}\|_2=1} \frac{N_{kl}^S(\mathbf{v}, \mathbf{X}) N_{lk}^S(\mathbf{v}, \mathbf{X})}{t_{lk}^S(\lambda^S)} \\
&\stackrel{(ii)}{\lesssim} \sum_{1 \leq k \neq l \leq K} \sup_{\mathbf{v} \in \Gamma_K, \|\mathbf{v}\|_2=1} \frac{N_{kl}^S(\mathbf{v}, \mathbf{X}) N_{lk}^S(\mathbf{v}, \mathbf{X})}{|G_l^*||G_k^*|(\|(\boldsymbol{\mu}_k^* - \boldsymbol{\mu}_l^*)_{S \cap S_0}\|_2^2 + |S|)} \\
&= \sum_{1 \leq k \neq l \leq K} \sup_{\mathbf{v} \in \Gamma_K, \|\mathbf{v}\|_2=1} \frac{(G_{1,kl}^S(\mathbf{v}) + G_{2,kl}^S(\mathbf{v}))(G_{1,lk}^S(\mathbf{v}) + G_{2,lk}^S(\mathbf{v}))}{|G_l^*||G_k^*|(\|(\boldsymbol{\mu}_k^* - \boldsymbol{\mu}_l^*)_{S \cap S_0}\|_2^2 + |S|)}
\end{aligned}$$

where step (i) uses the definition of  $T_{2,kl}^S(\mathbf{v})$  stated in (28) and step (ii) uses Lemma 22.

Expanding the numerator yields four terms. We establish the inequality for two of them, the  $G_1 \times G_1$  and  $G_2 \times G_2$  terms, as the cross terms can be easily handled by leveraging the results from these two cases. Before proceeding, we recall from (9) that  $\mathcal{S}$  is defined as

$$\mathcal{S} = \left\{ S : S \subset [p], |S| \leq \sqrt{p}, \Delta_{S \cap S_0}^2 \gtrsim \left( \log n + \frac{|S| \log p}{m} + \sqrt{\frac{|S| \log p}{m}} \right) \right\}.$$

**2. Inequality for the  $G_1 \times G_1$  term.** By Lemma 25, Uniformly across  $S \in \mathcal{S}$  and  $(k, l)$  such that  $1 \leq k \neq l \leq K$ , with probability at least  $1 - C_{11}/n$ , it holds that

$$\begin{aligned}
&\sum_{1 \leq k \neq l \leq K} \sup_{\mathbf{v} \in \Gamma_K, \|\mathbf{v}\|_2=1} \frac{G_{1,kl}^S(\mathbf{v}) G_{1,lk}^S(\mathbf{v})}{|G_l^*||G_k^*|(\|(\boldsymbol{\mu}_k^* - \boldsymbol{\mu}_l^*)_{S \cap S_0}\|_2^2 + |S|)} \\
&\stackrel{(i)}{\lesssim} \sum_{1 \leq k \neq l \leq K} \frac{|S|(\log n + |S| \log p)}{(\|(\boldsymbol{\mu}_k^* - \boldsymbol{\mu}_l^*)_{S \cap S_0}\|_2^2 + |S|)} \\
&\lesssim \frac{|S| \log n + |S|^2 \log p}{(\Delta_{S \cap S_0}^2 + |S|)}.
\end{aligned}$$

Therefore it suffices to show that

$$|S| \log n + |S|^2 \log p \lesssim (|S| + m \Delta_{S \cap S_0}^2)(\Delta_{S \cap S_0}^2 + |S|),$$

which is true since  $|S| \Delta_{S \cap S_0}^2 \gtrsim |S| \log n$  and  $m|S| \Delta_{S \cap S_0}^2 \gtrsim |S|^2 \log p$  under the separation condition of  $\mathcal{S}$ .

**3. Inequality for the  $G_2 \times G_2$  term.** By Lemma 26, Uniformly across  $S \in \mathcal{S}$  and  $(k, l)$

such that  $1 \leq k \neq l \leq K$ , with probability at least  $1 - C_{12}/n$ , it holds that

$$\begin{aligned}
& \sum_{1 \leq k \neq l \leq K} \sup_{\mathbf{v} \in \Gamma_K, \|\mathbf{v}\|_2=1} \frac{G_{2,kl}^S(\mathbf{v})G_{2,lk}^S(\mathbf{v})}{|G_l^*||G_k^*|(\|(\boldsymbol{\mu}_k^* - \boldsymbol{\mu}_l^*)_{S \cap S_0}\|_2^2 + |S|)} \\
& \stackrel{(i)}{\lesssim} \sum_{1 \leq k \neq l \leq K} \frac{\sqrt{|G_l^*|} \sqrt{|S| + 2\sqrt{|S|\xi^S} + 2\xi^S} \sqrt{|G_k^*| + \sqrt{\xi^S}} \sqrt{|G_k^*|} \sqrt{|S| + 2\sqrt{|S|\xi^S} + 2\xi^S} \sqrt{|G_l^*| + \sqrt{\xi^S}}}{|G_l^*||G_k^*|(\|(\boldsymbol{\mu}_k^* - \boldsymbol{\mu}_l^*)_{S \cap S_0}\|_2^2 + |S|)} \\
& = \sum_{1 \leq k \neq l \leq K} \frac{(|S| + 2\sqrt{|S|\xi^S} + 2\xi^S) \sqrt{|G_k^*||G_l^*|} + \sqrt{\xi^S}(|G_k^*| + |G_l^*|) + \xi^S}{\sqrt{|G_l^*||G_k^*|}(\|(\boldsymbol{\mu}_k^* - \boldsymbol{\mu}_l^*)_{S \cap S_0}\|_2^2 + |S|)} \\
& = \sum_{1 \leq k \neq l \leq K} \frac{(|S| + 2\sqrt{|S|\xi^S} + 2\xi^S) (\sqrt{|G_k^*||G_l^*|} + \sqrt{\sqrt{\xi^S}(|G_k^*| + |G_l^*|)} + \sqrt{\xi^S})}{\sqrt{|G_l^*||G_k^*|}(\|(\boldsymbol{\mu}_k^* - \boldsymbol{\mu}_l^*)_{S \cap S_0}\|_2^2 + |S|)},
\end{aligned}$$

where  $\xi^S = \log(n|S|^2 \binom{p}{|S|})$ . The last term can be decomposed into three parts, and we

establish an inequality for each one in turn, starting with the first term:

$$\begin{aligned}
& \sum_{1 \leq k \neq l \leq K} \frac{(|S| + 2\sqrt{|S|\xi^S} + 2\xi^S) (\sqrt{|G_k^*||G_l^*|})}{\sqrt{|G_l^*||G_k^*|}(\|(\boldsymbol{\mu}_k^* - \boldsymbol{\mu}_l^*)_{S \cap S_0}\|_2^2 + |S|)} \\
& = \sum_{1 \leq k \neq l \leq K} \frac{(|S| + 2\sqrt{|S|\xi^S} + 2\xi^S)}{(\|(\boldsymbol{\mu}_k^* - \boldsymbol{\mu}_l^*)_{S \cap S_0}\|_2^2 + |S|)} \\
& \lesssim \frac{(|S| + |S|\sqrt{\log p} + \sqrt{|S|\log n} + \log n + |S|\log p)}{\Delta_{S \cap S_0}^2 + |S|} \\
& \lesssim |S| + m\Delta_{S \cap S_0}^2,
\end{aligned}$$

where the last inequality holds due to the separation condition of  $\mathcal{S}$ .

Now, for the second term, we first recall from Theorem 1 that  $m = 2 \min_{1 \leq k \neq l \leq K} \left\{ \frac{|G_k^*||G_l^*|}{|G_k^*| + |G_l^*|} \right\}$ .

Then we have:

$$\begin{aligned}
& \sum_{1 \leq k \neq l \leq K} \frac{(|S| + 2\sqrt{|S|\xi^S} + 2\xi^S) (\sqrt{\sqrt{\xi^S}(|G_k^*| + |G_l^*|)})}{\sqrt{|G_l^*||G_k^*|}(\|(\boldsymbol{\mu}_k^* - \boldsymbol{\mu}_l^*)_{S \cap S_0}\|_2^2 + |S|)}, \\
& \lesssim \frac{(|S| + 2\sqrt{|S|\xi^S} + 2\xi^S)(\xi^S)^{1/4}}{\sqrt{m}(\Delta_{S \cap S_0}^2 + |S|)} \\
& \lesssim |S| + m\Delta_{S \cap S_0}^2,
\end{aligned}$$

where the last inequality holds because under the separation condition of  $\mathcal{S}$ , we have  $(|S| + 2\sqrt{|S|\xi^S} + 2\xi^S) \lesssim |S| + m\Delta_{S \cap S_0}^2$  and  $(\xi^S)^{1/4} \lesssim \sqrt{m}(\Delta_{S \cap S_0}^2 + |S|)$ .

Finally, for the third term, we have

$$\begin{aligned} & \sum_{1 \leq k \neq l \leq K} \frac{(|S| + 2\sqrt{|S|\xi^S} + 2\xi^S)\sqrt{\xi^S}}{\sqrt{|G_l^*||G_k^*|}(\|(\boldsymbol{\mu}_k^* - \boldsymbol{\mu}_l^*)_{S \cap S_0}\|_2^2 + |S|)} \\ & \lesssim \sum_{1 \leq k \neq l \leq K} \frac{(|S| + 2\sqrt{|S|\xi^S} + 2\xi^S)\sqrt{\xi^S}}{\sqrt{m}(\|(\boldsymbol{\mu}_k^* - \boldsymbol{\mu}_l^*)_{S \cap S_0}\|_2^2 + |S|)} \\ & \lesssim |S| + m\Delta_{S \cap S_0}^2, \end{aligned}$$

where the last inequality holds because under the separation condition of  $\mathcal{S}$ , we have  $(|S| + 2\sqrt{|S|\xi^S} + 2\xi^S) \lesssim |S| + m\Delta_{S \cap S_0}^2$  and  $(\xi^S)^{1/2} \lesssim \sqrt{m}(\Delta_{S \cap S_0}^2 + |S|)$ .

**4. Conclusion.** The inequalities for the cross terms can be verified in a straightforward manner. Combining all the inequalities established above, we conclude that, uniformly over  $S \in \mathcal{S}$  and all  $(k, l)$  with  $1 \leq k \neq l \leq K$ , the following holds with probability at least  $1 - C_{13}/n$ , where  $C_{13} > 0$  is a constant, it holds that:

$$\sup_{\mathbf{v} \in \Gamma_K, \|\mathbf{v}\|_2=1} \sum_{1 \leq k \neq l \leq K} \frac{T_{2,kl}^S(\mathbf{v})}{t_{lk}^S(\dot{\lambda}^S)}.$$

This completes the proof of Lemma 27.  $\square$

## D PROOF OF THEOREM 2

The proof proceeds in the following intermediate steps:

1. Reduction to symmetric two-cluster problem (68),
2. Reduction to average case risk (69),

3. Reduction to Bayes risk (70),

4. Bounding the Bayes risk (72).

*Proof.* We proceed by following the steps outlined above in sequence.

**1. Reduction to symmetric two-cluster problem.** We denote the separation by  $\rho > 0$  and leave its value unspecified for now. First, we define a reduced class of distributions consisting of two symmetric, sparse cluster centers.

$$\tilde{\Theta}(s, \rho, 2) := \tilde{\mathcal{M}}(s, \rho, 2) \times \mathcal{H}(2)$$

where

$$\begin{aligned} \tilde{\mathcal{M}}(s, \rho, 2) := \{(\boldsymbol{\mu}_1, \boldsymbol{\mu}_2) : \boldsymbol{\mu}_1 = \boldsymbol{\mu}, \boldsymbol{\mu}_2 = -\boldsymbol{\mu}, \boldsymbol{\mu} \in \mathbb{R}^p, \|\boldsymbol{\mu}_1 - \boldsymbol{\mu}_2\|_2^2 \geq \rho^2, \\ \text{supp}(\boldsymbol{\mu}) = S_0 \subset [p], |S_0| \leq s\}, \end{aligned}$$

Then we have (by augmenting the matrices in  $\mathcal{H}(2)$  with zero columns to match the dimensions):

$$\tilde{\Theta}(s, \rho, 2) \subset \Theta(s, \rho, K).$$

This inclusion immediately implies that

$$\inf_{\hat{\mathbf{H}}} \sup_{\boldsymbol{\theta} \in \Theta(s, \rho, K)} \mathbb{P}_{\boldsymbol{\theta}}(\hat{\mathbf{H}}(\mathbf{X}) \neq \mathbf{H}) \geq \inf_{\hat{\mathbf{H}}} \sup_{\boldsymbol{\theta} \in \tilde{\Theta}(s, \rho, 2)} \mathbb{P}_{\boldsymbol{\theta}}(\hat{\mathbf{H}}(\mathbf{X}) \neq \mathbf{H}), \quad (68)$$

since the supremum over a smaller set is less than or equal to that over a larger set.

**2. Reduction to average case risk.** Next, we lower bound the worst-case risk in (68) by the average risk.

$$\inf_{\hat{\mathbf{H}}} \sup_{\boldsymbol{\theta} \in \tilde{\Theta}(s, \rho, 2)} \mathbb{P}_{\boldsymbol{\theta}}(\hat{\mathbf{H}}(\mathbf{X}) \neq \mathbf{H}) = \inf_{\hat{\mathbf{H}}} \sup_{(\boldsymbol{\mu}_1, \boldsymbol{\mu}_2) \in \tilde{\mathcal{M}}(s, \rho, 2)} \sup_{\mathbf{H} \in \mathcal{H}(2)} \mathbb{P}_{\boldsymbol{\theta}}(\hat{\mathbf{H}}(\mathbf{X}) \neq \mathbf{H})$$

$$\geq \inf_{\hat{\mathbf{H}}} \sup_{(\boldsymbol{\mu}_1, \boldsymbol{\mu}_2) \in \tilde{\mathcal{M}}(s, \rho, 2)} \mathbb{E}_{\mathbf{H}(\mathbf{X}) \sim \pi} \mathbb{P}_{\boldsymbol{\theta}}(\hat{\mathbf{H}} \neq \mathbf{H}), \quad (69)$$

where  $\pi$  is a uniform prior on  $\mathcal{H}(2)$ , formally given by, for  $i = 1, \dots, n$ ,

$$H_{i,1} \stackrel{\text{i.i.d.}}{\sim} \text{Ber}(1/2), \quad H_{i2} = 1 - H_{i1}.$$

**3. Reduction to Bayes risk.** The risk (69) is equivalent to the minimax risk under zero-one loss, where the data is generated from a uniform hierarchical Gaussian mixture model defined as follows:

$$H_{i,1} \sim \text{Ber}(1/2),$$

$$\mathbf{X}_i \mid H_{i,1} \sim \mathcal{N}((-1)^{H_{i,1}} \boldsymbol{\mu}, \mathbf{I}_p).$$

In this setting, the algorithm that minimizes  $\mathbb{E}_{\mathbf{H} \sim \pi} \mathbb{P}_{\boldsymbol{\theta}}(\hat{\mathbf{H}}(\mathbf{X}) \neq \mathbf{H})$  is the Bayes classifier  $\mathbf{H}^{\boldsymbol{\mu}}$ , which assumes knowledge of the true cluster centers. It operates by thresholding the Gaussian likelihood ratio, and under symmetric cluster centers with isotropic covariance, this yields the decision rule  $H_{i,1}^{\boldsymbol{\mu}} = \mathbb{1}(\boldsymbol{\mu}^{\top} \mathbf{X}_i > 0)$  for  $i = 1, \dots, n$ . Its error probability for one observation, known as the Bayes rate, is explicitly given by (Cai and Zhang, 2019):

$$\mathcal{R}_{\boldsymbol{\mu}_1, \boldsymbol{\mu}_2}^* := \Phi\left(-\frac{\|\boldsymbol{\mu}_1 - \boldsymbol{\mu}_2\|_2}{2\sigma}\right), \quad (70)$$

where  $\Phi$  denotes the cumulative distribution function of standard normal distribution. Therefore we can bound (69) further from below:

$$\begin{aligned} \inf_{\hat{\mathbf{H}}} \sup_{(\boldsymbol{\mu}_1, \boldsymbol{\mu}_2) \in \tilde{\mathcal{M}}(s, \rho, 2)} \mathbb{E}_{\mathbf{H}(\mathbf{X}) \sim \pi} \mathbb{P}_{\boldsymbol{\theta}}(\hat{\mathbf{H}} \neq \mathbf{H}) &\stackrel{(i)}{\geq} \sup_{(\boldsymbol{\mu}_1, \boldsymbol{\mu}_2) \in \tilde{\mathcal{M}}(s, \rho, 2)} \inf_{\hat{\mathbf{H}}} \mathbb{E}_{\mathbf{H}(\mathbf{X}) \sim \pi} \mathbb{P}_{\boldsymbol{\theta}}(\hat{\mathbf{H}} \neq \mathbf{H}) \\ &\stackrel{(ii)}{=} \sup_{(\boldsymbol{\mu}_1, \boldsymbol{\mu}_2) \in \tilde{\mathcal{M}}(s, \rho, 2)} 1 - (1 - \mathcal{R}_{\boldsymbol{\mu}_1, \boldsymbol{\mu}_2}^*)^n \\ &\stackrel{(iii)}{=} 1 - (1 - \Phi(-\rho/\sigma))^n, \end{aligned} \quad (71)$$

where step (i) applies the max–min inequality (see, for example, Section 5.4.1 of Boyd and Vandenberghe, 2004), step (ii) follows from the optimality of Bayes classifier, and step (iii) uses (70).

**4. Bounding the Bayes risk.** If we set  $\rho^2 = C_4\sigma^2 \log n$ , we have

$$\Phi(-\rho/\sigma) = \Phi(-\sqrt{C_4 \log n}) = 1 - \mathbb{P}(Z > -\sqrt{C_4 \log n}) \stackrel{(i)}{\geq} 1 - \exp(-\frac{C_4}{2} \log n) = 1 - n^{-C_4/2},$$

where  $Z$  denotes a standard normal random variable and step (i) uses Gaussian tail bound.

Leveraging this, for any  $n \geq 2$ , we further bound (71) as:

$$1 - \{1 - \Phi(-\sqrt{C_4 \log n})\}^n \geq 1 - n^{-C_4 n/2} > C_5, \quad (72)$$

where  $C_5 > 0$  depends on  $C_4$ . Collecting the reductions (68), (69), (70), and the bound (72), we conclude that

$$\inf_{\hat{\mathbf{H}}} \sup_{\boldsymbol{\theta} \in \Theta(s, \sigma^2 \log n, K)} \mathbb{P}_{\boldsymbol{\theta}}(\hat{\mathbf{H}}(\mathbf{X}) \neq \mathbf{H}) > C_5.$$

This completes the proof of Theorem 2.  $\square$

**Remark 29.** *The reduction in step (i) of (71) is not tight in some regime. A sharper analysis can be obtained by decomposing the average risk  $\mathbb{E}_{\mathbf{H}(\mathbf{X}) \sim \pi} \mathbb{P}_{\boldsymbol{\theta}}(\hat{\mathbf{H}} \neq \mathbf{H})$  into the Bayes risk  $\mathcal{R}_{\boldsymbol{\mu}_1, \boldsymbol{\mu}_2}^*$  and the excess risk  $\mathbb{E}_{\mathbf{H}(\mathbf{X}) \sim \pi} \mathbb{P}_{\boldsymbol{\theta}}(\hat{\mathbf{H}} \neq \mathbf{H}) - \mathcal{R}_{\boldsymbol{\mu}_1, \boldsymbol{\mu}_2}^*$ . Cai et al. (2019) shows that the excess risk is of order  $(s \log p)/n$  in a setting slightly different from ours. Rather than modifying their analysis, we assume a standard high-dimensional sparse regime  $s \log p/n = o(1)$ , so that the Bayes risk term  $\log n$  dominates. In this regime, this lower bound matches the separation bound established in Theorem 1.*

## E DETAILS FOR THE SDP OBJECTIVE FUNCTION

This section presents supplementary information for the original SDP objective (Appendix E.1) and the reduced SDP objective in Algorithm 1 (Appendix E.2).

### E.1 Derivation of the SDP objective function

This section presents the derivation of the SDP objective (3), which was omitted from Section 2 for brevity. The derivation follows Sections 2 and 3 of Zhuang et al. (2023) and Section 1 of Chen and Yang (2021), and is included here for completeness. We proceed in the following order:

1. From Gaussian mixture likelihood to  $K$ -means objective,
2. From  $K$ -means objective to SDP objective.

**1. From Gaussian mixture likelihood to  $K$ -means objective.** We assume that the common covariance  $\Sigma^*$  is known. The log-likelihood for the parameters  $G_1, \dots, G_K$  and  $\mu_1, \dots, \mu_K$  is

$$\ell(G_1, \dots, G_K, \mu_1, \dots, \mu_K) = -\frac{np}{2} \log(2\pi|\Sigma^*|) - \frac{1}{2} \sum_{k=1}^K \sum_{i \in G_k} (\mathbf{X}_i - \mu_k)^\top \Omega^* (\mathbf{X}_i - \mu_k),$$

where  $|\Sigma^*|$  denotes the determinant of  $\Sigma^*$ ,  $G_1 \cup G_2 \cup \dots \cup G_K = [n]$  and  $G_k \cap G_l = \emptyset$  for all  $1 \leq k \neq l \leq K$ . Since the cluster center  $\mu_k$ 's are not of direct interest, we substitute each  $\mu_k$  with its maximum likelihood estimate given the clustering  $G_1, \dots, G_K$ :

$$\bar{\mathbf{X}}^k := \frac{1}{|G_k|} \sum_{j \in G_k} \mathbf{X}_j.$$

By further omitting constants that are irrelevant to the clustering assignment  $G_1, \dots, G_K$ , and multiplying the remaining term by 2, we define the scaled profile log-likelihood for the

clustering as follows:

$$\ell_{\text{lik}}(G_1, \dots, G_K; \mathbf{X}) := - \sum_{k=1}^K \sum_{i \in G_k} (\mathbf{X}_i - \bar{\mathbf{X}}^k)^\top \boldsymbol{\Omega}^* (\mathbf{X}_i - \bar{\mathbf{X}}^k). \quad (73)$$

The following is a well-known identity, which can be found in Equation 12.18 of James et al. (2013):

$$\begin{aligned} \ell_{\text{lik}}(G_1, \dots, G_K; \mathbf{X}) &= - \sum_{k=1}^K \sum_{i \in G_k} (\mathbf{X}_i - \bar{\mathbf{X}}^k)^\top \boldsymbol{\Omega}^* (\mathbf{X}_i - \bar{\mathbf{X}}^k) \\ &= - \sum_{k=1}^K \sum_{i \in G_k} (\mathbf{X}_i - \frac{1}{|G_k|} \sum_{j \in G_k} \mathbf{X}_j)^\top \boldsymbol{\Omega}^* (\mathbf{X}_i - \frac{1}{|G_k|} \sum_{j \in G_k} \mathbf{X}_j) \\ &= - \frac{1}{2} \sum_{k=1}^K \frac{1}{|G_k|} \sum_{i, j \in G_k} (\mathbf{X}_i - \mathbf{X}_j)^\top \boldsymbol{\Omega}^* (\mathbf{X}_i - \mathbf{X}_j). \end{aligned} \quad (74)$$

If  $\boldsymbol{\Sigma}^* = \mathbf{I}_p$ , the maximization of (74) is formulated as the following  $K$ -means problem, by removing the constant factor  $-1/2$ :

$$\min_{G_1, \dots, G_K} \sum_{k=1}^K \frac{1}{|G_k|} \sum_{i, j \in G_k} \|\mathbf{X}_i - \mathbf{X}_j\|_2^2 \quad (75)$$

$$s.t. \quad G_1 \cup G_2 \cup \dots \cup G_K = \{1, \dots, n\}, \text{ and}$$

$$G_k \cap G_l = \emptyset \text{ for all } 1 \leq k \neq l \leq K,$$

where within-cluster dissimilarity is quantified by the sum of squared Euclidean distances.

**2. From  $K$ -means objective to SDP objective.** The likelihood objective (74) can be further simplified as

$$\begin{aligned} \ell_{\text{lik}}(G_1, \dots, G_K; \mathbf{X}) &= - \frac{1}{2} \sum_{k=1}^K \frac{1}{|G_k|} \sum_{i, j \in G_k} (\mathbf{X}_i - \mathbf{X}_j)^\top \boldsymbol{\Omega}^* (\mathbf{X}_i - \mathbf{X}_j) \\ &= \frac{1}{2} \sum_{k=1}^K \frac{1}{|G_k|} \sum_{i, j \in G_k} (2\mathbf{X}_i^\top \boldsymbol{\Omega}^* \mathbf{X}_j - \mathbf{X}_i^\top \boldsymbol{\Omega}^* \mathbf{X}_i - \mathbf{X}_j^\top \boldsymbol{\Omega}^* \mathbf{X}_j) \\ &= \sum_{k=1}^K \left( \frac{1}{|G_k|} \sum_{i \in G_k} \mathbf{X}_i^\top \boldsymbol{\Omega}^* \mathbf{X}_i - \frac{1}{|G_k|} \sum_{i \in G_k} |G_k| (\mathbf{X}_i^\top \boldsymbol{\Omega}^* \mathbf{X}_i) \right) \end{aligned}$$

$$= \ell_{\text{sdp}}(G_1, \dots, G_k) - \sum_{i=1}^n \mathbf{X}_i^\top \boldsymbol{\Omega}^* \mathbf{X}_i, \quad (76)$$

where we recall that in (3) and (4), the SDP objective function is defined as follows:

$$\ell_{\text{sdp}}(G_1, \dots, G_k; \mathbf{X}) := \sum_{k=1}^K \frac{1}{|G_k|} \sum_{i,j \in G_k} \mathbf{X}_i^\top \boldsymbol{\Omega}^* \mathbf{X}_j. \quad (77)$$

From (76), we have the following relationship between the likelihood objective (73) and the SDP objective (77):

$$\ell_{\text{sdp}}(G_1, \dots, G_k; \mathbf{X}) = \ell_{\text{lik}}(G_1, \dots, G_k; \mathbf{X}) + \sum_{i=1}^n \mathbf{X}_i^\top \boldsymbol{\Omega}^* \mathbf{X}_i.$$

The second term of the SDP objective does not depend on the cluster structure.

## E.2 Intuition for the SDP objective in Algorithm 1

This section provides intuition on how the objective  $\langle \tilde{\mathbf{X}}_{\hat{S}^t, \cdot}^\top \boldsymbol{\Sigma}_{\hat{S}^t, \hat{S}^t}^* \tilde{\mathbf{X}}_{\hat{S}^t, \cdot}, \mathbf{Z} \rangle$  in Line 1 of Algorithm 1 arises from the original SDP objective  $\langle \mathbf{X}^\top \boldsymbol{\Omega}^* \mathbf{X}, \mathbf{Z} \rangle$  in (4), when restricted to a support set  $S$ , while capturing the key sparse clustering signal  $\boldsymbol{\beta}^* = \boldsymbol{\Omega}^* (\boldsymbol{\mu}_1^* - \boldsymbol{\mu}_2^*)$ .

We temporarily assume that  $\boldsymbol{\Omega}^*$  is known, and denote the transformed data matrix as  $\tilde{\mathbf{X}} := \boldsymbol{\Omega}^* \mathbf{X} \in \mathbb{R}^{p \times n}$ . Under this transformation, the similarity matrix in the original SDP objective (4) becomes

$$\mathbf{A} := \mathbf{X}^\top \boldsymbol{\Omega}^* \mathbf{X} = \tilde{\mathbf{X}}^\top \boldsymbol{\Sigma}^* \tilde{\mathbf{X}}.$$

We use the matrix-based notation introduced in Definition 12. Here,  $\mathbf{M}^*$  denotes the deterministic mean matrix, where each column is either  $\boldsymbol{\mu}_1^*$  or  $\boldsymbol{\mu}_2^*$ , and, the data matrix and its transformed version can be written as:

$$\mathbf{X} = \mathbf{M}^* + \mathcal{E} \text{ and } \tilde{\mathbf{X}} = \tilde{\mathbf{M}}^* + \tilde{\mathcal{E}}, \text{ where } \tilde{\mathbf{M}}^* := \boldsymbol{\Omega}^* \mathbf{M}^* \text{ and } \tilde{\mathcal{E}} := \boldsymbol{\Omega}^* \mathcal{E},$$

and the columns of  $\mathcal{E} = (\mathcal{E}_1, \dots, \mathcal{E}_n)$  are i.i.d. random vectors distributed as  $\mathcal{N}(\mathbf{0}, \Sigma^*)$ . Using this notation, the similarity matrix can be decomposed into:

$$\mathbf{A} = (\tilde{\mathbf{M}}^*)^\top \Sigma^* \tilde{\mathbf{M}}^* + (\tilde{\mathbf{M}}^*)^\top \Sigma^* \tilde{\mathcal{E}} + \tilde{\mathcal{E}}^\top \Sigma^* \tilde{\mathbf{M}}^* + \tilde{\mathcal{E}}^\top \Sigma^* \tilde{\mathcal{E}}.$$

In the above decomposition, both the second and third terms are zero-mean, and the fourth term is independent of the cluster structure. Thus we focus on  $(\tilde{\mathbf{M}}^*)^\top \Sigma^* \tilde{\mathbf{M}}^*$ .

Recall that  $S_0 \subset [p]$  denotes the index set where the corresponding entries of  $\boldsymbol{\mu}_1^*$  and  $\boldsymbol{\mu}_2^*$  differ (signal). Let  $N := [p] \setminus S_0$  denote the index set where the corresponding entries of  $\boldsymbol{\mu}_1^*$  and  $\boldsymbol{\mu}_2^*$  are identical (noise). Since  $\boldsymbol{\beta}^* = \boldsymbol{\Omega}^*(\boldsymbol{\mu}_1^* - \boldsymbol{\mu}_2^*)$  is sparse, the row indices of  $\tilde{\mathbf{M}}^*$  can also be decomposed into the signal set  $S_0$  and the noise set  $N$ . Then  $(\tilde{\mathbf{M}}^*)^\top \Sigma^* \tilde{\mathbf{M}}^*$  is decomposed into

$$\begin{aligned} (\tilde{\mathbf{M}}^*)^\top \Sigma^* \tilde{\mathbf{M}}^* &= (\tilde{\mathbf{M}}_{S_0, \cdot}^*)^\top \Sigma_{S_0, S_0}^* \tilde{\mathbf{M}}_{S_0, \cdot}^* + (\tilde{\mathbf{M}}_{S_0, \cdot}^*)^\top \Sigma_{S_0, N}^* \tilde{\mathbf{M}}_{N, \cdot}^* \\ &\quad + (\tilde{\mathbf{M}}_{N, \cdot}^*)^\top \Sigma_{N, S_0}^* \tilde{\mathbf{M}}_{S_0, \cdot}^* + (\tilde{\mathbf{M}}_{N, \cdot}^*)^\top \Sigma_{N, N}^* \tilde{\mathbf{M}}_{N, \cdot}^*. \end{aligned}$$

In the above decomposition, the first term,  $(\tilde{\mathbf{M}}_{S_0, \cdot}^*)^\top \Sigma_{S_0, S_0}^* \tilde{\mathbf{M}}_{S_0, \cdot}^*$ , contains all the essential information for clustering, by the following reason. By expressing  $\mathbf{Z}$  as  $\mathbf{H}\mathbf{B}\mathbf{H}$  and tracing back the derivation in Appendix E.1, we have:

$$\begin{aligned} &\langle (\tilde{\mathbf{M}}_{S_0, \cdot}^*)^\top \Sigma_{S_0, S_0}^* \tilde{\mathbf{M}}_{S_0, \cdot}^*, \mathbf{Z} \rangle \\ &= \sum_{k=1}^K \frac{1}{|G_k|} \sum_{i, j \in G_k} \mathbf{M}_{S_0, i}^* \Sigma_{S_0, S_0}^* \mathbf{M}_{S_0, i}^* \\ &= -\frac{1}{2} \sum_{k=1}^K \frac{1}{|G_k|} \sum_{i, j \in G_k} (\mathbf{M}_{S_0, i}^* - \mathbf{M}_{S_0, j}^*)^\top \Sigma_{S_0, S_0}^* (\mathbf{M}_{S_0, i}^* - \mathbf{M}_{S_0, j}^*) + \sum_{i=1}^n \mathbf{M}_{S_0, i}^* \Sigma_{S_0, S_0}^* \mathbf{M}_{S_0, i}^*. \end{aligned}$$

The first term contains  $\boldsymbol{\beta}^*$ . Therefore, we propose running the SDP-relaxed  $K$ -means (4) using a noisy version of  $(\tilde{\mathbf{M}}_{S_0, \cdot}^*)^\top \Sigma_{S_0, S_0}^* \tilde{\mathbf{M}}_{S_0, \cdot}^*$ , given by the matrix  $\tilde{\mathbf{X}}_{\hat{S}^t, \cdot}^\top \Sigma_{\hat{S}^t, \hat{S}^t}^* \tilde{\mathbf{X}}_{\hat{S}^t, \cdot}$ .

## F DETAILS FOR PROPOSED ITERATIVE ALGORITHMS

This section supplements the iterative algorithms presented in Section 3 by providing omitted details. Appendix F.1 derives the uniform bound presented in (11), which is used in the feature selection step of Algorithm 2. Appendix F.2 provides additional details for the ISEE subroutine, which plays a central role in Algorithm 3.

### F.1 Derivation of the uniform bound in the feature selection step of Algorithm 2

This section derives the uniform bound presented in equation (11) in Section 3.1. Since  $\mathbf{X}_i \sim \mathcal{N}(0, \Sigma^*)$ , it follows that  $\tilde{\mathbf{X}}_i = \mathbf{X}_i \boldsymbol{\Omega}^* \sim \mathcal{N}(0, \boldsymbol{\Omega}^* \Sigma^* \boldsymbol{\Omega}^*)$ . Therefore, for any  $j \notin S_0$ , we have  $\tilde{X}_{j,i} \sim \mathcal{N}(0, \omega_{jj})$ , where  $\omega_{jj}$  is the  $j$ th diagonal entry of  $\boldsymbol{\Omega}^*$ .

Given cluster assignments  $G_1$  and  $G_2$ , the empirical transformed cluster means are defined as

$$\bar{\tilde{\mathbf{X}}}_{G_1} := \frac{1}{|G_1|} \sum_{i \in G_1} \tilde{\mathbf{X}}_i, \quad \text{and} \quad \bar{\tilde{\mathbf{X}}}_{G_2} := \frac{1}{|G_2|} \sum_{i \in G_2} \tilde{\mathbf{X}}_i.$$

Regardless of the accuracy of the cluster assignments, for  $j \notin S_0$ , the  $j$ th entry of  $\bar{\tilde{\mathbf{X}}}_{G_1}$  and  $\bar{\tilde{\mathbf{X}}}_{G_2}$  follows the distributions

$$\mathcal{N}\left(0, \frac{\omega_{jj}}{|G_1|}\right) \quad \text{and} \quad \mathcal{N}\left(0, \frac{\omega_{jj}}{|G_2|}\right),$$

respectively. Let  $\hat{\boldsymbol{\beta}}(G_1, G_2) := \bar{\tilde{\mathbf{X}}}_G - \bar{\tilde{\mathbf{X}}}_{G_2}$ . Then, for each  $j \notin S_0$ , the scaled  $j$ th element satisfies:

$$\frac{1}{\sqrt{\omega_{jj}}} \hat{\beta}_j(G_1, G_2) \sim \mathcal{N}\left(0, \frac{n}{|G_1| \cdot |G_2|}\right),$$

because  $|G_1| + |G_2| = n$ . Although the entries of  $\hat{\boldsymbol{\beta}}(G_1, G_2)$  are not independent, the Gaussian maximal inequality still applies. Consequently, for any  $\delta > 0$ , with probability at least  $1 - \delta$ ,

we have:

$$\max_{G_1, G_2} \max_{j \in S \setminus S_0} \left| \sqrt{\frac{|G_1| \cdot |G_2|}{\omega_{jj}}} \hat{\beta}_j(G_1, G_2) \right| \leq \sqrt{2n \log(2(p - |S_0|)/\delta)}.$$

This completes the derivation of the bound in equation (11).

## F.2 Supplementary details for ISEE subroutine

This section provides the omitted details for the ISEE subroutine. We proceed in the following steps:

1. Regression relationship on the data sub-vectors (Appendix F.2.1),
2. Key identities on transformed cluster center and noise (Appendix F.2.2),
3. Estimation error bound for the ISEE subroutine (Appendix F.2.3),

Without loss of generality, we focus on the case where  $i \in G_1^*$ . The derivations build on those in Fan and Lv (2016), with the key distinction that they only consider the special case  $\mu_1^* = \mathbf{0}$ . At the end of this section, Algorithm 4 formulates the ISEE subroutine presented in Section 3.2.1 as an algorithm.

### F.2.1 Regression relationship on the data sub-vectors

Using the conditional distribution property of multivariate Gaussians and the Schur complement, we derive the following regression relationship between sub-vectors of  $\mathbf{X}_i \sim \mathcal{N}(\mu_1^*, \Sigma^*)$  for  $i \in G_1^*$ , as presented in equation (13) in Section 3.2.1. Given a small index set  $A \subset [p]$ , we recall the following relationship:

$$\underbrace{\mathbf{X}_{A,i}}_{\text{response} \in \mathbb{R}^{|A|}} = \underbrace{(\mu_1^*)_A + (\Omega_{A,A}^*)^{-1} \Omega_{A,A^c}^* (\mu_1^*)_{A^c}}_{:= (\alpha_1)_A \in \mathbb{R}^{|A|} \text{ (intercept)}} - \underbrace{(\Omega_{A,A}^*)^{-1} \Omega_{A,A^c}^*}_{\text{slope} \in \mathbb{R}^{|A| \times (p-|A|)}} \underbrace{\mathbf{X}_{A^c,i}}_{\text{predictor} \in \mathbb{R}^{p-|A|}} + \underbrace{\mathbf{E}_{A,i}}_{\text{residual} \in \mathbb{R}^{|A|}},$$

where  $\mathbf{E}_{A,i} \sim \mathcal{N}(0, (\boldsymbol{\Omega}_{A,A}^*)^{-1})$ . Let us partition  $\mathbf{X}_i$ ,  $\boldsymbol{\mu}_1^*$ , and  $\boldsymbol{\Omega}^*$  according to :

$$\mathbf{X}_i = \begin{bmatrix} \mathbf{X}_{A,i} \\ \mathbf{X}_{A^c,i} \end{bmatrix}, \quad \boldsymbol{\mu}_1^* = \begin{bmatrix} (\boldsymbol{\mu}_1^*)_A \\ (\boldsymbol{\mu}_1^*)_{A^c} \end{bmatrix}, \quad \boldsymbol{\Sigma}^* = \begin{bmatrix} \boldsymbol{\Sigma}_{A,A}^* & \boldsymbol{\Sigma}_{A,A^c}^* \\ \boldsymbol{\Sigma}_{A^c,A}^* & \boldsymbol{\Sigma}_{A^c,A^c}^* \end{bmatrix}.$$

Then the conditional distribution  $\mathbf{X}_{A,i} \mid \mathbf{X}_{A^c,i}$  follows  $\mathcal{N}(\bar{\boldsymbol{\mu}}, \bar{\boldsymbol{\Sigma}})$ , where

$$\bar{\boldsymbol{\mu}} := (\boldsymbol{\mu}_1^*)_A + \boldsymbol{\Sigma}_{A,A^c}^* (\boldsymbol{\Sigma}_{A^c,A^c}^*)^{-1} (\tilde{\mathbf{X}}_{A^c,i} - (\boldsymbol{\mu}_1^*)_{A^c}), \quad (78)$$

and

$$\bar{\boldsymbol{\Sigma}} := \boldsymbol{\Sigma}_{A,A}^* - \boldsymbol{\Sigma}_{A,A^c}^* (\boldsymbol{\Sigma}_{A^c,A^c}^*)^{-1} \boldsymbol{\Sigma}_{A^c,A}^*. \quad (79)$$

Next, to apply the Schur complement, we first introduce the following simplified notation for the matrix partition:

$$\boldsymbol{\Sigma}^* = \begin{bmatrix} \boldsymbol{\Sigma}_{A,A}^* & \boldsymbol{\Sigma}_{A,A^c}^* \\ \boldsymbol{\Sigma}_{A^c,A}^* & \boldsymbol{\Sigma}_{A^c,A^c}^* \end{bmatrix} = \begin{bmatrix} \mathbf{A} & \mathbf{B} \\ \mathbf{C} & \mathbf{D} \end{bmatrix}, \quad (80)$$

Then by the Schur complement, we have:

$$\boldsymbol{\Omega}^* = (\boldsymbol{\Sigma}^*)^{-1} = \begin{bmatrix} \boldsymbol{\Omega}_{A,A}^* & \boldsymbol{\Omega}_{A,A^c}^* \\ \boldsymbol{\Omega}_{A^c,A}^* & \boldsymbol{\Omega}_{A^c,A^c}^* \end{bmatrix} = \begin{bmatrix} \mathbf{W} & -\mathbf{WBD}^{-1} \\ -\mathbf{D}^{-1}\mathbf{CW} & \mathbf{D}^{-1} + \mathbf{D}^{-1}\mathbf{CWBD}^{-1} \end{bmatrix}, \quad (81)$$

where

$$\mathbf{W} := (\mathbf{A} - \mathbf{BD}^{-1}\mathbf{C})^{-1}. \quad (82)$$

Leveraging this representation of  $\boldsymbol{\Omega}^*$ , we can derive:

$$-\boldsymbol{\Sigma}_{A,A^c}^* (\boldsymbol{\Sigma}_{A^c,A^c}^*)^{-1} \stackrel{(i)}{=} -\mathbf{BD}^{-1} \stackrel{(ii)}{=} \mathbf{W}^{-1} (-\mathbf{WBD}^{-1}) \stackrel{(iii)}{=} (\boldsymbol{\Omega}_{A,A}^*)^{-1} \boldsymbol{\Omega}_{A,A^c}^*,$$

where step (i) uses (80), step (ii) uses (82), and step (iii) uses (81). This lets us rewrite  $\bar{\boldsymbol{\mu}}$  in (78) as follows:

$$\bar{\boldsymbol{\mu}} = (\boldsymbol{\mu}_1^*)_A + \boldsymbol{\Sigma}_{A,A^c}^* (\boldsymbol{\Sigma}_{A^c,A^c}^*)^{-1} (\tilde{\mathbf{X}}_{A^c,i} - (\boldsymbol{\mu}_1^*)_{A^c})$$

$$\begin{aligned}
&= (\boldsymbol{\mu}_1^*)_A - (\boldsymbol{\Omega}_{AA}^*)^{-1} \boldsymbol{\Omega}_{AA^c}^* (\tilde{\mathbf{X}}_{A^c,i} - (\boldsymbol{\mu}_1^*)_{A^c}) \\
&= (\boldsymbol{\mu}_1^*)_A + \underbrace{(\boldsymbol{\Omega}_{A,A}^*)^{-1} \boldsymbol{\Omega}_{A,A^c}^* (\boldsymbol{\mu}_1^*)_{A^c} - (\boldsymbol{\Omega}_{A,A}^*)^{-1} \boldsymbol{\Omega}_{A,A^c}^* \tilde{\mathbf{X}}_{A^c,i}}_{(\boldsymbol{\alpha}_1)_A},
\end{aligned}$$

Likewise, we can also simplify  $\bar{\boldsymbol{\Sigma}}$  in (79) as follows:

$$\bar{\boldsymbol{\Sigma}} = \boldsymbol{\Sigma}_{A,A}^* - \boldsymbol{\Sigma}_{A,A^c}^* (\boldsymbol{\Sigma}_{A^c,A^c}^*)^{-1} \boldsymbol{\Sigma}_{A^c,A}^* \stackrel{(i)}{=} \mathbf{A} - \mathbf{B} \mathbf{D}^{-1} \mathbf{C} \stackrel{(ii)}{=} \mathbf{W}^{-1} = (\boldsymbol{\Omega}_{A,A}^*)^{-1},$$

where step (i) uses (80), step (ii) uses (82), and step (iii) uses (81). Substituting these expressions into the conditional distribution  $\mathbf{X}_{A,i} \mid \mathbf{X}_{A^c,i} \sim \mathcal{N}(\bar{\boldsymbol{\mu}}, \bar{\boldsymbol{\Sigma}})$ , we obtain the regression relationship (13).

### F.2.2 Key identities on transformed cluster center and noise

Next, we turn to the two key identities presented in (14):

$$(\tilde{\boldsymbol{\mu}}_1^*)_A = \boldsymbol{\Omega}_{A,A}^* (\boldsymbol{\alpha}_1)_A,$$

and

$$(\tilde{\mathcal{E}}_i)_A = \boldsymbol{\Omega}_{A,A} \mathbf{E}_{A,i},$$

which play a central role in the ISEE subroutine.

We start with the first identity. By pre-multiplying  $\boldsymbol{\Omega}_{A,A}^*$  to  $(\boldsymbol{\alpha}_1)_A$ , we have:

$$\boldsymbol{\Omega}_{A,A}^* (\boldsymbol{\alpha}_1)_A = \boldsymbol{\Omega}_{A,A}^* (\boldsymbol{\mu}_1^*)_A + \boldsymbol{\Omega}_{A,A^c}^* (\boldsymbol{\mu}_1^*)_{A^c}.$$

Therefore, we can express  $(\tilde{\boldsymbol{\mu}}_1^*)_A$  as follows:

$$(\tilde{\boldsymbol{\mu}}_1^*)_A = \boldsymbol{\Omega}_{A,A}^* \boldsymbol{\mu}_1^* = \boldsymbol{\Omega}_{A,A}^* (\boldsymbol{\mu}_1^*)_A + \boldsymbol{\Omega}_{A,A^c}^* (\boldsymbol{\mu}_1^*)_{A^c} = \boldsymbol{\Omega}_{A,A}^* (\boldsymbol{\alpha}_1)_A.$$

This completes the derivation of the first identity.

Next, we derive the second identity:

$$\begin{aligned}
\tilde{\mathcal{E}}_{A,i} &= \boldsymbol{\Omega}_{A,.}^* \mathbf{X}_i - \boldsymbol{\Omega}_{A,.}^* \boldsymbol{\mu}_1^* \\
&= \boldsymbol{\Omega}_{A,A}^* \mathbf{X}_{A,i} + \boldsymbol{\Omega}_{A,A^c}^* \mathbf{X}_{A^c,i} - \boldsymbol{\Omega}_{A,A}^* (\boldsymbol{\mu}_1^*)_A + \boldsymbol{\Omega}_{A,A^c}^* (\boldsymbol{\mu}_1^*)_{A^c} \\
&= \boldsymbol{\Omega}_{A,A}^* \left( \mathbf{X}_{A,i} + (\boldsymbol{\Omega}_{A,A}^*)^{-1} \boldsymbol{\Omega}_{A,A^c}^* \mathbf{X}_{A^c,i} - (\boldsymbol{\mu}_1^*)_A + (\boldsymbol{\Omega}_{A,A}^*)^{-1} \boldsymbol{\Omega}_{A,A^c}^* (\boldsymbol{\mu}_1^*)_{A^c} \right) \\
&= \boldsymbol{\Omega}_{A,A}^* \mathbf{E}_{A,i}.
\end{aligned}$$

where the last equality uses the regression relationship (13). This completes the derivation of the second identity.

### F.2.3 Estimation error bound for the ISEE subroutine

We derive the estimation error bound presented in (15) in Section 3.2.2, recalled below:

$$\|((\hat{\tilde{\boldsymbol{\mu}}}_1)_{A_\ell} - (\hat{\tilde{\boldsymbol{\mu}}}_2)_{A_\ell}) - ((\tilde{\boldsymbol{\mu}}_1^*)_{A_\ell} - (\tilde{\boldsymbol{\mu}}_2^*)_{A_\ell})\|_2 \lesssim C_6 \max\{J \log p/n, \sqrt{\log p/n}\},$$

where  $J$  is the maximum number of nonzero off-diagonal entries per row of  $\boldsymbol{\Omega}^*$ , and  $C_6 =$

$$\|\boldsymbol{\Omega}_{A_\ell,A_\ell}^*\|_2 + \|(\hat{\boldsymbol{\alpha}}_1)_{A_\ell}\|_2 + \|(\hat{\boldsymbol{\alpha}}_2)_{A_\ell}\|_2.$$

We start by using the triangle inequality to obtain the following bound:

$$\|((\hat{\tilde{\boldsymbol{\mu}}}_1)_{A_\ell} - (\hat{\tilde{\boldsymbol{\mu}}}_2)_{A_\ell}) - ((\tilde{\boldsymbol{\mu}}_1^*)_{A_\ell} - (\tilde{\boldsymbol{\mu}}_2^*)_{A_\ell})\|_2 \leq \|(\hat{\tilde{\boldsymbol{\mu}}}_1)_{A_\ell} - (\tilde{\boldsymbol{\mu}}_1^*)_{A_\ell}\|_2 + \|(\hat{\tilde{\boldsymbol{\mu}}}_2)_{A_\ell} - (\tilde{\boldsymbol{\mu}}_2^*)_{A_\ell}\|_2.$$

We can bound the  $\|(\hat{\tilde{\boldsymbol{\mu}}}_1)_{A_\ell} - (\tilde{\boldsymbol{\mu}}_1^*)_{A_\ell}\|_2$  term as follows:

$$\begin{aligned}
&\|(\hat{\tilde{\boldsymbol{\mu}}}_1)_{A_\ell} - (\tilde{\boldsymbol{\mu}}_1^*)_{A_\ell}\|_2 \\
&\stackrel{(i)}{=} \|(\hat{\boldsymbol{\Omega}}_{A_\ell,A_\ell}(\hat{\boldsymbol{\alpha}}_1)_{A_\ell} - \boldsymbol{\Omega}_{A_\ell,A_\ell}^*(\boldsymbol{\alpha}_1)_{A_\ell})\|_2 \\
&\stackrel{(ii)}{=} \|(\hat{\boldsymbol{\Omega}}_{A_\ell,A_\ell}(\hat{\boldsymbol{\alpha}}_1)_{A_\ell} - \boldsymbol{\Omega}_{A_\ell,A_\ell}^*(\hat{\boldsymbol{\alpha}}_1)_{A_\ell}) + (\boldsymbol{\Omega}_{A_\ell,A_\ell}^*(\hat{\boldsymbol{\alpha}}_1)_{A_\ell} - \boldsymbol{\Omega}_{A_\ell,A_\ell}^*(\boldsymbol{\alpha}_1)_{A_\ell})\|_2 \\
&= \|(\hat{\boldsymbol{\Omega}}_{A_\ell,A_\ell} - \boldsymbol{\Omega}_{A_\ell,A_\ell}^*)(\hat{\boldsymbol{\alpha}}_1)_{A_\ell} + \boldsymbol{\Omega}_{A_\ell,A_\ell}^*((\boldsymbol{\alpha}_1)_{A_\ell} - (\hat{\boldsymbol{\alpha}}_1)_{A_\ell})\|_2
\end{aligned}$$

$$\begin{aligned}
&\leq \|(\hat{\Omega}_{A_\ell, A_\ell} - \Omega_{A_\ell, A_\ell}^*)(\hat{\alpha}_1)_{A_\ell}\|_2 + \|\Omega_{A_\ell, A_\ell}^*((\alpha_1)_{A_\ell} - (\hat{\alpha}_1)_{A_\ell})\|_2 \\
&\stackrel{(iii)}{\leq} \|\hat{\Omega}_{A_\ell, A_\ell} - \Omega_{A_\ell, A_\ell}^*\|_2 \|(\hat{\alpha}_1)_{A_\ell}\|_2 + \|\Omega_{A_\ell, A_\ell}^*\|_2 \|(\alpha_1)_{A_\ell} - (\hat{\alpha}_1)_{A_\ell}\|_2,
\end{aligned}$$

where step (i) uses the key identity from equation (14) and the fact that the ISEE subroutine employs a plug-in estimator, step (ii) adds and subtracts the term  $\Omega_{A_\ell, A_\ell}^*(\hat{\alpha}_1)_{A_\ell}$ , and step (iii) applies the operator norm bound  $\|\mathbf{A}\mathbf{x}\|_2 \leq \|\mathbf{A}\|_2 \|\mathbf{x}\|_2$ . We can also derive a similar bound for  $\|(\hat{\tilde{\mu}}_2)_{A_\ell} - (\tilde{\mu}_2^*)_{A_\ell}\|_2$ . Therefore we have:

$$\begin{aligned}
&\|((\hat{\tilde{\mu}}_1)_{A_\ell} - (\hat{\tilde{\mu}}_2)_{A_\ell}) - ((\tilde{\mu}_1^*)_{A_\ell} - (\tilde{\mu}_2^*)_{A_\ell})\|_2 \\
&\leq \|\hat{\Omega}_{A_\ell, A_\ell} - \Omega_{A_\ell, A_\ell}^*\|_2 \|(\hat{\alpha}_1)_{A_\ell}\|_2 + \|\Omega_{A_\ell, A_\ell}^*\|_2 \|(\alpha_1)_{A_\ell} - (\hat{\alpha}_1)_{A_\ell}\|_2 \\
&\quad + \|\hat{\Omega}_{A_\ell, A_\ell} - \Omega_{A_\ell, A_\ell}^*\|_2 \|(\hat{\alpha}_2)_{A_\ell}\|_2 + \|\Omega_{A_\ell, A_\ell}^*\|_2 \|(\alpha_2)_{A_\ell} - (\hat{\alpha}_2)_{A_\ell}\|_2.
\end{aligned}$$

Under some regularity conditions, Fan and Lv (2016) proves that  $\|\hat{\Omega}_{A_\ell, A_\ell} - \Omega_{A_\ell, A_\ell}^*\|_2$ ,  $\|(\hat{\alpha}_1)_{A_\ell} - (\alpha_1)_{A_\ell}\|_2$ , and  $\|(\hat{\alpha}_2)_{A_\ell} - (\alpha_2)_{A_\ell}\|_2$  all have convergence rates of order  $\max\{J \log p/n, \sqrt{\log p/n}\}$ . Therefore, we can conclude that

$$\begin{aligned}
&\|((\hat{\tilde{\mu}}_1)_{A_\ell} - (\hat{\tilde{\mu}}_2)_{A_\ell}) - ((\tilde{\mu}_1^*)_{A_\ell} - (\tilde{\mu}_2^*)_{A_\ell})\|_2 \\
&\lesssim (\|(\hat{\alpha}_1)_{A_\ell}\|_2 + \|(\hat{\alpha}_2)_{A_\ell}\|_2 + 2\|\Omega_{A_\ell, A_\ell}^*\|_2) \max\left\{\frac{J \log p}{n}, \sqrt{\frac{\log p}{n}}\right\} \\
&\lesssim C_6 \max\left\{\frac{J \log p}{n}, \sqrt{\frac{\log p}{n}}\right\}.
\end{aligned}$$

This completes the estimation error bound presented in (15).

## G DETAILS FOR NUMERICAL STUDY

This section provides additional details on the numerical studies, omitted from Section 4. Appendix G.1 provides details on parameter tuning, early stopping criterion, implementation

---

**Algorithm 4** ISEE subroutine: `isee`


---

**Require:** Data matrix  $\mathbf{X}$ , cluster estimate  $\hat{G}_1, \hat{G}_2$

- 1:  $A_1, \dots, A_L \leftarrow$  non-overlapping subsets of  $[p]$  of size 2 or 3
- 2: **for**  $\ell = 1, 2, \dots, L$  **do**
- 3:    $\mathcal{D}_1^\ell \leftarrow \{(\mathbf{X}_{A_\ell^c, i}, \mathbf{X}_{A_\ell, i}) : i \in \hat{G}_1\}$
- 4:    $(\hat{\boldsymbol{\alpha}}_1)_{A_\ell}, \{\hat{\mathbf{E}}_{A_\ell, i}\}_{i \in \hat{G}_1} \leftarrow$  slope and residuals obtained from running lasso on  $\mathcal{D}_1^\ell$
- 5:    $\mathcal{D}_2^\ell \leftarrow \{(\mathbf{X}_{A_\ell^c, i}, \mathbf{X}_{A_\ell, i}) : i \in \hat{G}_2\}$
- 6:    $(\hat{\boldsymbol{\alpha}}_2)_{A_\ell}, \{\hat{\mathbf{E}}_{A_\ell, i}\}_{i \in \hat{G}_2} \leftarrow$  slope and residuals obtained from running lasso on  $\mathcal{D}_2^\ell$
- 7:    $\hat{\mathbf{E}}_{A_\ell, \cdot} \leftarrow (\hat{\mathbf{E}}_{A_\ell, 1}, \dots, \hat{\mathbf{E}}_{A_\ell, n})$  ▷ Residual block
- 8:    $\hat{\boldsymbol{\Omega}}_{A_\ell, A_\ell} \leftarrow (\frac{1}{n} \hat{\mathbf{E}}_{A_\ell, \cdot} \hat{\mathbf{E}}_{A_\ell, \cdot}^\top)^{-1}$ , ▷ Precision matrix block
- 9:    $(\hat{\hat{\boldsymbol{\mu}}}_1)_{A_\ell} \leftarrow \hat{\boldsymbol{\Omega}}_{A_\ell, A_\ell} (\hat{\boldsymbol{\alpha}}_1)_{A_\ell}$ , ▷ Transformed cluster 1 center block
- 10:    $(\hat{\hat{\boldsymbol{\mu}}}_2)_{A_\ell} \leftarrow \hat{\boldsymbol{\Omega}}_{A_\ell, A_\ell} (\hat{\boldsymbol{\alpha}}_2)_{A_\ell}$  ▷ Transformed cluster 2 center block
- 11:    $\hat{\tilde{\mathbf{M}}}_{A_\ell, \cdot} \leftarrow$  an  $|A_\ell| \times n$  matrix where the  $i$ th column is  $(\hat{\hat{\boldsymbol{\mu}}}_1)_{A_\ell}$  if  $i \in \hat{G}_1$ , and  $(\hat{\hat{\boldsymbol{\mu}}}_2)_{A_\ell}$  if  $i \in \hat{G}_2$
- 12:    $\hat{\tilde{\mathbf{X}}}_{A_\ell, \cdot} \leftarrow \hat{\tilde{\mathbf{M}}}_{A_\ell, \cdot} + \boldsymbol{\Omega}_{A_\ell, A_\ell} \hat{\mathbf{E}}_{A_\ell, \cdot}$  ▷ Transformed data block
- 13:    $\hat{\hat{\boldsymbol{\mu}}}_1 \leftarrow ((\hat{\hat{\boldsymbol{\mu}}}_1)_{A_1}^\top, \dots, (\hat{\hat{\boldsymbol{\mu}}}_1)_{A_L}^\top)^\top$ , ▷ Aggregate cluster 1 center blocks
- 14:    $\hat{\hat{\boldsymbol{\mu}}}_2 \leftarrow ((\hat{\hat{\boldsymbol{\mu}}}_2)_{A_1}^\top, \dots, (\hat{\hat{\boldsymbol{\mu}}}_2)_{A_L}^\top)^\top$  ▷ Aggregate cluster 2 center blocks
- 15:    $\hat{\tilde{\mathbf{X}}} \leftarrow (\hat{\tilde{\mathbf{X}}}_{A_1, \cdot}^\top, \dots, \hat{\tilde{\mathbf{X}}}_{A_L, \cdot}^\top)^\top$  ▷ Aggregate transformed data blocks
- 16:   Output  $\hat{\hat{\boldsymbol{\mu}}}_1, \hat{\hat{\boldsymbol{\mu}}}_2, \hat{\tilde{\mathbf{X}}}$

---

details, and computing resources. Appendix G.2 describes sparsity-aware high-dimensional clustering methods used for comparison.

## G.1 Supplementary details for the simulation studies

This section provides details on hyperparameter tuning, software implementation, early stopping criteria, and computing resources related to the simulation studies presented in Section 4 and Appendix H.

**Initialization** Unless specified, we use spectral clustering (Han et al., 2023) for initialization of our iterative algorithms.

**High-dimensional regression** We use the lasso (Tibshirani, 1996) for high-dimensional regression between nodes in the ISEE subroutine (Algorithm 4) of Algorithm 3. At each iteration, the regularization parameter is tuned by computing the lasso path and selecting the value that minimizes the Akaike Information Criterion (AIC). This procedure is implemented using functions from the MATLAB package `penalized` (McIlhagga, 2016).

**Early stopping** For efficiency, we employ a data-driven stopping criterion to terminate the algorithm before reaching the  $T$ th iteration. At each iteration  $t$ , the stopping condition is met if either of the following conditions is met: (1) the relative change in the objective value falls below  $\pi\%$ ; or (2) after a warm-up period of  $w$  iterations, the best objective value observed shows less than  $\pi\%$  improvement over the most recent  $\eta$  iterations. The algorithm terminates only when this condition holds for both the SDP objective in SDP  $K$ -means subroutine (line 1 of Algorithm 1) and the original  $K$ -means objective. Unless stated otherwise, we set  $w = 10$ ,  $\eta = 5$ , and  $\pi = 1\%$  in our experiments. Appendix H provides a numerical evaluation of this

stopping criterion.

**Software implementation** Our algorithms are implemented in MATLAB, and all simulations are run using version R2023b. To solve the SDP problems, we use the ADMM-based solver SDPNAL++ (Sun et al., 2020). In the final step of the SDP-relaxed  $K$ -means, we extract the leading eigenvector (an  $n$ -dimensional vector) from the output matrix  $Z$  and apply the `kmeans` function from MATLAB Statistics and Machine Learning Toolbox. For the ISEE subroutine, we utilize the MATLAB Parallel Computing Toolbox to simultaneously estimate the cluster centers and precision matrix blocks. For graphical lasso in Algorithm 5, we use the implementation provided by Leung et al. (2016). In Scenario 1, hierarchical clustering is performed using the `linkage` function with default options, also from MATLAB Statistics and Machine Learning Toolbox. When comparing against baseline methods, we use their original implementations, some in MATLAB and others in R, executed within their respective environments. All implementations and simulation codes, including those for the baseline methods written by their original authors, are available at our GitHub repository.

**Computing resources.** All simulations are conducted on a Linux machine equipped with an AMD EPYC 7542 processor (32 cores, 2.90 GHz) and 16 GB of RAM. A single run of Algorithm 3, from initialization to the final iteration, completes in under one minute on this system.

## G.2 Sparsity-aware clustering methods used for benchmarking

This section describes the baseline sparsity-aware methods used for comparison with our algorithms in the numerical studies presented in Section 4.

**IFPCA** Influential Feature PCA (IFPCA; Jin and Wang, 2016) is a two step method. In the feature selection step, features with the highest Kolmogorov-Smirnov (KS) scores are selected, with the selection threshold determined in a data-driven manner using the Higher Criticism principle (Donoho and Jin, 2004). In the clustering step, spectral clustering is applied: the top  $K - 1$  left singular vectors are extracted from the normalized data matrix after feature selection and used as inputs to the classical  $K$ -means algorithm to estimate cluster labels. For simulations, we use the authors' MATLAB implementation.

**SAS** Sparse Alternate Similarity clustering (SAS; Arias-Castro and Pu, 2017) is an iterative method that uses the fact that the within-cluster dissimilarity of  $K$ -means, measured by the squared  $\ell_2$  distances, can be decomposed coordinate-wise. The algorithm alternates between clustering and support estimation: given a support set, it applies  $K$ -means to estimate the clusters; given the cluster assignments, it selects the top  $|\hat{S}_0|$  coordinates with the largest average within-cluster dissimilarity. The tuning parameter  $|\hat{S}_0|$ , which denotes the number of signal features, is selected using the following permutation-based approach: For each  $|\hat{S}_0| = 1, \dots, p$ , run the SAS algorithm to obtain corresponding cluster and support estimates. For each run, compare the within-cluster dissimilarity of the selected features under the estimated cluster assignment to that under a randomly permuted cluster assignment. The discrepancy between the two is quantified using the gap statistic (Tibshirani et al., 2001). Then choose the value of  $|\hat{S}_0|$  that yields the largest gap statistic. We use the authors' R implementation.

**SKM** Sparse  $K$ -means (SKM; Witten and Tibshirani, 2010 ) is an iterative method which exploits the fact that the within-cluster dissimilarity in  $K$ -means, measured by squared  $\ell_2$  distances, can be decomposed coordinate-wise. The method assigns a feature weight  $w_j$  to each variable  $j = 1, \dots, p$ , and constructs a feature-weighted version of the  $K$ -means

objective. It then optimizes this objective over both feature weights and cluster assignments, subject to a combined lasso and ridge penalty. The proposed algorithm alternates between maximizing the objective with respect to the cluster assignments (given fixed feature weights) and with respect to the feature weights (given fixed cluster assignments). For simulations, we use the authors' R package `sparcl`.

**CHIME** CHIME (Cai et al., 2019) is an EM-type iterative method, where the E-step updates the cluster assignments based on current Gaussian mixture model parameters, and the M-step updates the model parameters with cluster labels fixed. Notably, CHIME avoids explicit covariance estimation by employing an  $\ell_1$ -regularized estimation of the sparse discriminative direction  $\boldsymbol{\beta}^* = \boldsymbol{\Omega}^*(\boldsymbol{\mu}_1^* - \boldsymbol{\mu}_2^*)$ . After a suitable number of iterations, the estimated  $\boldsymbol{\beta}^*$  is plugged into the Fisher discriminant rule to produce the final cluster assignments. For simulations, we use the authors' MATLAB implementation. This algorithm requires careful initialization of the model parameters. For simulations, we used the true values of model parameters with very small Gaussian noise (standard deviation 0.01) added to each entry as the initial values.

## H ADDITIONAL NUMERICAL RESULTS

This section supplements Section 4 by presenting additional simulation results.

### H.1 Evaluation of Algorithm 2 under known non-isotropic covariance

As argued in Section 3.1 and further justified in Appendix E.2, the SDP problem in line 1 of Algorithm 1:

$$\arg \max_{\mathbf{Z} \in \mathbb{R}^{n \times n}} \langle \tilde{\mathbf{X}}_{\hat{S}^t, \cdot}^\top, \boldsymbol{\Sigma}_{\hat{S}^t, \hat{S}^t} \tilde{\mathbf{X}}_{\hat{S}^t, \cdot}, \mathbf{Z} \rangle$$

$$\text{s.t. } \mathbf{Z}^\top = \mathbf{Z}, \mathbf{Z} \succeq 0, \text{tr}(\mathbf{Z}) = 2, \mathbf{Z}\mathbf{1}_n = \mathbf{1}_n$$

captures the key sparse clustering signal encoded in  $\beta^*$ . To validate this claim, we evaluate Algorithm 2 under the same setting as Figure 1 (line 1 of Table 1), but with a non-isotropic covariance. In particular, we adopt an AR(1) covariance structure. The data are generated under the model (16), with parameter settings following the line 1 of Table 3. The result presented in Figure 3 highlights two key findings. First, Algorithm 2 successfully adapts to the sparsity of  $\beta^*$ : its performance remains stable, particularly when  $\Delta_{\Sigma^*} = 4$ , as sparsity increases while the total clustering signal is held fixed. Second, when the covariance structure is known, stronger correlations improve clustering. As  $\rho$  increases, mis-clustering rates deteriorate more slowly with increasing sparsity while the total clustering signal is held fixed. This is expected, since knowing a high-correlation structure is effectively equivalent to working in a lower-dimensional space.

## H.2 Impact of Parameter Estimation and Threshold Choice on Algorithm 3

We argued in Section 3.2 that the strength of Algorithm 3 lies in avoiding full estimation of the precision matrix. On the other hand, its threshold choice is based on the theoretical guarantee of ISEE (Fan and Lv, 2016), which involves many constants (we suppressed this by  $\sqrt{\log n}$ ). Recall that for the threshold in Algorithm 2, only a single constant  $\delta$  arises from the family-wise error rate derived by maximal inequality for Gaussians, which was also conveniently set to a fixed constant without theoretical background. Nevertheless, we argue that these constant factors have little practical impact, since the threshold can be set slightly conservative without loss of performance. This is justified by Theorem 1, which shows that

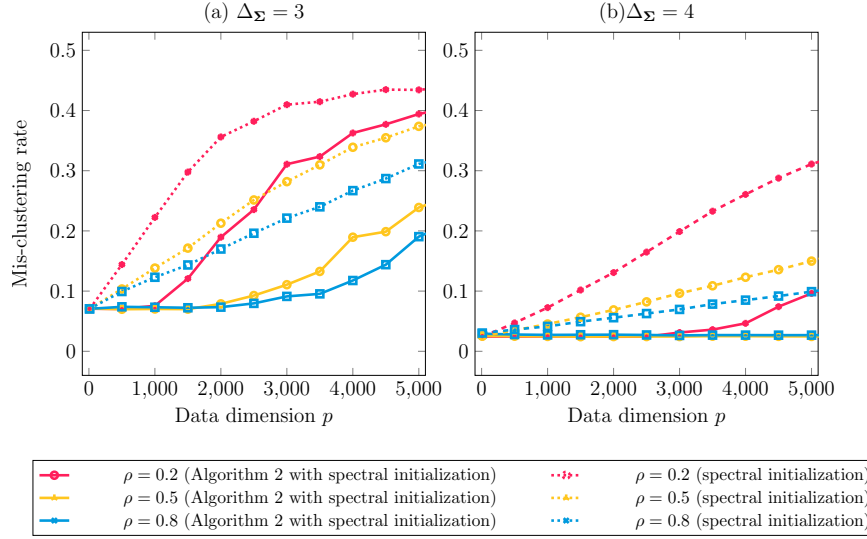


Figure 3: Mis-clustering rates of Algorithm 2 with spectral initialization under AR(1) correlation structures with  $\rho = 0.2, 0.5, 0.8$ . The data generation follows line 1 of Table 3. Dotted lines of the same color indicate the mis-clustering rates of spectral initialization under the corresponding covariance structure.

Table 3: Summary of Parameter Settings for Model (16) used in Appendices H.1 - H.3, with  $i, j = 1, \dots, p$ .

Section	Methods Evaluated	Covariance structure	$p$	$n$	Separation
H.1	Algorithm 2 (for known $\Sigma^*$ )	known, $\Sigma_{i,j}^* = \rho^{ i-j }$ , $\rho \in \{0.2, 0.5, 0.8\}$	50-5000	200	$\Delta_{\Sigma^*}^2 = 3^2, 4^2$
H.2	Algorithm 3 and its variants	unknown, $\Omega_{i,i+1}^* = \Omega_{i+1,i}^* = \rho$ , $\Omega_{i,i}^* = 1, \Omega_{i,j}^* = 0$ o.w., $\rho \in \{0.2, 0.45\}$	400	500	$\Delta_{\Sigma^*}^2 = 3^2, 4^2$
H.3	Early stopping of Algorithm 3	unknown, $\Omega_{i,i+1}^* = \Omega_{i+1,i}^* = \rho$ , $\Omega_{i,i}^* = 1, \Omega_{i,j}^* = 0$ o.w., $\rho = 0.45$	400	500	$\Delta_{\Sigma^*}^2 = 4^2$

SDP  $K$ -means is robust to overestimation of  $S_0$ . In this section, we numerically validate these points by comparing Algorithm 3 with two specially designed variants.

**Algorithm 5: Algorithm 3 with graphical lasso** At each iteration  $t$ , Algorithm 5 fully estimates the precision matrix using graphical lasso (**GraphicalLasso**; Friedman et al., 2008), and uses it to compute the necessary quantities:  $\tilde{\mathbf{X}}$ ,  $\beta^*$ , and  $\Sigma_{\hat{S}^t, \hat{S}^t}$ . These estimates are then used in feature selection and clustering steps.

---

**Algorithm 5** Iterative SDP  $K$ -means with unknown covariance using graphical lasso

---

**Require:** Data matrix  $\mathbf{X}$ , maximum number of iteration  $T$

- 1: Let  $\hat{G}_1^0, \hat{G}_2^0$  be cluster estimates obtained by running spectral clustering on  $\mathbf{X}$
- 2: **for**  $t = 1, 2, \dots, T$  **do**
- 3:      $\hat{\mathbf{X}}_1^t \leftarrow |\hat{G}_1^{t-1}|^{-1} \sum_{i \in \hat{G}_1^{t-1}} \mathbf{X}_i$
- 4:      $\hat{\mathbf{X}}_2^t \leftarrow |\hat{G}_2^{t-1}|^{-1} \sum_{i \in \hat{G}_2^{t-1}} \mathbf{X}_i$
- 5:      $\dot{\mathbf{X}}^t \leftarrow (\mathbf{X}_{\cdot, \hat{G}_1^{t-1}} - \hat{\mathbf{X}}_1^t \mathbf{1}_{\hat{G}_1^{t-1}}^\top, \mathbf{X}_{\cdot, \hat{G}_2^{t-1}} - \hat{\mathbf{X}}_2^t \mathbf{1}_{\hat{G}_2^{t-1}}^\top) \triangleright$  Cluster-wise demeaned data matrix
- 6:      $\hat{\Omega}^t \leftarrow \text{GraphicalLasso}(\dot{\mathbf{X}}^t)$
- 7:      $\hat{\omega}_{11}^t, \dots, \hat{\omega}_{pp}^t \leftarrow \text{diag}(\hat{\Omega}^t)$
- 8:      $\hat{\beta}^t \leftarrow \hat{\Omega}^t (\hat{\mathbf{X}}_1^t - \hat{\mathbf{X}}_2^t)$
- 9:      $\hat{S}^t \leftarrow \left\{ j \in \{1, \dots, p\} : |\hat{\beta}_j^t| > \sqrt{2\hat{\omega}_{jj}^t n \log(2p)} / \sqrt{|\hat{G}_1^{t-1}| \cdot |\hat{G}_2^{t-1}|} \right\} \triangleright$  feature selection
- 10:      $\hat{\tilde{\mathbf{X}}}^t \leftarrow \hat{\Omega}^t \mathbf{X}$
- 11:      $\hat{\Sigma}_{\hat{S}^t, \hat{S}^t}^t \leftarrow ((\hat{\Omega}^t)^{-1})_{\hat{S}^t, \hat{S}^t}$
- 12:      $\hat{G}_1^t, \hat{G}_2^t \leftarrow \text{clust}(\hat{\tilde{\mathbf{X}}}^t_{\hat{S}^t, \cdot}, \hat{\Sigma}_{\hat{S}^t, \hat{S}^t}^t) \triangleright$  Clustering (Algorithm 1)
- 13: Output  $\hat{G}_1^T, \hat{G}_2^T$

---

---

**Algorithm 6: Algorithm 3 with threshold based on Gaussian maximal inequality**

The estimated submatrix blocks of the precision matrix, computed in line 8 of Algorithm 4, also provide precision matrix diagonal estimates, denoted  $\hat{\omega}_{11}, \dots, \hat{\omega}_{pp}$ . Algorithm 6 leverages these diagonal estimates to compute plug-in estimates for the quantities required by Algorithm 3, instead of using  $\hat{\boldsymbol{\mu}}_1^t$  and  $\hat{\boldsymbol{\mu}}_2^t$ .

---

**Algorithm 6** Iterative SDP  $K$ -means with unknown covariance using threshold based on Gaussian maximal inequality

---

**Require:** Data matrix  $\mathbf{X}$ , maximum number of iteration  $T$

- 1: Let  $\hat{G}_1^0, \hat{G}_2^0$  be cluster estimates obtained by running spectral clustering on  $\mathbf{X}$
- 2: **for**  $t = 1, 2, \dots, T$  **do**
- 3:      $\hat{\mathbf{X}}^t, \omega_{11}^t, \dots, \omega_{pp}^t \leftarrow \text{isee}(\mathbf{X}, \hat{G}_1^{t-1}, \hat{G}_2^{t-1})$   $\triangleright$  Algorithm 4 modified to output  $\hat{\omega}_{11}^t, \dots, \hat{\omega}_{pp}^t$
- 4:      $\hat{\boldsymbol{\beta}}^t \leftarrow |\hat{G}_1^{t-1}|^{-1} \sum_{i \in \hat{G}_1^{t-1}} \hat{\mathbf{X}}_i^t - |\hat{G}_2^{t-1}|^{-1} \sum_{i \in \hat{G}_2^{t-1}} \hat{\mathbf{X}}_i^t$ .
- 5:      $\hat{S}^t \leftarrow \left\{ j \in \{1, \dots, p\} : |\hat{\beta}_j^t| > \sqrt{2\hat{\omega}_{jj}^t n \log(2p)} / \sqrt{|\hat{G}_1^{t-1}| \cdot |\hat{G}_2^{t-1}|} \right\}$   $\triangleright$  feature selection
- 6:      $\hat{\boldsymbol{\Sigma}}_{\hat{S}^t, \hat{S}^t}^t \leftarrow$  pooled covariance of covariances computed from  $\mathbf{X}_{\hat{S}^t, \hat{G}_1^{t-1}}$  and  $\mathbf{X}_{\hat{S}^t, \hat{G}_2^{t-1}}$
- 7:      $\hat{G}_1^t, \hat{G}_2^t \leftarrow \text{clust}(\hat{\mathbf{X}}_{\hat{S}^t, \cdot}^t, \hat{\boldsymbol{\Sigma}}_{\hat{S}^t, \hat{S}^t}^t)$   $\triangleright$  Clustering (Algorithm 1)
- 8: Output  $\hat{G}_1^T, \hat{G}_2^T$

---

Figure 4 compares Algorithm 3 with the two variants under the setting specified in line 2 of Table 3. Figure 4 highlights two key findings. First, Algorithm 5 performs poorly compared to Algorithm 3, indicating that avoiding full estimation of the precision matrix improves performance. Second, Algorithm 6 performs slightly worse than Algorithm 3 in some scenarios, suggesting that an exact feature selection cutoff is not necessary and reconfirming the robustness of SDP  $K$ -means to slight overestimation of  $S_0$ .

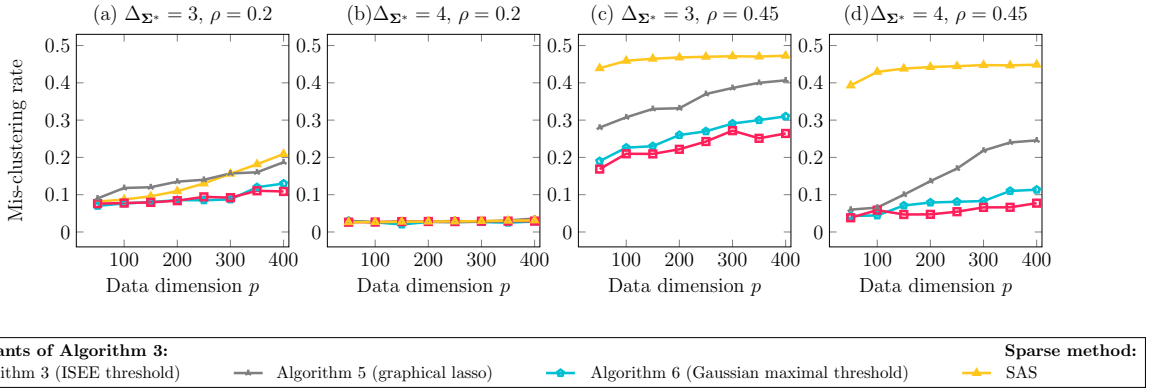


Figure 4: Mis-clustering rates of Algorithm 3, its two variants, and SAS (the best-performing baseline method in Figure 2). The settings follow the unknown covariance scenario with varying conditional correlations, as specified in line 2 of Table 3.

### H.3 Numerical Evidence Supporting the Convergence of Our Algorithm

We provide numerical evidence supporting the convergence of Algorithm 3 under the stopping criterion in Appendix G.1, and reaffirm that slight overestimation of  $S_0$  is not harmful. We reuse one setting from Appendix H.2, specifically the scenario  $(p, \Delta_{\Sigma^*}, \rho) = (400, 4, 0.45)$ . Line 3 of Table 3 provides the details of this setting. The stopping criteria are applied using the hyperparameters  $T = 100$ ,  $\pi = 0.5\%$ ,  $w = 40$ , and  $\eta = 20$ . We conduct 200 independent replications to record when Algorithm 3 terminates its iteration. At each stopping point, we record the mis-clustering rate, the number of true positives (signal entries retained), and false positives (noise entries retained). The results in Figure 5 reveal two main insights about the behavior of our stopping criteria and the performance of Algorithm 3: First, the stopping criteria are effective. Figure 5-(a) shows that the algorithms consistently stop before reaching the maximum iteration limit, providing empirical evidence of convergence. Across

different estimation-cutoff strategies, the stopping points are similarly concentrated. Second, true discoveries contribute more to clustering performance than the avoidance of false ones. As shown in Figure 5-(b), the original Algorithm 3 demonstrates more stable clustering performance compared to its variant, which often yields mis-clustering rates near 0.5. Figures 5-(c) and 5-(d) shows that Algorithm 3 incurs many more false discoveries. Since Figure 4 shows that Algorithm 3 slightly outperforms Algorithm 6, these plots reaffirm that modest over-selection of features is not particularly harmful.

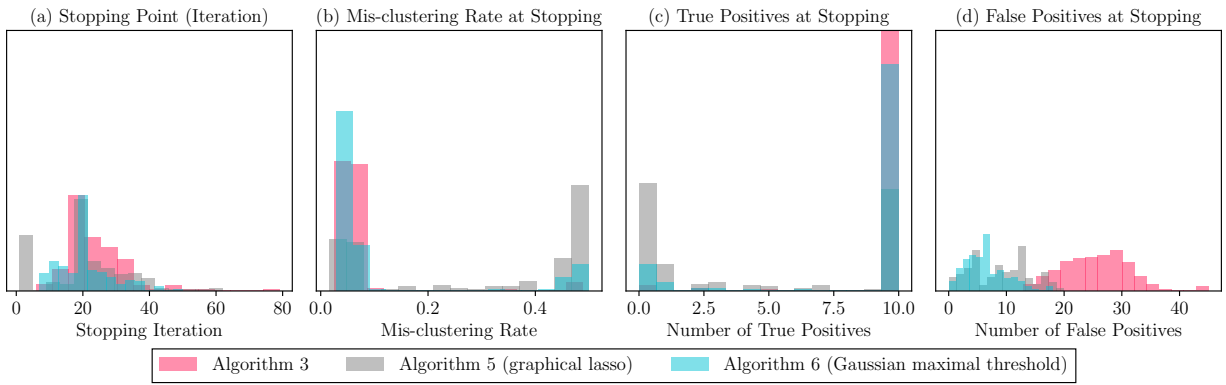


Figure 5: Histograms from 200 independent runs comparing Algorithm 3 and its variants (Algorithms 5 and 6). The data setting follows line 1 of Table 3, and the stopping criteria are applied using the hyperparameters  $T = 100$ ,  $\pi = 0.5\%$ ,  $w = 40$ , and  $\eta = 20$ .

## H.4 Assumption Robustness

We address the robustness of our method by discussing each type of model misspecification separately:

- Section H.4.1 addresses the assumption of Gaussian noises.
- Section H.4.2 addresses the assumption of covariance homogeneity.

- Section H.4.3 addresses the assumption of exact sparsity in the cluster centers and the precision matrix.

Each subsection discusses the potential consequences of assumption violations and provides numerical experiments addressing a single type of misspecification, based on our established baselines (line 1 of Table 1 for isotropic scenarios and line 2 for non-isotropic scenarios). All reported values represent average accuracy over 100 independent experiments.

#### H.4.1 Assumption of Gaussian Noises

Algorithm 2 relies on a Gaussian distribution assumption both on theoretical development and algorithmic standpoint. On the theoretical front, the separation bound for exact recovery in Theorem 1 assumes Gaussian distribution. As existing exact recovery separation bounds without sparsity were established under this condition (Chen and Yang, 2021), Theorem 1 extends these findings with new perspectives on high dimensionality and sparse signals. Leveraging Gaussian properties, we derive the separation bound for exact recovery whose rate explicitly depends on sample size  $n$ , sparsity  $s$ , and dimension  $p$ . Such explicit dependency clarifies how  $n$  and  $s$  can affect the separation bound, motivating the critical role of feature selection in high-dimensional clustering. Relaxing the Gaussian assumption would likely alter these dependency rates on critical parameters, with the exact form determined by the data's tail behavior. For example, heavy-tailed distributions would likely lead to a separation bound where the  $n$  dependency grows faster than  $s$ , since the  $n$  term in our bound stems from the Gaussian's exponential tails. From an algorithmic standpoint, in the isotropic case, Gaussianity guides our algorithm's feature selection threshold (10). The SDP algorithm does not require Gaussianity (although our theory requires it for obtaining the separation bound). Deviation from Gaussianity will make our threshold less accurate in measuring the noise

Table 4: Comparison of clustering accuracy for Algorithm 2 under isotropic  $t$ -distributed and Gaussian noise. All other settings follow line 1 of Table 1 with  $\Delta = 4$ .

Noise distribution	$p = 1000$	$p = 2000$	$p = 3000$	$p = 4000$	$p = 5000$
$\mathcal{N}(\mathbf{0}, \mathbf{I}_p)$	0.97	0.92	0.86	0.74	0.67
Entrywise $t(6)$	0.97	0.93	0.78	0.71	0.70
Entrywise $t(8)$	0.97	0.91	0.81	0.72	0.66

level, potentially affecting feature selection accuracy. However, this may not be a concern because our ultimate goal is clustering, and feature selection is conducted to reduce the noise caused by null features and thus is only of secondary importance.

We conduct an additional simulation to show that our algorithm maintains strong performance even when the data are generated from heavy-tailed distributions. Extending the isotropic Gaussian scenario in Figure 1, we consider settings where the noise is generated i.i.d. from a  $p$ -dimensional distribution, with each entry independently drawn from a  $t$ -distribution with 6 or 8 degrees of freedom. The result displayed in Table 4 shows that Algorithm 2 has robust performance even when data are generated from multivariate  $t$ -distributions.

Under unknown non-isotropic covariance  $\Sigma^*$ , Algorithm 3 works on the transformed data  $\tilde{\mathbf{X}}_i = \Omega^* \mathbf{X}_i$  whose estimator  $\hat{\tilde{\mathbf{X}}}_i$  is built on node-wise Lasso regressions derived from the Gaussian distribution. The estimation accuracy of  $\hat{\tilde{\mathbf{X}}}_i$  is only theoretically justified when the data have Gaussian distribution. Nevertheless our simulation result shown in Table 5 demonstrates that Algorithm 3 has robust performance even when data are generated from multivariate  $t$ -distributions with covariance  $\Sigma^*$ .

Developing the companion theoretical justification is technically challenging and left as a

Table 5: Comparison of clustering accuracy for Algorithm 3 under  $t$ -distributed and Gaussian noise with unknown non-isotropic covariance  $\Sigma^*$ . All other settings follow line 2 of Table 1 with  $\Delta_{\Sigma^*} = 4$ .

Noise distribution	$p = 100$	$p = 200$	$p = 300$	$p = 400$
$\mathcal{N}(\mathbf{0}, \Sigma^*)$	0.94	0.95	0.93	0.92
Entrywise $t(6)$ , pre-multiplied by $(\Sigma^*)^{1/2}$	0.97	0.91	0.94	0.89
Entrywise $t(8)$ , pre-multiplied by $(\Sigma^*)^{1/2}$	0.97	0.95	0.93	0.92

future research direction.

#### H.4.2 Assumption of Covariance Homogeneity

When cluster covariances differ, our theoretical results no longer apply and the optimal (Bayes) clustering boundary becomes nonlinear (quadratic for Gaussian distributions). Blindly applying our algorithm under covariance heterogeneity presents a common model misspecification challenge, as our algorithm learns a linear boundary. Under mild heterogeneity, we expect Algorithm 2 to retain strong performance. To verify this, we conduct a simulation in which the data distribution remains Gaussian but with two different covariance matrices,  $(1 + \delta)\mathbf{I}_p$  and  $(1 - \delta)\mathbf{I}_p$ . The results, reported in Table 6, show an interesting phenomenon of higher clustering accuracy for larger  $\delta$ . A plausible explanation is that larger  $\delta$  corresponds to larger difference in clusters and hence an easier clustering problem. Theoretical understanding of the impact of such heterogeneity is an interesting future research direction.

Table 6: Comparison of clustering accuracy for Algorithm 2 under heterogeneous and homogeneous covariances. All other settings follow line 1 of Table 1 with  $\Delta = 4$ .

$\delta$	$p = 1000$	$p = 2000$	$p = 3000$	$p = 4000$	$p = 5000$
0 (homogeneous covariance)	0.97	0.93	0.86	0.74	0.68
0.05 (homogeneous covariance)	0.98	0.92	0.84	0.76	0.74
0.1 (heterogeneous covariance)	0.98	0.92	0.91	0.87	0.88

#### H.4.3 Assumption of Sparsity

In the second paragraph of Section 1, rather than the cluster centers themselves being exactly sparse, we assume that their difference  $(\boldsymbol{\mu}_1^* - \boldsymbol{\mu}_2^*)$  is exactly sparse. When this difference is approximately sparse, it implies that all entries have clustering power, just that some have weak signals.

Under the known covariance setting, our Theorem 1 is specific to SDP relaxed  $K$ -means algorithm under the sparse signal setting, and Theorem 2 characterizes the fundamental difficulty in high-dimensional sparse clustering and is not specific to any algorithm. Thus, from the theoretical perspective, we only discuss Theorem 1 results when approximate instead of exact sparsity in  $\boldsymbol{\mu}_1^* - \boldsymbol{\mu}_2^*$  holds. Our separation bound in Theorem 1 is derived for the difference  $\boldsymbol{\mu}_1^* - \boldsymbol{\mu}_2^*$ , and it does not rule out the approximately sparse scenario where  $\|\boldsymbol{\mu}_1^* - \boldsymbol{\mu}_2^*\|_0 \approx s$ . Indeed, our result ensures that for any subset  $S$  containing enough signals such that the cumulative signal strength satisfies the inequality in (9), exact recovery of cluster IDs can be achieved.

In practice, having weak signals can cause challenges in feature selection. However, since

Table 7: Comparison of clustering accuracy for Algorithm 2 under exact and approximate sparsity of the cluster centers. All other settings follow line 1 of Table 1 with  $\Delta = 4$ .

$\delta$	$p = 1000$	$p = 2000$	$p = 3000$	$p = 4000$	$p = 5000$
0 (exact sparsity)	0.97	0.93	0.86	0.74	0.68
0.02 (approximate sparsity)	0.98	0.95	0.81	0.70	0.63
0.05 (approximate sparsity)	0.97	0.96	0.85	0.75	0.68

our goal is clustering and feature selection is conducted only to reduce noise, including a few weak signals does not necessarily make clustering much worse. We conduct additional experiments to support this claim. First, in the known covariance setting of line 1 of Table 1, we add  $\delta \in \{0.02, 0.05\}$  to  $\lfloor p/10 \rfloor$  noise entries of  $\boldsymbol{\mu}_1^*$ . The result presented in Table 7 shows that Algorithm 2 retains strong performance under approximate sparsity of the cluster centers. Note that the slight increase in clustering accuracy stems from the increased cumulative signal strength from these weak signals.

Under the unknown covariance setting, the feature selection threshold in Algorithm 3 depends on the exact sparsity of the precision matrix, as described in (15). We demonstrate numerically that Algorithm 3 remains robust under approximate sparsity of the precision matrix. Starting from an exactly sparse precision matrix  $\boldsymbol{\Omega}^*$ , we introduce approximate sparsity in two ways. First, we add  $\delta \in \{0.02, 0.05\}$  to 10% of the zero entries of  $\boldsymbol{\Omega}^*$ . Second, we add 0.01 to all zero entries of  $\boldsymbol{\Omega}^*$ . The result presented in Table 8 shows that Algorithm 3 retains strong performance under approximate sparsity of the precision matrix.

Table 8: Comparison of clustering accuracy for Algorithm 3 under exact and approximate sparsity of the precision matrix. All other settings follow line 2 of Table 1 with  $\Delta_{\Sigma^*} = 4$ .

$\delta$	$p = 100$	$p = 200$	$p = 300$	$p = 400$
0 (exact sparsity)	0.94	0.95	0.93	0.92
0.02 (added to 10% of zero entries)	0.95	0.96	0.93	0.94
0.05 (added to 10% of zero entries)	0.96	0.91	0.91	0.88
0.001 (added to all zero entries)	0.96	0.95	0.95	0.93

## H.5 Scalability to Large Samples and Alternative Solvers

The computational cost of Algorithms 2 and 3 is largely determined by the sample size  $n$ , since the decision variable in the clustering step (Algorithm 1) is an  $n \times n$  matrix. The feature selection steps prune irrelevant variables, so  $p$  primarily affects only the initial clustering stage. However, our current ADMM-based solver SDPNAL+ (Sun et al., 2020) does not scale well beyond  $n > 1000$  (see Table 5 of Sun et al., 2020 for details).

For moderately large sample sizes (up to  $n = 10,000$ ), instead of solving the full SDP in Algorithm 1, we recommend solving its nonnegative low-rank restriction using a nonconvex Burer–Monteiro factorization (Zhuang et al., 2024). Zhuang et al. (2024) shows that this approach retains the same statistical guarantees as the full SDP problem in Algorithm 1. Under the same setting as line 1 of Table 1, we numerically compare the clustering accuracy of Algorithm 2, where the clustering step is performed either by solving the original SDP formulation or its low-rank restriction. The results in Table 9 show that the low-rank SDP formulation achieves comparable clustering accuracy in the small-sample setting. For

$p = 5000$ , the average end-to-end runtime was 121.33 s for the original SDP-based iterative algorithm and 26.66 s for the low-rank SDP-based version (Intel Core i7-1270P CPU, 16 GB RAM).

Table 9: Clustering accuracy of Algorithm 2 with different clustering step formulations. Original SDP solved by ADMM-based solver (Sun et al., 2020); low-rank restriction solved via Burer–Monteiro factorization. Other settings follow line 1 of Table 1 with  $\Delta = 4$ .

Clustering step formulation	$p = 1000$	$p = 2000$	$p = 3000$	$p = 4000$	$p = 5000$
Original SDP	0.97	0.93	0.86	0.74	0.68
Low-rank restriction of SDP	0.97	0.93	0.83	0.74	0.66

We further verify numerically that the low-rank restriction–based algorithm efficiently handles sample sizes up to  $n = 10,000$ , achieving reliable clustering accuracy (Table 10). For  $n = 10,000$ , the average end-to-end runtime of the iterative algorithm was about seven minutes (Intel Core i7-1270P CPU, 16 GB RAM).

To further demonstrate scalability to extremely large sample sizes (e.g.,  $n = 100,000$ ), we incorporate the sketch-and-lift technique of Zhuang et al. (2022). This method randomly subsamples observations, solves the smaller clustering problem, and then propagates the clustering results. Zhuang et al. (2022) show that this approach enjoys a similar statistical guarantees as the inner algorithm applied to the sub-problems. In our implementation, we solve the low-rank restriction of the SDP proposed by Zhuang et al. (2024) for the sub-problems of sample size  $n^{3/7}$ . Table 11 reports strong clustering accuracy and favorable end-to-end timing of this approach, for sample sizes up to  $n = 100,000$  (Intel Core i7-1270P CPU, 16 GB RAM). The runtime increases only modestly with  $n$ , since feature selection and

Table 10: Clustering accuracy of Algorithm 2 with clustering step formulated as low-rank restriction of SDP, under varying  $n$  with fixed ambient dimension  $p = 10000$ . Low-rank restriction solved via Burer–Monteiro factorization. Other settings follow line 1 of Table 1 with  $\Delta = 3$ .

Clustering step formulation	$n = 7000$	$n = 8000$	$n = 9000$	$n = 10000$
Low-rank restriction of SDP	0.92	0.92	0.92	0.93

Table 11: Scalability of Algorithm 2 with clustering step formulated as sketch-and-lift with low-rank restriction of SDP, for fixed ambient dimension  $p = 10000$  and varying sample sizes. Other settings follow line 1 of Table 1 with  $\Delta = 3$ .

	$n = 60000$	$n = 80000$	$n = 100000$
Clustering accuracy	0.957	0.962	0.969
End-to-end timing (s)	196.80	277.58	345.03
Iterations until stop	11.26	10.54	10.34

the sketch-and-lift technique keep the per-iteration cost manageable. Moreover, the algorithm tends to stop earlier for larger sample sizes, further reducing the overall runtime.

## H.6 Comparison with Subspace Clustering Approach

While both subspace clustering and sparse clustering involve dimensionality reduction, they differ fundamentally. Subspace clustering achieves dimensionality reduction via linear combinations of features, whereas feature selection explicitly identifies and prunes individual

Table 12: Comparison of clustering accuracy of JL  $K$ -means with different intrinsic dimension parameter  $t$  and Algorithm 2. Other settings follow line 1 of Table 1 with  $\Delta = 4$ .

	$p = 2000$	$p = 3000$	$p = 4000$	$p = 5000$
JL $K$ -means ( $t = 10$ )	0.53	0.54	0.53	0.52
JL $K$ -means ( $t = 20$ )	0.53	0.53	0.52	0.54
Algorithm 2	<b>0.93</b>	<b>0.86</b>	<b>0.74</b>	<b>0.68</b>

variables. Beyond this conceptual distinction, we empirically compared our method against a subspace clustering approach with theoretical guarantees: the Johnson-Lindenstrauss (JL) transform-based  $K$ -means (JL  $K$ -means; Boutsidis et al., 2010). After applying their JL transform, we ran the SDP-relaxed  $K$ -means (Chen and Yang, 2021) on the dimension-reduced data. This JL transform is theoretically guaranteed to preserve the  $K$ -means objective up to a constant. Under the setting identical to Figure 1 (line 1 of Table 1), which has 10 signal features, we provided the JL algorithm with intrinsic dimension parameters  $t = 10$  and  $t = 20$ . The results, displayed in Table 12, show that Algorithm 2 outperforms JL  $K$ -means in terms of clustering accuracy.